ÇUKUROVA UNIVERSITY
INSTITUTE OF NATURAL AND APPLIED SCIENCES

PhD THESIS

Mustafa ERDEN

INVESTIGATION OF HYDROGEN PRODUCTION PERFORMANCE OF VARIOUS SALTS WITH CHLOR–ALKALI METHOD

DEPARTMENT OF PHYSICS

ADANA-2022

ÇUKUROVA UNIVERSITY
INSTITUTE OF NATURAL AND APPLIED SCIENCES

INVESTIGATION OF HYDROGEN PRODUCTION PERFORMANCE OF VARIOUS SALTS WITH CHLOR-ALKALI METHOD

Mustafa ERDEN

PhD THESIS

DEPARTMENT OF PHYSICS

We certify that the thesis titled above was reviewed and approved for the award of the degree of the Philosophy of Doctorate by the board of jury on 16 / 09 / 2022.

…….....	.....…….……..	……..……
Prof. Dr.Mehmet KARAKILÇIK	Prof. Dr.Süleyman ÇABUK	Prof. Dr.Hüseyin AKILLI
SUPERVISOR	MEMBER	MEMBER
…….....	…….…….	
Prof. Dr. İsmail BOZKURT	Assoc. Prof. Dr. Hacı SOĞUKPINAR	
MEMBER	MEMBER	

This PhD thesis is written at the Department of Physics of the Institute of Natural and Applied Sciences of Çukurova University.
Registration Number:

Prof. Dr. Sadık DİNÇER
Director
Institute of Natural and Applied Sciences

This thesis was supported by the Scientific Research Project Unit of Çukurova University.
Project No: FDK-2017-7005

ABSTRACT

PhD THESIS

INVESTIGATION OF HYDROGEN PRODUCTION PERFORMANCE OF VARIOUS SALTS WITH CHLOR-ALKALI METHOD

Mustafa ERDEN

ÇUKUROVA UNIVERSITY
INSTITUTE OF NATURAL AND APPLIED SCIENCES
DEPARTMENT OF PHYSICS

Supervisor : Prof. Dr. Mehmet KARAKILÇIK
Year: 2022, Pages: 137
Jury : Prof. Dr. Süleyman ÇABUK
: Prof. Dr. Hüseyin AKILLI
: Prof. Dr. İsmail BOZKURT
: Assoc. Prof. Dr. Hacı SOĞUKPINAR

Three important products, namely chlorine gas, caustic soda, and hydrogen gas, are obtained with a Chlor-alkali process generally. Therefore, a Chlor-alkali process powered by the electricity generated from any renewable sources is an important industrial application as it produces three important products without emitting carbon. According to the activity series of K, Na, and Ca metals, the most hydrogen production was obtained with the aqueous solution of KCl, while the least with the aqueous solution of $CaCl_2$ in a certain period. The increase in the operating temperature, cell voltage, and mass flow rate, which are the experimental parameters, also increased the hydrogen production rate. The most effective of these three parameters on the hydrogen production rate was the cell voltage, and the least effective was the mass flow rate. The minimum hydrogen production rate is 27.36 mL/h when the aqueous solution of $CaCl_2$ is used with a mass flow rate of 0.3 g/s and cell voltage of 2.5 V at the operating temperature of 25 °C with energy and exergy efficiencies of 10.81 % and 8.47 %, respectively. The maximum hydrogen production rate is 295.68 mL/h when KCl salt solution is used with a mass flow rate of 0.7 g/s and cell voltage of 3.5 V at the operating temperature of 60 °C with energy and exergy efficiencies of 23.78 % and 17.63 %, respectively.

Keywords: Chlor-Alkali, Hydrogen, Energy, Exergy.

ÖZ

DOKTORA TEZİ

KLOR-ALKALİ YÖNTEM İLE FARKLI TUZLARIN HİDROJEN ÜRETİM PERFORMANSLARININ İNCELENMESİ

Mustafa ERDEN

ÇUKUROVA ÜNİVERSİTESİ
FEN BİLİMLERİ ENSTİTÜSÜ
FİZİK ANA BİLİM DALI

Danışman : Prof. Dr. Mehmet KARAKILÇIK
Yıl: 2022, Sayfa: 137
Jüri : Prof. Dr. Süleyman ÇABUK
: Prof. Dr. Hüseyin AKILLI
: Prof. Dr. İsmail BOZKURT
: Doç. Dr. Hacı SOĞUKPINAR

Genel olarak klor-alkali prosesi ile klor gazı, kostik soda ve hidrojen gazı olmak üzere üç önemli ürün elde edilmektedir. Bu nedenle, herhangi bir yenilenebilir kaynaktan üretilen elektrikle çalışan bir klor-alkali prosesi, karbon salmadan üç önemli ürün ürettiği için önemli bir endüstriyel uygulamadır. K, Na ve Ca metallerinin aktivite serilerine uygun olarak belirli bir zaman diliminde en fazla hidrojen üretimi KCl tuz çözeltisi ile en az ise $CaCl_2$ tuz çözeltisi ile elde edilmiştir. Deneysel parametreler olan çalışma sıcaklığı, hücre voltajı ve kütle akış hızındaki artış hidrojen üretim hızını da artırmıştır. Bu üç parametreden hidrojen üretim hızı üzerinde en etkili olanı hücre voltajı, en az etkili olanı ise kütle akış hızıdır. 25 °C çalışma sıcaklığında 0,3 g/s kütle akış hızı ve 2,5 V hücre voltajı ile $CaCl_2$ tuz çözeltisi kullanıldığında minimum hidrojen üretim hızı 27,36 mL/saat olmuştur. Enerji ve ekserji verimleri sırasıyla % 10.81 ve % 8.47 olarak hesaplanmıştır. 60 °C çalışma sıcaklığında 0,7 g/s kütle akış hızı ve 3,5 V hücre voltajı ile KCl tuz çözeltisi kullanıldığında maksimum hidrojen üretim hızı 295,68 mL/saat olmuştur. Enerji ve ekserji verimleri sırasıyla % 23.78 ve % 17.63 olarak hesaplanmıştır.

Anahtar Kelimeler: Chlor-Alkali, Hidrojen, Enerji, Ekserji.

EXTENDED SUMMARY

Hydrogen produced with renewable energies contributes to the decarbonisation of various sectors. So, hydrogen from Chlor-alkali can be a low-carbon option for industrial processes. Sodium chloride ($NaCl$) is used in industrial Chlor-alkali applications dominantly. But another salt like potassium chloride (KCl) or calcium chloride ($CaCl_2$) can be used.

The Chlor-alkali process is a widely used electrolytic process that produces mainly chlorine and caustic soda as well as hydrogen. This method can be called killing three birds with one stone, not two. However, this study focuses only on hydrogen production. There are three electrolytic processes for producing Chlor-alkali: the mercury cell process, the diaphragm cell process, and the membrane cell process.

In the mercury cell process, a saturated brine solution floats on top of a thin layer of mercury in an electrolytic cell. The mercury layer in this cell behaves as a cathode due to the polarity of the applied potential. Thus sodium forms amalgam with mercury and chlorine is produced at the anode simultaneously. The amalgam (a mixture of two metals, e.g. Na/Hg) is continuously transferred from the electrolytic cell to a decomposer where it reacts with water and decomposes into sodium hydroxide, hydrogen, and mercury. This method has been abandoned in Europe because mercury is a toxic heavy metal and poses an environmental risk.

In the diaphragm cell process, a permeable asbestos fibers diaphragm is often used to separate the anode and the cathode compartments of the cell. The anode compartment is fed with the brine and the chloride ions are oxidized at the anode to produce chlorine gas. The remaining brine from the input brine flows through the diaphragm into the cathode compartment where sodium hydroxide and hydrogen are produced. The diaphragm also prevents the reaction between chlorine and sodium hydroxide.

In the membrane cell process, the electrolysis of brine (mostly an aqueous solution of sodium chloride) takes place in a membrane cell. An ion-exchange membrane separates the anode and the cathode compartments of the cell and allows only sodium ions and a small amount of water to pass through it. Thus, chloride ions are oxidized at the anode to produce chlorine gas, and water is reduced to hydrogen gas and hydroxide ions at the cathode. In addition, sodium hydroxide is formed in the cathode compartment.

The experimental proceeding is based on the membrane cell Chlor-alkali process. Experiments started following electrolyte preparation at operating temperature after checking the system components. When the experiments were started directly while the membrane was dry, inconsistent circuit current was observed in response to the applied voltage for several hours. To overcome this problem, it has been seen that it is beneficial to keep the membrane in the electrolyte one day beforehand. During the experimental runs, applied cell voltage and resulting current, and the hydrogen level in the graduated cylinder concerning time were monitored and registered. Each experiment was repeated to increase consistency and reliability.

Experiments were continued by varying the parameters namely mass flow rate, operating temperature, and cell voltage. These experimental parameters are:

- Mass flow rate: 0.3 g/s, 0.5 g/s, 0.7 g/s.
- Operating temperature: 25 °C, 45 °C, 60 °C.
- Cell voltage: 2.5 V, 3 V, 3.5 V.

Depending on the kind of salt solution ($NaCl_{(aq)}$, $KCl_{(aq)}$ and $CaCl_{2(aq)}$) entering the anode compartment, the membrane allows positive ions only (Na^+, K^+ and Ca^{2+}) to pass from the anode compartment to the cathode compartment. Thus, hydrogen gas (H_2) is released from the cathode compartment and Sodium Hydroxide ($NaOH$), Potassium Hydroxide (KOH), and Calcium Hydroxide ($Ca(OH)_2$) solutions are formed depending on the kind of positive ion passing

through the membrane in the cathode compartment simultaneously. The volume of the produced hydrogen gas is measured by the volumetric displacement technique with the help of a graduated cylinder. On the other hand, in the anode compartment, a large amount of chlorine-based chemical species such as chlorine gas, chlorate, and hypochlorous acid are available for reduction at the anode. An appropriate electrode should be used for chlorine gas discharge in the anode compartment.

According to the activity series of K, Na, and Ca metals, KCl salt solution produced the most hydrogen, while $CaCl_2$ salt solution produced the least hydrogen. Increasing the operating temperature, cell voltage, or mass flow rate increased hydrogen production for all three salt types. For hydrogen production, the voltage increase was more effective than the mass flow rate. More hydrogen was produced as the charge movement increased with the voltage.

The minimum hydrogen production rate was 27.36 mL/h when $CaCl_2$ salt solution was used with a mass flow rate of 0.3 g/s and cell voltage of 2.5 V at the operating temperature of 25 °C. The maximum hydrogen production rate was 295.68 mL/h when KCl salt solution was used with a mass flow rate of 0.7 g/s and cell voltage of 3.5 V at the operating temperature of 60 °C.

GENİŞLETİLMİŞ ÖZET

Yenilenebilir enerjilerle üretilen hidrojen, çeşitli sektörlerin karbondan arındırılmasına katkıda bulunur. Bu nedenle, klor-alkaliden elde edilen hidrojen, endüstriyel prosesler için düşük karbonlu bir seçenek olabilir. Sodyum klorür (NaCl) endüstriyel klor-alkali uygulamalarında baskın olarak kullanılmaktadır. Ancak potasyum klorür (KCl) veya kalsiyum klorür ($CaCl_2$) gibi başka tuzlarda kullanılabilir.

Klor-alkali işlemi, hidrojenin yanı sıra esas olarak klor ve kostik soda üreten, yaygın olarak kullanılan bir elektrolitik işlemdir. Bu yönteme bir taşla iki değil üç kuş vurmak denilebilir. Ancak bu çalışma sadece hidrojen üretimine odaklanmaktadır. Klor-alkali üretmek için üç elektrolitik süreç vardır: cıva hücre süreci, diyafram hücre süreci ve membran hücre süreci.

Cıva hücresi işleminde, doymuş bir tuzlu su çözeltisi, elektrolitik bir hücrede ince bir cıva tabakasının üzerinde yüzer. Bu hücredeki cıva tabakası, uygulanan potansiyelin polaritesinden dolayı bir katot gibi davranır. Böylece sodyum, cıva ile amalgam oluşturur ve aynı anda anotta klor üretilir. Amalgam (İki metalin karışımıdır. Örneğin Na/Hg), elektrolitik hücreden sürekli olarak su ile reaksiyona girdiği ve sodyum hidroksit, hidrojen ve cıvaya ayrıştığı bir ayrıştırıcıya aktarılır. Bu yöntem, cıvanın toksik bir ağır metal olması ve çevresel risk oluşturması nedeniyle Avrupa'da terk edilmiştir.

Diyafram hücresi işleminde, hücrenin anot ve katot bölmelerini ayırmak için genellikle geçirgen bir asbest lifli diyafram kullanılır. Anot bölmesi tuzlu su ile beslenir ve klor gazı üretmek için klorür iyonları anotta oksitlenir. Girilen tuzlu suyun geri kalanı diyaframdan sodyum hidroksit ve hidrojenin üretildiği katot bölmesine geçer. Diyafram ayrıca klor ve sodyum hidroksit arasındaki reaksiyonu da önler.

Membran hücre işleminde, tuzlu suyun (çoğunlukla sulu sodyum klorür çözeltisi) elektrolizi bir membran hücresinde gerçekleşir. Bir iyon değişim zarı,

hücrenin anot ve katot bölmelerini ayırır ve sadece sodyum iyonlarının ve az miktarda suyun içinden geçmesine izin verir. Böylece klorür iyonları anotta oksitlenerek klor gazı üretilir ve su katotta hidroksit iyonlarına ve hidrojen gazına indirgenir. Ek olarak, katot bölmesinde sodyum hidroksit oluşur.

Deneysel işlem, membran hücreli klor-alkali işlemine dayanmaktadır. Sistem bileşenleri kontrol edildikten sonra çalışma sıcaklığında elektrolit hazırlığının ardından deneylere başlandı. Deneyler doğrudan membran kuru iken başlatıldığında, uygulanan voltajla uyumsuz olarak birkaç saat boyunca tutarsız devre akımı gözlendi. Bu sorunu aşmak için membranın bir gün öncesinden elektrolit içinde tutulmasının faydalı olduğu görülmüştür. Deneysel çalışmalar sırasında, uygulanan hücre voltajı ve ortaya çıkan akım ile dereceli silindirdeki hidrojen seviyesi zamana göre izlenmiş ve kaydedilmiştir. Tutarlılığı ve güvenilirliği artırmak için her deney tekrarlanmıştır.

Kütle akış hızı, çalışma sıcaklığı ve hücre voltajı gibi parametreler değiştirilerek deneylere devam edilmiştir.

Bu deneysel parametreler şunlardır:

• Kütle akış hızı: 0,3 g/s, 0,5 g/s, 0,7 g/s.

• Çalışma sıcaklığı: 25 °C, 45 °C, 60 °C.

• Hücre voltajı: 2,5 V, 3 V, 3,5 V.

Anot bölmesine giren tuz çözeltisinin (NaCl, KCl ve $CaCl_2$) türüne bağlı olarak, membran sadece pozitif iyonların (Na^+, K^+ ve Ca^{2+}) anot bölmesinden katot bölmesine geçmesine izin verir. Böylece katot bölmesinden hidrojen gazı (H_2) salınır ve membrandan geçen pozitif iyonun türüne bağlı olarak Sodyum Hidroksit (NaOH), Potasyum Hidroksit (KOH) ve Kalsiyum Hidroksit ($Ca(OH)_2$) çözeltileri oluşur. Üretilen hidrojen gazının hacmi, dereceli silindir yardımıyla hacimsel yer değiştirme tekniği ile ölçülür. Öte yandan, anot bölmesinde klor gazı, klorat ve hipokloröz asit gibi büyük miktarda klor bazlı kimyasal türler indirgenmek üzere bulunmaktadır. Anot bölmesinde klor gazı deşarjı için uygun elektrot kullanılmalıdır.

K, Na ve Ca metallerinin aktivite sıralarına göre belli bir süre içinde en fazla hidrojeni KCl tuz çözeltisi, en az hidrojeni ise $CaCl_2$ tuz çözeltisi üretmiştir. Çalışma sıcaklığının, hücre voltajının ve kütle akış hızının her birinin tek tek arttırılması, her üç tuz türü için de hidrojen üretimini arttırdı. Hidrojen üretimi için voltaj artışı kütle akış hızından daha etkiliydi. Artırılan voltajla birlikte iyon hareketi de arttığı için daha fazla hidrojen üretildi.

25 °C çalışma sıcaklığında 0,3 g/s kütle akış hızı ve 2,5 V hücre voltajı ile $CaCl_2$ tuz çözeltisi kullanıldığında minimum hidrojen üretim hızı 27,36 mL/saat olmuştur. 60 °C çalışma sıcaklığında 0,7 g/s kütle akış hızı ve 3,5 V hücre voltajı ile KCl tuz çözeltisi kullanıldığında maksimum hidrojen üretim hızı 295,68 mL/saat olmuştur.

ACKNOWLEDGMENTS

I would like to express my sincere gratitude to my supervisor Prof. Dr. Mehmet KARAKILÇIK for giving me the great opportunity to work on this interesting project at Çukurova University. I also appreciate his steady guidance and encouragement throughout my PhD study.

I would like to especially thank my dissertation committee members Prof. Dr. Süleyman ÇABUK, Prof. Dr. Hüseyin AKILLI, Prof. Dr. İsmail BOZKURT, and Assoc. Prof. Dr. Hacı SOĞUKPINAR for their constructive support.

I wish to thank the Scientific Research Project Unit of Çukurova University for financially supporting this thesis (FDK-2017-7005).

TABLE OF CONTENTS **PAGE**

LIST OF TABLES **PAGE**

LIST OF FIGURES **PAGE**

LIST OF ABBREVIATIONS

CA	: Chlor-Alkali
CE	: Current Efficiency
CEM	: Cation Exchange Membrane
CNC	: Computer Numeric Control
DC	: Direct Current
EES	: Engineering Equation Solver
GHG	: Greenhouse Gas
HHV	: Higher Heating Value
PS	: Power Supply
PV	: Photovoltaic
PV/T	: Photovoltaic Thermal
UV	: Ultraviolet

NOTATIONS

A	: Area (m^2)
E	: Energy (kJ)
$\dot{E}$	: Energy rate (kW)
E°	: Decomposition voltage (V)
ex	: Specific exergy (kJ/kg)
Ex	: Exergy (kJ)
$\dot{E}x$	: Exergy rate (kW)
F	: Faraday constant (9.6485 x 10^4 C/mol)
g	: Gravitational acceleration (9.80665 m/s2)
G	: Gibbs free energy (kJ)
h	: Specific enthalpy (kJ/kg)

H : Enthalpy (kJ)

i : Current (A)

J : Current density (A/m^2)

K : Electrical conductivity ($ohm^{-1}.m^{-1}$)

m : Mass (kg)

$\dot{m}$: Mass flow rate (kg/s)

N : Normality

n : Number of moles (mol or kmol)

P : Pressure (kPa)

Q : Heat (kJ)

$\dot{Q}$: Heat transfer rate (kW)

R : Universal gas constant (8.314 kJ/kmol-K)

s : Specific entropy (kJ/kg.K)

S : Entropy (kJ/K)

$\dot{s}$: Entropy rate (kW/K)

t : Time (s)

T : Temperature (°C or K)

v : Velocity (m/s)

V : Voltage (V)

W : Work (kJ)

$\dot{W}$: Work transfer rate (kW)

z : Altitude (m)

Greek Symbols

Δ : Change

η : Efficiency

σ_M : Thickness of the membrane

Subscript and Superscripts

A	: Anode
C	: Cathode
cv	: Control volume
d	: Destruction
en	: Energy
env	: Enviroment
ex	: Exergy
in	: Inlet stream
ke	: Kinetic
mix	: Mixture
out	: Outlet stream
pe	: Potential
ph	: Physical
pro	: Produced
u	: Internal

1. INTRODUCTION

Energy use, which is an indispensable element of daily life and an indicator of industrialization, is the primary problem of countries. In parallel with the increase in population and industrialization, the energy needs of countries are also increasing. Since non-renewable energy resources will be depleted in the future, many countries are looking for ways to use their energy resources with high efficiency without wasting them, on the other hand, they are trying to benefit more from the potential of renewable energy resources, especially solar and wind energy. Although it significantly increases environmental problems, a large part of the world's energy needs is obtained from fossil fuels today. To minimize the dependency of countries such as Türkiye with no or insufficient fossil fuel reserves and to prevent environmental disasters, it has become a necessity to identify renewable energy sources and to search for ways to benefit from them with high efficiency. Therefore, it is of great importance that a clean energy source that can be produced using renewable energy sources replaces fossil fuels as soon as possible. The properties sought in a clean energy source can be listed as carbon-free, inexhaustible, light, storable, safe to transport, high calorific value per unit mass, easily converted to other types of energy, and economical. Considering these features, hydrogen stands out as the fuel of the future. Hydrogen is a clean fuel that can be produced, stored, and transported by various methods.

Hydrogen is an odorless and colorless gas at normal temperature and pressure. When the hydrogen combustion process takes place, a significant amount of energy is obtained with water. In 1781, Cavendish has determined this process experimentally. The density of hydrogen, the simplest element in the universe, is 1/14 compared to air and 1/9 compared to natural gas. The density of hydrogen, which becomes liquid when cooled to –253 °C under atmospheric pressure, is 1/10 of gasoline. Hydrogen, the basic substance of stars and planets, is found in more than 90 % of the universe. The fuel of the sun and other stars is hydrogen, and it is

the main energy source of the universe. Table 1.1 shows the particular properties of hydrogen and some other fuels (Noor et al., 2013).

Table 1.1. Specifics of some fuels.

Fuel	Molar mass (g/mole)	Specific heat (MJ/kg)	Density (kg/m^3)
Hydrogen	2.01	141.8	0.0899
Natural gas	18	50	0.8
Gasoline	100-110	47.3	719.7
Diesel	170-200	44.4	832

While a hydrogen atom normally has one proton and one electron, one of the 5000 hydrogen atoms has a neutron in its nucleus. The hydrogen atom in this state is called deuterium. The water obtained by enriching deuterium and combining it with oxygen is called 'heavy water'. It is used as a moderator in nuclear reactors to slow down the neutrons released during the fission of uranium. Another much less common isotope of hydrogen is tritium which has two neutrons in its nucleus. Radioactive tritium is used to make a hydrogen bomb.

1.1. Storage of Hydrogen

A suitable method for storing large amounts of energy has not yet been found. If it were possible to store the electricity produced from hydroelectric power plants, it would be possible to solve the energy problem to some extent. This storage problem seems to be overcome by the underground hydrogen storage method. Perhaps the cheapest method of storing hydrogen gas is to store it in underground geological areas such as depleted oil or natural gas reservoirs, aquifers, and salt caverns (Karakilçik and Karakilçik, 2020). Another form of storage, which is somewhat expensive, is to store it in caves in mines. The most used method for medium or small-scale storage is to hold liquefied hydrogen in

steel tubes under high pressure. However, this application is seen as a very expensive method for large quantities. Another practical solution is to store liquid hydrogen in low-temperature tanks. Liquid hydrogen used as rocket fuel in space programs is stored with this method. The largest liquid hydrogen tank in the world is at Kennedy Space Center and can hold 3400 m^3 of liquid hydrogen. The energy value of this amount of hydrogen as fuel corresponds to 29×10^6 MJ or 8×10^6 kWh. Another important property of hydrogen is that it can easily react exothermically with some metals and alloys and return to its hydride form in large quantities. To better store hydrogen, studies on various metal alloys continue today. The necessary conditions for the best storage can be listed as follows:

- The metal or alloy should be fairly cheap.
- It should store the most hydrogen per unit volume.
- The metal should react readily with hydrogen to form hydrides and should be stable at room temperature.
- Hydrogen gas must be able to separate from the metal at a very high temperature and a certain pressure.

Among the most studied and promising alloys are Lanthanum-Nickel ($LaNi_3$), Magnesium-Nickel (Mg_2Ni) and Iron-Titanium ($FeTi$). The molecular formulas of these alloys showing the hydrogen storage amounts can also be written as $(LaNi_3)H_6$, $(Mg_2Ni)H_4$ and $(FeTi)H_2$. In addition to these alloys, studies have also been carried out on the hydrogen storage performance of nano-doped metal hydrides (Luo et al., 2020). On the other hand, due to its flammable and explosive nature, hydrogen storage is a process that requires extreme attention and security measures at the highest level. Singla et al. (2022) have addressed hydrogen production techniques and emphasized that the storage and using of

hydrogen is a serious process regarding security. They have mentioned safety measures in the storage of hydrogen due to its inflammability.

1.2. Transport of Hydrogen

Hydrogen gas can be transported easily and safely through pipes like natural gas. It is also possible for natural gas pipe networks to be used in hydrogen with little change in the future. Today, hydrogen is transported by pipelines with a length of 80 km in Texas, USA, and 204 km in the Ruhr basin in Germany. Mijim et al. (2020) have studied probabilistic design factors for pipes used for hydrogen transportation through urban and rural areas. This method includes a risk equation obtained from the probabilities of some failures such as leakage, ignition, lethal effects, etc. In addition to pipelines, hydrogen can also be transported by tankers as pressurized gas or by liquefying. Liquefied hydrogen placed in double-layered insulated tanks with a volume of 25 m^3 can be transported by road and liquefied hydrogen put into tanks with a volume of 130 m^3 can be transported by rail. Today, thousands of tons of crude oil that leak from oil tankers or spill into the seas as a result of accidents cause irreparable damages. There are also large energy losses in electrical energy distribution lines. Since natural gas and oil reserves are located in certain regions, they require high investment costs as they have to be transported to other countries by pipelines of thousands of kilometers. Since hydrogen can be produced locally everywhere, there is no need for very long pipelines.

1.3. Use of Hydrogen as a Fuel

Fuel can be used in many areas, including industry, homes, vehicles, etc. When other fuels are examined, we see that most of them can only be used for certain applications. For example, it is not practical to use coal in automobiles and airplanes. However, hydrogen can easily be used in oven and heating systems instead of natural gas, vehicles instead of gasoline as well as power rockets. It is also possible to convert it into electricity in fuel cells. In recent years, great

progress has been achieved as a result of intensive studies on fuel cells. The fact that hydrogen can be used instead of gasoline in vehicles also attracts the attention of vehicle manufacturing companies. Hydrogen-fueled engines have many advantages over gasoline engines. One of them is the high efficiency of hydrogen engines, and the other, perhaps most importantly, is that they mainly produce water vapor instead of harmful waste. Hydrogen can be used instead of gasoline in internal combustion engines, as well as to generate electricity with fuel cells and power vehicles with electric motors. The main problem to be solved here is the safe storage of hydrogen in vehicles. Due to the limited availability of oil and increasing environmental pollution, this problem must be solved. Despite the many advantages of hydrogen fuel cell systems, Foorginezhad et al. (2021) have drawn attention to the safety issues associated with possible leakage, fire, and explosion. They have also presented a comprehensive review of safety issues with hydrogen fuel cell vehicles.

1.4. Use of Hydrogen in Industry

It is seen that hydrogen, which is very important in the industry, is produced in large quantities and widely used in many areas from margarine making to metal processing. The main areas where hydrogen is used in industry are listed below.

1.4.1. Catalytic Hydrogenation

It is the process of adding hydrogen (H_2) to organic compounds under pressure and with the help of a catalyst.

- Ammonia synthesis
- Methyl alcohol synthesis
- Solidification of vegetable oil
- Obtaining alcohol from fatty acids

- Synthetic yarn production
- Pharmaceutical production

1.4.2. Hydrogen in Metallurgy

- Reducing agent
- Welding flame
- Tungsten and molybdenum extraction
- In the preparation of metal hydrides

1.5. Hydrogen Production

Today, reserves of fossil fuels are used rapidly at the expense of polluting the environment. Since these reserves will be depleted soon, the search for new and clean fuel sources continues intensively. It is seen that humanity, which used resources such as wood, water, wind, and sun in the periods before fossil fuels, will start to use them again as the main energy source with different technologies and more efficiently soon. Today, it is accepted by all scientists that the most advanced and only energy source that can provide the world's increasing energy needs is the solar-hydrogen system. Producing hydrogen from water via electrolysis with renewable energy sources is the right choice. Hydrogen, which is produced with all kinds of primary energy sources, is used in various fields such as artificial fertilizer, vegetable oil, and rocket fuel. For this, 600 billion cubic meters of hydrogen are produced every year in the world. While describing hydrogen production methods, it would be appropriate to specify the primary energy sources that can be used. Accordingly, hydrogen can be produced with the help of fossil fuels, as well as with all of the primary energy sources such as sun, wind, wave, geothermal, and biomass, by any of the methods described following.

1.5.1. Fossil Fuel Methods

Most of the hydrogen used in industry today is obtained from fossil fuels such as natural gas, petroleum products, or coal. The most commonly used methods are catalytic steam reforming of natural gas, partial oxidation of petroleum, and coal gasification. Longden et al. (2022) emphasized that the process of producing hydrogen from fossil fuels causes greenhouse gas emissions (GHG) even if the released carbon is tried to be controlled. They have also stated that electrolysis with renewable energy could become cheaper than fossil fuel soon. In addition to the fossil fuel methods, although the main purpose is not hydrogen production, there are also methods where hydrogen is obtained as a by-product during the production of other industrial materials. For example, hydrogen gas is produced in the refining process of crude oil, in the baking process of coal for coke production as well as the Chlor-alkali process.

1.5.2. Electrolysis of Water

The process of splitting water into hydrogen and oxygen using direct current is called electrolysis. It is known as the simplest method for hydrogen production. In principle, an electrolysis cell contains two electrodes and a conductive liquid called an electrolyte in which they are immersed. Nickel-plated steel electrodes are used in electrolysis cells used in practice. When a direct current source is connected to these electrodes, current will flow from the positive electrode to the negative electrode in the conductive liquid. As a result, hydrogen gas will come out from the cathode and oxygen gas from the anode. However, since water is not a good conductor, a substance such as potassium-hydroxide is usually added to increase the conductivity. Ideally, 1.23 V is sufficient for the electrolysis of water at normal pressure and temperature. However, higher voltage is used in the electrolysis process due to voltage losses in the electrolysis components. Therefore, in practice, the voltage applied per electrolysis cell for the separation of water is usually around 2 V. Theoretically, 2.8 kWh of electrical energy is sufficient for

each cubic meter of hydrogen, but due to voltage losses, the amount of electrical energy used in practice varies between 3.9-4.6 kWh for one cubic meter of hydrogen production. Accordingly, the efficiency of the electrolysis process is around 70 %. However, 90 % efficiency has been achieved in recent years thanks to the studies and developing technology in this field.

1.5.3. Thermochemical Method

The efficiency of converting primary energies from fossil or nuclear fuels to hydrogen by electrolysis depends on how efficiently electrical energy is produced from these fuels. Electricity generation efficiency is around 38 % for modern fossil fuel plants and 32 % for nuclear plants. Considering that the electrolysis cell operates at 80 % efficiency, the total efficiency of obtaining hydrogen from fossil fuels by electrolysis is 25-30 %. It is possible to obtain higher efficiency when the heat energy generated during electricity production is used for the separation of water. However, a temperature of at least 2500 °C is required for the separation of water with this method. Here, instead of a single-step thermo-chemical process, several-step processes are required. As a result of the studies carried out in this field, the required temperature in multi-step thermochemical processes was reduced to 950 °C and the total efficiency was found to be 50 %. Safari and Dincer (2020) express that thermochemical cycles are promising technologies for clean and sustainable hydrogen production. They have discussed and comparatively evaluated the various hydrogen production methods through thermochemical and hybrid cycles, including two-step (Zinc oxide), three-step (Sulfur-Iodine), four-step (Iron-Chlorine, Magnesium-Chlorine, and Copper-Chlorine), and hybrid types (Hybrid Sulfur). In addition, they have analyzed the major challenges, recent advancements, and future directions of these methods.

1.5.4. Solar-Hydrogen System

The production of hydrogen using solar energy is of great importance both in terms of the environment and the economy. Even if we put aside the environmental harm that fossil-based fuels cause due to carbon emissions, the fact that they will run out soon has led people to seek new sustainable and clean energy. For this purpose, intensive studies have been carried out on the solar-hydrogen system in recent years. The solar-hydrogen system is an extremely clean and safe energy production method with a lower carbon footprint. This fact is seen when compared with fossil-based fuels in terms of pollutants. The conversion of solar energy into useful energy can be divided into two parts thermal and photonic. In heat treatment, the heat energy obtained from the sun can be used in various heating processes as well as converted into mechanical or electrical energy with different cycles. In the photonic process, photons are directly absorbed by a semiconductor absorber and converted into electrical energy. Photons are also used in the formation of biomass through photosynthesis. As in all conversion processes, it is important to know what the losses are to increase the solar-hydrogen efficiency. Song et al. (2022) have provided a comprehensive review of solar-hydrogen production processes including photocatalytic, photoelectrochemical, photovoltaic–electrochemical, solar thermochemical, photothermal catalytic, and photobiological technologies. They have evaluated these processes regarding efficiency, durability, economic viability, and environmental sustainability. They have also mentioned the problems that may be encountered for solar-hydrogen production in the future.

To obtain hydrogen using solar energy, one of the following fundamental methods may be used.

- Photochemical systems
- Semiconductor systems
- Photobiological systems

1.5.4.1. Photochemical Method

After obtaining hydrogen and oxygen in the cell using titanium dioxide (TiO_2) coated electrodes, which were first developed by Fujishima and Honda (1972), a great development has been experienced in this field. This method uses the ultraviolet (UV) region of direct solar energy to decompose water into hydrogen and oxygen, without the need for high temperatures or electricity. Although UV radiation from the sun has enough energy to directly decompose water, very little of it can come to earth because they are absorbed in large quantities by the ozone layer in the atmosphere. Therefore, for the photochemical method, it is necessary to strengthen these radiations or increase their absorption by water. For this, the UV effect is increased by adding some minerals and metals to the water with a set of devices that intensify the solar radiation. Although this method is not very efficient, it is cheaper than other methods. Xing et al. (2013) stated that it is a very promising way to produce clean hydrogen fuel by decomposing water under sunlight in the presence of a semiconductor photocatalyst. They also emphasized that while scientists are making efforts to discover new semiconductor materials suitable for photoelectrochemical and photochemical systems, less attention has been paid to the design of photocatalytic reaction systems or reactors. Ahmad et al. (2015) revealed that there is a great interest in producing hydrogen from solar energy, and many studies have been carried out to develop photocatalysts that work not only under ultraviolet light but also under visible light, to use solar energy efficiently. One of the best-known photocatalysts used in the last four decades is TiO_2. Although it has excellent properties as a photocatalyst, TiO_2 also have some disadvantages such as a wide band gap, high potential for hydrogen production, and rapid assembly of photoelectron-hole pairs. To overcome these disadvantages, methods such as adding sacrificial substances such as methanol to the solution, combining TiO_2 with carbon materials, removing the particles accumulated on the surface with

various absorbents, using dyes, doping TiO_2 with non-metallic elements such as carbon, sulfur and boron are applied.

1.5.4.2. Semiconductor (solar-cell) Systems

In these systems, hydrogen production with solar energy is carried out in two steps. In the first step, direct electric current (DC) is obtained using solar cells made of semiconductors. Solar cells, which consist of many photovoltaic (PV) cells, are semiconductor systems that directly convert solar energy into electrical energy. The electrical current produced in this way is delivered to the electrodes of an electrolysis cell, and the water is decomposed into oxygen and hydrogen. When the efficiency of solar cells is 15 % on average and the electrolysis cell efficiency is 80 % on average, it can be said that hydrogen can be produced with remarkable efficiency. It is clear that if the efficiency of solar cells can be further increased, the overall efficiency will also increase. Considering that two-thirds of our world is covered with water and the solar energy falling on the world every day is greater than the total energy used in a year, the size of the potential that emerges is promising for the future. Zafar and Dincer (2014) proposed and analyzed a combined renewable energy system consisting of a photovoltaic-thermal (PV/T) panel, electrolyzer, and fuel cell that produces electricity, hydrogen, and pure water. While some of the electricity produced by PV/T and the cooling water flowing through it are sent to domestic use, the remaining part of the electricity is stored by producing hydrogen with the help of an electrolyzer. In cases where the need for electricity increases, the stored hydrogen is sent to the fuel cell to produce electricity and pure water. Energy, exergy, and economic analyzes were performed to analyze the performance of the system under different operating conditions. Bhattacharyya et al. (2017) designed and analyzed a system that produces hydrogen by alkaline water electrolysis using electricity generated by a photovoltaic (PV) panel. Since the amount of electricity required for electrolysis depends on the hydrogen production rate and operating conditions, PV power

system design and analysis for an electrolysis-based hydrogen production cell also become important. According to the calculations, approximately 60 kW is required for an average hydrogen production of 10 m^3/h at 70 °C and 5 bars.

1.5.4.3. Photobiological Systems

Photosynthetic organisms have a mechanism that harvests and store large amounts of solar energy. Normally, when photosynthetic systems convert carbon dioxide and water to carbohydrates, they give off oxygen but not hydrogen directly. But green algae and cyanobacteria are unicellular photosynthetic organisms that possess the enzymatic equipment for photosynthetic hydrogen production. It was found that as a result of the incubation of green algae in an airless environment, hydrogen was produced with approximately 10 % yield. A study by Greenbaum and Lee (1997) showed that yields approaching 15-20 % may be possible in some mutants such as "Chlamydomonas reinhardtii". In recent years, extensive research has been done on photobiological hydrogen production by green microalgae, and Chlamydomonas reinhardtii microalgae have emerged as one of the most promising eukaryotic hydrogen producers (Torzillo et al. 2015). Besides bacteria that produce hydrogen directly, other types of bacteria produce biogas from waste. Biogas is an important form of energy and can be used in many fields. Safari and Dincer (2019) discussed the energy and exergy analyzes of a combined system based on the anaerobic digestion of sewage sludge from a wastewater treatment plant for multiple productions. The useful outputs of this system are fresh water, heat, power, and hydrogen. To increase efficiency in the system, recovery methods such as generating electricity with organic Rankine cycle (ORC) using waste heat are also used. Most of the electricity produced in the system is provided by the open-air Brayton cycle powered by biogas produced by the digestion process. In case of excess electricity generation in the system, a proton exchange membrane (PEM) electrolyzer is used to produce hydrogen by the electrochemical method. The energy and exergy efficiencies of the proposed system are 63.6 % and 40 %,

respectively, and the amounts of power, hydrogen, and fresh water produced are 1102 kW, 0.94 kg/h, and 0.347 kg/h, respectively.

1.5.5. An Overview of Integrated Hydrogen Production Systems

It is also possible to establish integrated systems in which more than one hydrogen production method is used together to increase hydrogen production efficiency and to benefit from various energy sources in the same system. Acar et al. (2018) emphasized that hydrogen, which is considered the basic component of energy systems for a sustainable future, should be produced in a clean, reliable, cost-effective, and safe manner without harming the environment and society. However, according to the literature review, there is a lack of studies focusing on a complete technical, environmental, social, and economic evaluation of hydrogen production systems when reliability is taken into account. Therefore, they have conducted a comprehensive study and research on the types of electrolysis, nuclear and solar thermochemical water separation cycles, and photoelectrochemical cells, to provide comprehensive knowledge to the people involved in this business. To overcome the hesitations observed in the preferences of the decision-makers about which system to apply, a new approach, the hesitant fuzzy method, was used to evaluate the sustainability of the selected hydrogen production methods. This method is applied in some uncertain situations, by highlighting some criteria that are thought to be effective in the system and evaluating their effects on the system. In this study, economic performance (investment cost and operating cost), environmental performance (Greenhouse gas emissions, land use, solid and liquid waste), social performance (impact on public health, employment and education opportunities, and public acceptance), technical performance (energy and exergy efficiency, process control and raw material input) and usability/reliability (dependence on imported resources, predictability and scalability) were taken into consideration. The results showed that grid electrolysis will come to the fore in sustainable hydrogen production soon and that the technologies of other methods

are also advancing and the associated costs are decreasing. Yilmaz et al. (2016) emphasized that using solar energy instead of fossil sources for hydrogen production is the most appropriate option and compared and discussed the advantages and disadvantages of four different solar hydrogen production methods. The first method studied is photoelectrolysis. In this method, water is decomposed into hydrogen and oxygen with the help of a semiconductor material under direct sunlight. Secondly, water is decomposed into hydrogen and oxygen by the electrolysis method of water using the electricity produced under the sunlight with the photovoltaic panel. Third, some microorganisms produce hydrogen under sunlight and in a suitable environment by a photo-biological method. Fourth and lastly, it is the thermal decomposition method, which is the direct separation of water into hydrogen and oxygen at a temperature of about 2500 K under concentrated solar energy, that is, thermolysis. According to these methods, it is emphasized that the most important advantage of these methods is that no or very little greenhouse gas is emitted during solar-based hydrogen production. Karapekmez and Dincer (2020) designed and analyzed a new system equipped with renewable energy-based multiple generation units for heating, drying, cooling, domestic hot water, electricity, and hydrogen production. Electricity generation in the system is provided by a large number of parabolic solar collectors and an organic Rankine cycle fed by geothermal resources. It was also emphasized that it would be a logical way to produce hydrogen with the help of an electrolyzer from hydrogen sulfide (H_2S), which is released from geothermal power plants and can cause adverse effects on the environment. To analyze the system performance, the effects of various parameters such as ambient temperature, inlet mass flow rate of geothermal steam, and water inlet temperature on the efficiency were investigated and the results were discussed comparatively. Acar and Dincer (2019b) examined various hydrogen production sources and systems and some hydrogen storage options in detail and compared the economic, environmental, social, and technical performances and reliability of the options discussed in detail. The sources of

hydrogen production under consideration are biomass, geothermal, hydro, nuclear, solar, and wind; hydrogen production methods are biological, thermal, photonic, and electrical; hydrogen storage systems are also chemical hydrides, compressed gas, cryogenic liquid, metal hydrides, and nanomaterials. Obtained results;

- In terms of environmental performance, the solar option appears to be the most advantageous hydrogen production source with a ranking of 8/10, while nuclear is in the last place with a ranking of 3/10.
- Considering all of the economic, environmental, social, technical, and reliability criteria as an average, the wind has the highest performance ranking (7.40/10), while geothermal has the lowest (4.60/10).
- In the comparison of hydrogen production systems in terms of environmental performance, photonic systems have the highest ranking (8/10) and thermal systems have the lowest ranking (5/10).
- Considering all the performance criteria, electric hydrogen production systems have the most advantageous (7.60/10), while biological systems have the lowest ranking (4.80/10).
- Among the hydrogen storage options, nanomaterials have the most advantage in terms of environmental performance (9/10) and cryogenic liquid has the lowest ranking (3/10).
- Considering all performance criteria, nanomaterials have the most advantage in terms of hydrogen storage (8.40/10), while cryogenic liquid has the lowest overall average (3.40/10).

As a result, it has been emphasized that the method of electrical (such as photoelectrochemical) hydrogen production based on solar energy and hydrogen storage with nanomaterials can be the most harmless and sustainable option for the environment.

1.5.6. A Brief Assessments of Some Hydrogen Production Systems

Hydrogen can be produced from a wide range of feedstock including both fossil and non-fossil-based materials via different technologies. Steam reforming and gasification technologies are the most mature hydrogen production technology today. Currently, a great amount of hydrogen is produced through steam reforming, gasification, and partial oxidation technologies using fossil fuels. But these technologies have a drawback as carbon emissions. Therefore, the hydrogen production process by the electrolysis method of water using electricity produced from renewable sources is gaining importance day by day. Photobiological methods are also an important method for the environment as they produce carbon-free hydrogen. A chlorine-alkali process, the main goal of which is to produce chlorine gas, is an extremely strategic process because both important chemicals and hydrogen are produced.

Many hydrogen production technologies still have some drawbacks namely high energy consumption and carbon emissions. Therefore, continuous research is needed to develop new technologies to overcome these problems.

Table 1.2 shows some hydrogen production technologies and their efficiencies (source: El-Shafie, M., Kambara, S., Hayakawa, Y., 2019).

Table 1.2. The hydrogen production technology efficiencies.

Technology	Feed stock	Efficiency	Maturity
Steam reforming	Hydrocarbons	70-80 %	Commercial
Partial oxidation	Hydrocarbons	60-75 %	Commercial
Ammonia decomposition	Ammonia	28.3 %	Near term
Biomass gasification	Biomass	35-50 %	Commercial
Photolysis	Sunlight+H_2O	0.5 %	Long term
Alkaline electrolyzer	Electricity+H_2O	50-60 %	Commercial
PEM electrolyzer	Electricity+H_2O	55-70 %	Near term
Photoelectrochemical water splitting	Sunlight+H_2O	12.4 %	Long term

1.6. Importance and Purpose of the Study

Environmental pollution and global warming caused by the use of fossil resources have led to the shift of studies in the field of energy production to the side of renewable and clean energy sources in recent years. Therefore, much research is carried out on the production, storage, and transportation of hydrogen, which is accepted as an energy carrier in the future. For hydrogen to be the most important energy carrier in the future, it must be produced using renewable energy sources. In addition, safety problems during storage, transportation, and use must be overcome. It is possible to store and transport hydrogen as a compressed gas or liquefied in a smaller volume. However, it should not be forgotten that the liquefaction of hydrogen requires high energy consumption and advanced cooling techniques. There are many methods used in the production of hydrogen. In these methods which require electrical energy and heat, renewable energy sources such as solar, wind, and hydroelectricity as well as waste heat of nuclear power plants can be utilized. In addition, the Chlor-alkali process, which is currently used extensively, can also be considered one of the hydrogen production methods.

The Chlor-alkali process is a widely used electrolytic process that produces mainly chlorine and caustic soda as well as hydrogen. This method can be called killing three birds with one stone, not two. However, this study focuses only on hydrogen production. There are three electrolytic processes for producing Chlor-alkali: the diaphragm cell process, the mercury cell process, and the membrane cell process. Detailed explanations about the Chlor-alkali processes are given in section 3.1. While chlorine and caustic soda are produced in Chlor-alkali processes, high-quality hydrogen is already produced with a lower carbon footprint. But, while 80 % of the total hydrogen produced by the members of Eurochlor (It is the association of chloralkali plant operators in Europe) in Chlor-alkali processes is used, the rest is vented into the atmosphere because there is not enough use area (Chlor-Alkali Industry Review 2019-2020). In China, approximately 1.8 billion m^3 of hydrogen produced in the industrial Chlor-alkali process is wasted each year. In

the USA, nearly 40 %-50 % of the hydrogen produced in the Chlor-alkali process is burned for industrial heat processes, while 30 %-40 % is sold to the commercial hydrogen market. The remaining 10 %-30 % is vented into the atmosphere Li et al. (2021). Unfortunately, these are a very significant waste of energy.

Hydrogen produced with renewable energies has the potential to contribute to the decarbonisation of various sectors. So, hydrogen from Chlor-alkali can be a low-carbon option for industrial processes. Sodium chloride (NaCl) is used in industrial Chlor-alkali applications dominantly. Although it is a mature technology, there is no information in the literature that other types of salts are used in the Chlor-alkali process. These are the driving force of this study.

The purpose of the present study is to investigate the hydrogen production performances of potassium chloride (KCl) and calcium chloride ($CaCl_2$) as well as sodium chloride (NaCl) using the membrane cell method experimentally. In addition, energy and exergy performance analyses are also made on the hydrogen production of the system using the Engineering Equation Solver software (EES, version 2020).

The particular objectives of the present study are:

- To carry out mass, energy, entropy, and exergy balance equations for the reactor.
- To investigate hydrogen production performance depending on the mass flow rate, operating temperature, and cell voltage.

2. LITERATURE REVIEW

In recent years, diaphragm cell and mercury cell methods that use asbestos and mercury, which are known to be harmful to the environment, have been avoided for Chlor-alkali processes. Nowadays membrane cell method is a dominant Chlor-alkali process with its energy efficiency and environmentally benign. Therefore this study is conducted on the membrane cell Chlor-alkali process. So, the relevant literature reviews for the membrane cell method are presented as follows.

Due to its increasing importance in recent years, many researchers have done extensive research on membrane cell Chlor-alkali technology.

Hofmann et al. (2022) conducted a study on electricity consumption in Chlor-alkali processes in Germany. For the operation of the Chlor-alkali electrolysis, direct current is required in general at a voltage of 3 V per cell. When a sufficient amount of aqueous sodium chloride solution is electrolyzed, 1000 kg of chlorine, 1128.3 kg of sodium hydroxide, and 316.3 m3 of hydrogen are produced corresponding to a consumption of 2.58 MWh power. Since chlorine and hydrogen are highly reactive they need to be separated during the Chlor-alkali process by a cation-exchange membrane to avoid explosive reactions. Na^+ ions can easily pass through the membrane. Conversely OH^- and Cl^- are only able to pass in small quantities. The addition of hydrochloric acid to the anolyte compartment enhances the chlorine quality and reduces oxygen evolution. Madaeni and Kazemi (2008) used reverse osmosis and nanofiltration membranes to remove polluting ions such as Fe^{2+}, Mg^{2+}, Ca^{2+} and SO_4^{2-} in saturated brine. For this purpose, they have used seven polymeric membranes (FT30, PVD, DOW-PS, TFC-SR, BW30, 37100, and NF45) to treat the saturated brine. They have seen that the PVD membrane has the best performance with moderate flux, appropriate removal of impurities, and minimum NaCl rejection at 8 bars and 40 °C. In addition, it was found that the

NF45 membrane performed well in removing Fe^{2+} ion, while the DOW-PS membrane performed best in removing SO_4^{2-} ion. Jalali et al. (2009) investigated various parameters affecting cell voltage and current efficiency of a laboratory-scale Chlor-alkali reactor at low caustic concentrations (5-22 g/L). The parameters whose effects were examined were the anolyte pH value (2-5), cell temperature (25-90 °C), electrolyte mass flow rate (2.2-8.4 cm/s), brine concentration (200-300 g/L), and current density (1-4 kA/m^2). In the reactor, DSA-Cl_2 was used as the anode electrode, nickel as the cathode electrode, and Flemion® 892 as the membrane. It has been found that the most affecting parameters of the cell voltage are current density and cell temperature. According to the results obtained from the voltage balance analysis, the effects of the membrane, nickel cathode, and catholyte liquid on the cell voltage were found to be high. The effect of other components was also found to be small. It was also found that the measured and predicted cell voltages converged at higher current densities. Taguchi and ANOVA techniques were used for experimental design and data analysis, respectively. Taguchi is a method that aims to minimize the variability in the experimental result by using the most appropriate combination of controllable variables to minimize the effect of uncontrollable variables in any experiment. ANOVA, on the other hand, is a statistical analysis method known as the analysis of variance. Rabbani et al. (2014a) experimentally investigated the effects of different process parameters on hydrogen, chlorine, and sodium hydroxide production in a newly designed multi-membrane Chlor-alkali reactor. The process parameters in this study are the applied cell voltage varying between 3 V and 20 V, the concentration of brine entering the anode chamber varying between 150 g/L and 225 g/L, and the concentration of base entering the cathode chamber varying between 35.3 g/L and 58.8 g/L, electrode surface area, cell temperature, and different anode materials (copper, aluminum, nickel, steel, and graphite). Analysis of variance (ANOVA), a statistical method, was used to see the effect of each processing parameter. The results showed that graphite is the most stable anode material, brine and electrolyte

concentration values do not affect the production rate of the products, increasing the cell temperature increases the production, but also causes a decrease in both energy and exergy efficiency because it increases the energy input to the system. They also showed that changing the electrode surface area changes the current density, which has a significant effect on the hydrogen generation rate, and the efficiency increases in the case of low cell voltage. Safizadeh et al. (2015) researched the development of efficient electrocatalysts in systems containing alkaline solutions. Efficient electrocatalysts should be low cost and at the same time show good catalytic activity and high corrosion resistance, creating a low cell potential for hydrogen production. Amorphous alloys meet these desired properties because they have many properties such as high corrosion resistance, electrochemical, and good mechanical properties. On the other hand, some pure metals and some rare earth elements are also discussed as alloyed composites. Particular emphasis was placed on the electrodeposition method used in the preparation of alloys for Chlor-alkali industry applications. Budiarto et al. (2017) have expressed that energy consumption is a major production cost for the Chlor-alkali industry. To overcome this problem, they proposed to develop a model that predicts the voltage and current density of the cell for process dynamics. For this purpose, a material balance model (sodium ion balance, hydroxide ion balance, and chloride balance) and voltage balance for the Chlor-alkali process were developed and studied. The results showed that chlorine production with high current density also increases energy costs. Franco et al. (2019) stated that in an industrial Chlor-alkali membrane system, the cell current has to be recorded continuously and this process is important in terms of monitoring the efficiency of the system and performing the necessary maintenance. Because in this process, to maintenance or replacement of aging membrane and electrodes without delay is important for system efficiency. In a case study, they examined eight years of data and calculated the mean relative errors in the ohmic overpotential (associated with the membrane) and the activation overpotential (associated with the electrodes) to be 3 % and 6 %,

respectively. Khasawneh et al. (2019) state that the hydrogen produced from the Chlor-alkali processes in Jordan is directly vented to the atmosphere. Whereas, the utilization produced hydrogen as an energy resource can play a significant role in energy policy. For this purpose, they examined a Chlor-alkali plant based on membrane cells, in the northern part of Jordan, as a case study. They proposed to install a hydrogen boiler next to the plant and utilize the hydrogen to generate steam for on-site process heating purposes. Thus, they calculated that around 1810 tons of carbon dioxide emissions could be reduced in two years. Rosales-Huamani et al. (2021) evaluated the factors that influence the formation of sodium hydroxide (NaOH) through an electrolytic cell with an ion exchange membrane and graphite electrodes. They have stated that the best-operating conditions are found at a cell voltage of 7.5 V, an initial concentration in the cathodic compartment of 0.1 N NaOH, and a temperature of 45 °C. They have calculated the average electric current efficiency as 80.2 % depending on the experimental conditions of 25 °C, initial NaOH concentration of 0.01 N, and voltages of 5.0 V, 6.5 V, and 7.5 V. Li et al. (2021) stated that there is a need for serious improvements and developments in the Chlor-alkali industry, which consumes high amounts of electricity and causes environmental problems. They proposed to combine experimental and theoretical methods to better understand the formation of chlorine and oxygen at the anode and to improve the selectivity and activity of the anode. They also stated that the hydrogen produced by the Chlor-alkali industry is released directly into the atmosphere as there is not a sufficient market to use it. Moreover, they have mentioned that hydrogen may become the major fuel in the future as a promising clean energy. Thummar et al. (2022) showed that a Chlor-alkali plant connected to a wind energy system can be operated effectively depending on the wind profile. They have stated that when a fluctuation occurs due to a change in current wind strength during the day, the model provides stable operation with minimal deflection around the set points. They made steady state and dynamic simulation

studies including both electrochemical and equilibrium equations at a constant temperature.

Although the Chlor-alkali industry has a history of over 100 years, it remains a high-energy-consuming industry today, consuming nearly 10 % of global electricity every year. Since one of the most important problems of Chlor-alkali processes is the high amount of electricity consumption, solar-assisted hybrid systems have been preferred to reduce it to some extent. Acar and Dincer (2017a,b,c) presented both experimental research and thermodynamic evaluation of a hybrid photoelectrochemical Chlor-alkali system for hydrogen production using the solar energy spectrum at the maximum level. This system produces chlorine gas and sodium hydroxide, which are important industrial products, together with hydrogen gas. The system was tested at four different temperatures (20, 40, 60, and 80 °C) and three different light settings (no light, 600 W/m^{2,} and 1200 W/m^2). According to the parametric study, the system produces approximately 145 mL/h of hydrogen with energy and exergy efficiencies of 25.4 % and 18.76 %, respectively, at 20 °C and under no light conditions. Likewise, at a temperature of 80 °C and under 1200 W/m^2 solar radiation, it produces approximately 295 mL/h of hydrogen with energy and exergy efficiencies of 19.6 % and 13.72 %, respectively. According to the experimental results, the system produces approximately 145 mL/h of hydrogen with energy and exergy efficiencies of 49.3 % and 35.1 %, respectively, at 20 °C and under no light conditions. Likewise, at a temperature of 80 °C and under 1200 W/m^2 solar radiation, it produces approximately 295 mL/h of hydrogen with energy and exergy efficiencies of 8.2 % and 7.3 %, respectively. Bicer and Dincer (2018) evaluated the experimental performance of a newly developed photoelectrochemical reactor for hydrogen production under concentrated sunlight and in the absence of light. In this experimental setup, sunlight was concentrated about ten times and separated into an infrared and visible light spectrum with a special dielectric mirror for better use. To increase the hydrogen production rate under sunlight, a cathode plate covered

with photosensitive Cu_2O was used and the amount of hydrogen production at different potentials was measured. According to the results of the study, while the applied potential was 2.5 V, the hydrogen production rates under concentrated light and without light were found to be 41.34 mg/s and 34.73 mg/s, respectively. In addition, the photocurrent produced under concentrated light is 0.63 mA/cm^2. It is quite clear that the hydrogen production rate increases significantly under concentrated sunlight with its contribution to the photocurrent. Chehade et al. (2018) conducted an experimental study to examine the effect of photosensitive titanium dioxide (TiO_2) coated on a 316 stainless steel anode with a surface area of 180 cm^2 on photoelectrochemical hydrogen production. TiO_2 nanoparticles prepared by the sol-gel method were coated on 316 stainless steel anode with a dip coating device. Potentiostatic studies have shown that the photoactivity properties of TiO_2 nanoparticles increase when exposed to ultraviolet light. While hydrogen is produced at a rate of 51 mL/s under 600 W/m^2 light intensity with a TiO_2 coated stainless steel electrode, this production rate is 42 mL/s in the absence of light. In addition, a 10 mA increase in photocurrent value was found with this electrode under 1.6 V potential, with energy and exergy efficiencies of 1.32 % and 3.42 %, respectively. The present results show that TiO_2 coatings have good potential in photoelectrochemical hydrogen generation applications. Qureshy et al. (2019) proposed two different photoelectrochemical reactor designs (Design 1 and 2) and analyzed them numerically. The height of the reactor is 200 mm, its width is 34 mm, the height of the photoelectrodes is 100 mm and the thickness is 2 mm. The distance between the electrodes was chosen as 10 mm in Design 1 and 6 mm in Design 2 and calculations were made accordingly. To examine the effects of important design parameters on system performance, equations related to transport events in the reactor were developed and solved numerically. According to the present results, as solar radiation increases in proposed designs, volumetric hydrogen production and solar-hydrogen conversion efficiency also increase.

Solar-hydrogen conversion efficiencies were calculated as 12.65 % for Design 1 and 12.48 % for Design 2. The volumetric hydrogen production rate was calculated as 78.3 L/m^2h with Design 1 and 74.8 L/m^2h with Design 2. Karakilcik et al. (2018) conceptually investigated the hydrogen production performance of a reactor supported by a solar pond using the photoelectrochemical method. In this system, the extra energy contribution of the solar pond to the reactor is aimed. The main components of the system are a solar pond, a photovoltaic panel (PV), a photocathode, and a hybrid Chlor-alkali reactor. The system produces sodium hydroxide as well as hydrogen and chlorine gases while consuming NaCl solution and water. It is aimed to increase production efficiency by using the heated brine in the storage area of the solar pool in the reactor. The electrical energy required for electrolysis is provided by the PV panel. The results show that the thermal energy stored in the pool plays an important role in the reactor efficiency.

3. BACKGROUND

Hydrogen is a well-known energy carrier today. However, although they are abundant in nature, they are not found alone. Therefore, hydrogen should be produced using different energy sources with the least environmental impact. Table 3.1 shows an overview of the relation between primary energy sources and the methods to produce hydrogen.

Table 3.1. Some hydrogen production methods and primary energy sources.

Methods	Wind power	Hydro power	Solar energy	Biomass	Fossil fuels	Nuclear energy
Electrolysis	✓	✓	✓			
Photoelectrolysis			✓			
Photoelectrochemical			✓			
Gasification				✓	✓	
Biological processes				✓		
Reforming processes				✓	✓	
High temperature electrolysis						✓
Thermochemical water splitting						✓

In this study, it is necessary to highlight electrolysis among these methods. Electrolysis is a method of separating compounds by direct current (DC). The main components of an electrolytic cell are a DC supply, an electrolyte containing positive (anions) and negative (cations) ions, and two electrodes (anode and cathode). Oxidation occurs at the anode and reduction occurs at the cathode. Oxidation is the loss of electron(s) by an atom (or ion) while reduction is the gain of electron(s) by an atom (or ion). Some reactions such as chlorine evolving require an inert electrode (graphite, platinum, gold, etc.) that does not participate.

3.1. Chlor-Alkali Process

The Chlor-alkali (CA) process is an important industrial process including the electrolysis of an aqueous solution of dominantly sodium chloride ($NaCl$) for the production of mainly chlorine gas (Cl_2) besides sodium hydroxide ($NaOH$) and hydrogen gas (H_2). In the Chlor-alkali process, hydrogen is produced as a by-product, and some of it is released into the atmosphere, not fully utilized. A typical Chlor-alkali process consists of two half-reactions. One of them is the chlorine gas (Cl_2) evolution reaction at the anode and the other one is the hydrogen gas (H_2) evolution reaction at the cathode with sodium hydroxide ($NaOH$) formation in the electrolyte in the cathode compartment simultaneously. The anode, cathode, and overall reactions are given as:

Anode: $$2Cl^- \rightarrow Cl_2 + 2e^- \quad (3.1)$$

Cathode: $$2H_2O + 2e^- \rightarrow H_2 + 2OH^- \quad (3.2)$$

Overall: $$2H_2O_{(l)} + 2NaCl_{(aq)} \rightarrow 2NaOH_{(aq)} + Cl_{2(g)} + H_{2(g)} \quad (3.3)$$

In this process, where $NaCl$ is generally used other salts such as KCl and $CaCl_2$ can be used. In this case, K or Ca elements are included in the products instead of Na elements. For example, when $NaCl$ is used, $NaOH$ is produced, and when KCl and $CaCl_2$ are used, KOH and $Ca(OH)_2$ are produced, respectively. All of them are valuable industrial chemicals. The main methods used to produce Chlor-alkali are:

- mercury cell process
- diaphragm cell process
- membrane cell process

3.1.1. Mercury Cell Process

Figure 3.1 shows the schematic representation of the mercury cell process. In this process, a saturated brine solution floats on top of a thin layer of mercury in an electrolytic cell. The mercury layer in this cell behaves as a cathode due to the polarity of the applied potential. Thus sodium forms amalgam with mercury and chlorine is produced at the anode simultaneously. The amalgam (a mixture of two metals, e.g. Hg/Na) is continuously transferred from the electrolytic cell to a decomposer where it reacts with water and decomposes into sodium hydroxide, hydrogen, and mercury. The sodium hydroxide can be produced at nearly 50 % concentration. Since this percentage is commercially sufficient, no further purification is required. However, this method has been abandoned in Europe because mercury is a toxic heavy metal and poses an environmental risk. Therefore, it will not be considered further.

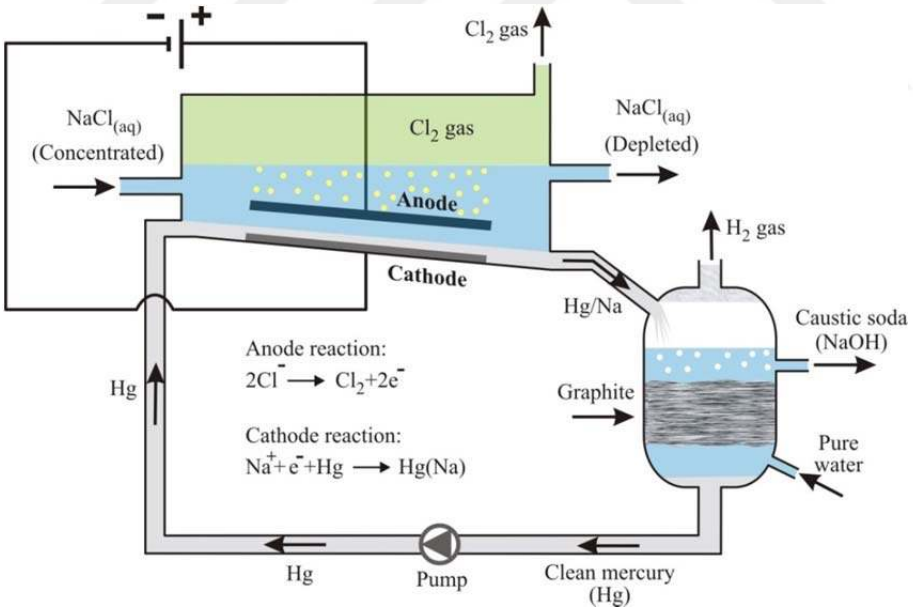

Figure 3.1. Schematic of the mercury cell Chlor-alkali process.

3.1.2. Diaphragm Cell Process

Figure 3.2 shows the schematic of the diaphragm cell process. In this process, a permeable asbestos fibers diaphragm is often used to separate the anode and the cathode compartments of the cell. The anode compartment is fed with the concentrated brine. Thus the chloride ions are oxidized at the anode to produce chlorine gas. The produced chlorine gas also contains oxygen. So it must often be purified by liquefaction and evaporation. The remaining brine from the input brine flows through the diaphragm into the cathode compartment where sodium hydroxide and hydrogen are produced. The produced sodium hydroxide can be concentrated to 50 % by using an evaporative process. However, this process requires three tons of steam for one ton of sodium hydroxide. The diaphragm also prevents the reaction between chlorine and sodium hydroxide. The anode reaction takes place like Equation 3.1, and the cathode reaction takes place like Equation 3.2.

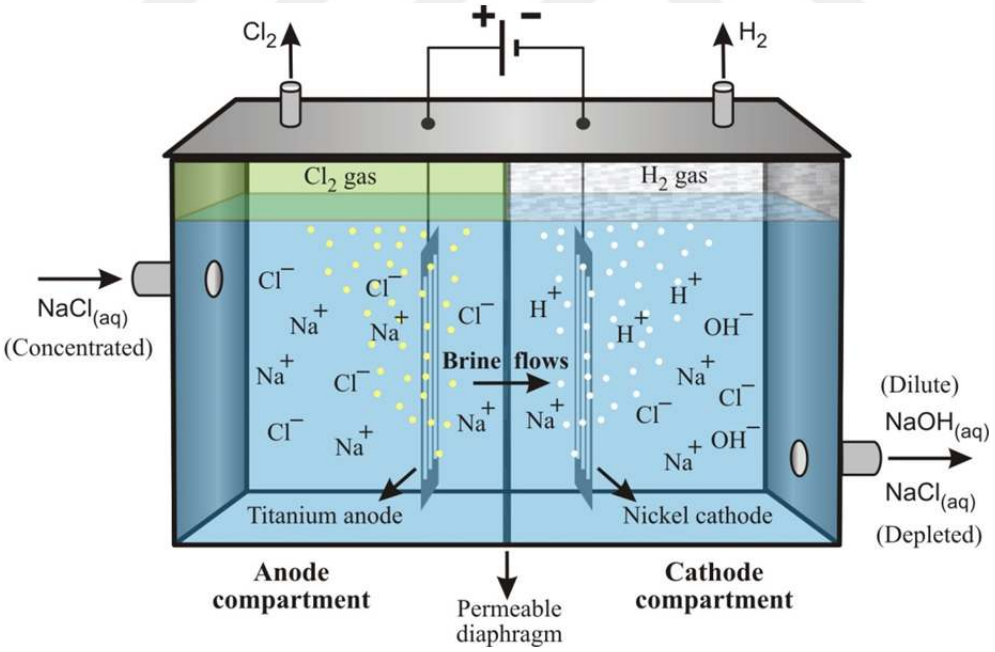

Figure 3.2. Schematic of the diaphragm cell Chlor-alkali process.

3.1.3. Membrane Cell Process

Figure 3.3 shows the membrane cell Chlor-alkali process. Since this study is focused on the membrane cell process, let's examine this method in more detail. The anode and the cathode compartments of the cell are separated by a cation exchange membrane. The anode compartment is fed with concentrated aqueous sodium chloride solution ($NaCl_{(aq)}$) and the cathode compartment is fed with dilute aqueous sodium hydroxide solution ($NaOH_{(aq)}$). The cation exchange membrane allows only sodium ions to pass from the cathode compartment to the anode compartment as well as a small amount of water can pass through it. The brine entering the anode chamber decomposes into Na^+ and Cl^- ions. Thus Cl^- ions are oxidized to chlorine gas at the anode and Na^+ ions migrate to the cathode compartment through the cation exchange membrane. The water reduces to hydrogen gas (H_2) and hydroxide ions (OH^-) at the cathode. Then Na^+ and OH^- ions form NaOH in the cathode compartment.

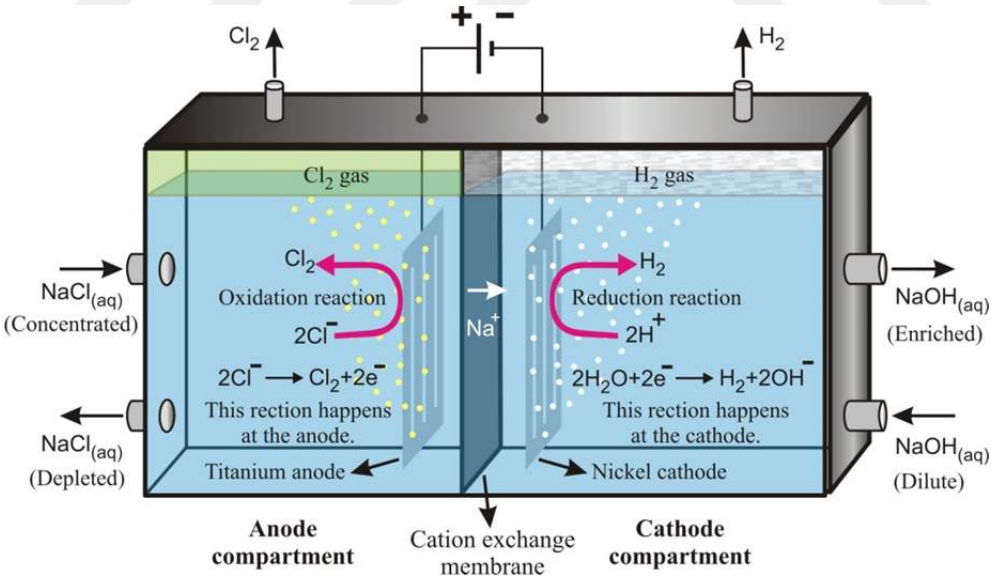

Figure 3.3. Schematic of the membrane cell Chlor-alkali process.

Figure 3.4 shows the share of the total capacity of chlorine production depending on the production method between the years 2001 and 2019 in Europe.

The share of the mercury cell process has decreased dramatically in recent years due to the highest electricity consumption and environmental contamination. This method has been phased out since 2017 and it is no longer used in Europe.

Similar to the mercury cell process the share of the diaphragm cell process has also been continuously decreasing in recent years due to the adverse effects of asbestos fibers on human health.

Oppose to other Chlor-alkali processes the increasing trend of the membrane cell process can be seen in recent years. Because this process has the lowest electricity consumption and the fact that it does not produce environmentally harmful waste. This method is the dominant technology today to produce Chlor-alkali in Europe.

HCl electrolysis and molten salt electrolysis can be considered in other methods.

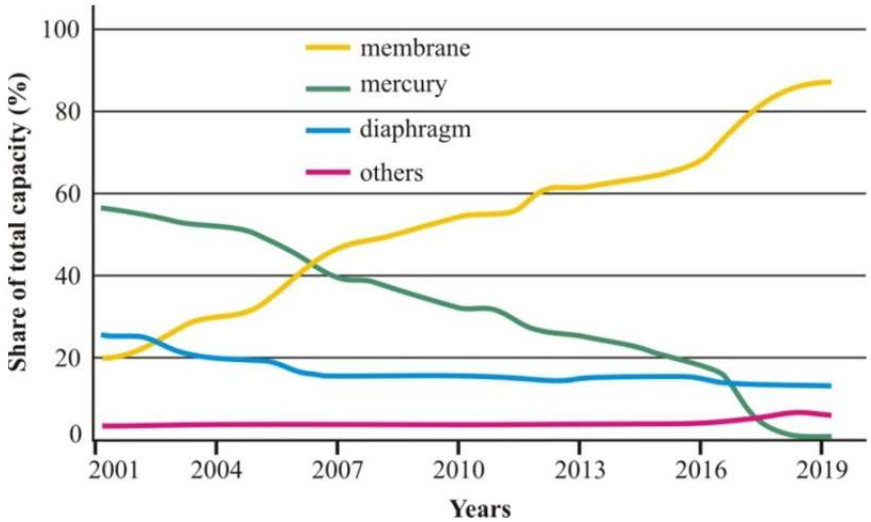

Figure 3.4. Share of Chlor-alkali technologies (source: Eurochlor (17.) 2019-2020).

3.2. Electrochemical Analysis

The minimum required input work (electrical energy for the process) for an electrochemical process under constant temperature and pressure is equal to the change in Gibbs free energy (ΔG). So, ΔG of an electrochemical reaction at constant temperature and pressure can be written as:

$$\Delta G = -nFE^0 \tag{3.4}$$

where n is the number of moles of electron transferred, F is the Faraday's constant and E^0 is the standard electrode potential that can be easily found in the literature. If $\Delta G < 0$, the electrode reactions take place spontaneously as in galvanic cells. If $\Delta G > 0$, the electrode reactions should be driven by a direct current (DC) power supply (PS) as in electrolytic cells. The minimum theoretical DC potential (decomposition voltage or standard electrode potential) requirement for a typical Chlor-alkali membrane cell is given in Table 3.2 (Jalali et al., 2009).

Table 3.2. Minimum theoretical DC potential requirement for the membrane cell.

Anode	$Cl^- \rightarrow Cl_2 + 2e^-$	$E^0 = -1.358$ V
Cathode	$2H_2O + 2e^- \rightarrow H_2 + 2OH^-$	$E^0 = -0.825$ V
Total	$2H_2O + 2NaCl \rightarrow 2NaOH + Cl_2 + H_2$	$E^0 = -2.183$ V

The theoretical cell voltage for electrolysis of brine ($NaCl_{(aq)}$) is around 2.2 V as shown in Table 3.2. But in real applications, the applied cell potential to drive the Chlor-alkali reactions is always larger than the minimum theoretical DC potential requirement due to the irreversibilities. Therefore, the practical operating potential lies around 3 V. It is extremely important for efficiency to determine the voltage losses regarding the system components and to carry out studies to fix them. So, electrochemical analysis is needed to find the required potential by taking into account the decomposition voltage and ohmic losses between the

different components of the reactor. Since the electric field between the anode and the cathode electrodes provides ion transport across the electrolytes and the membrane, it is necessary to pay attention to the ohmic losses when determining the cell voltage. For the Chlor-alkali membrane system shown in Figure 3.2, the overall voltage balance equation across the reactor can be written as:

$$V = E^0 + V_A + V_{anolyte} + V_M + V_{catholyte} + V_C \quad (3.5)$$

where E^0 is the decomposition voltage, V_A is the voltage drop across the anode electrode, $V_{anolyte}$ is the voltage drop across the anolyte (brine) in the anode compartment, V_M is the voltage drop across the ion-exchange membrane, $V_{catholyte}$ is the voltage drop across the catholyte in the cathode compartment and V_C is the voltage drop across the cathode electrode.

In the Chlor-alkali process, voltage drops (ohmic losses) across the cell components and electrolytes are important trouble that reduces the system performance, and hence, increases the energy consumption. Therefore, system designs must be done very well to reduce losses and save energy. The voltage drop across the anolyte is calculated as:

$$V_{anolyte} = \frac{i}{A} \times \frac{L_a}{K_a} \quad (3.6)$$

where i is the total current traveling between the electrodes, A is the surface area of the electrode, L_a is the distance between the anode and the membrane and K_a is the conductivity of anolyte depending on the concentration and the operating temperature. The voltage drop across the catholyte is calculated as:

$$V_{catholyte} = \frac{i}{A} \times \frac{L_c}{K_c} \quad (3.7)$$

where L_c is the distance between the cathode and the membrane and K_c is the conductivity of the catholyte depending on the concentration and the operating temperature. As seen from Equations 3.6 and 3.7, when the distance between the electrodes decreases, the voltage drop along the electrolytes also decreases. On the other hand, it is necessary to adjust the electrolyte density and operating temperature in a way that will increase the electrical conductivity of the electrolyte. The voltage drop across the membrane is calculated as:

$$V_M = \frac{i}{A} \times \frac{\sigma_M}{K_M} \tag{3.8}$$

where σ_M is the thickness of the membrane and K_M is the electrical conductivity of the membrane which depends on many factors such as the chemical structure of the membrane, operating temperature, pH of the electrolyte, and permeability. These values are generally provided by the manufacturer. Assessment of the voltage drops across the anode and cathode is a very complex process as many parameters affect it. Detailed explanations on this subject are abundant in the literature. Rabbani et al. (2014b) designed a new photoelectrochemical hydrogen production reactor combining photochemical hydrogen production with an electrochemical Chlor-alkali process and evaluated the electrochemical properties of this model. The ideal minimum potential required to neutralize the hydroxyl ions in the Chlor-alkali process was calculated as 2.18 volts. It is important to calculate the voltage losses in the electrodes, solution, and membrane used in the system to find the required voltage requirement of the photoelectrochemical hydrogen production reactor. The results showed that salt water and electrolyte density did not have a significant effect on the cell voltage for the electrochemical process, but it was observed that the cell voltage increased as the distance between the electrodes increased, and the cell voltage decreased with

the increase in temperature. It has also been emphasized that the voltage loss across the membrane is the highest due to its low conductivity.

3.3. Efficiency Analysis

Efficiency analysis is needed to understand how inputs are translated into valuable outputs. Thus, potential sources of inefficiency can be identified, and can be taken necessary measures to improve them. Therefore, energy and exergy analyzes are needed to evaluate the thermodynamic performance of a Chlor-alkali process. For this, it is necessary to know the theoretical energy requirement of the system.

So, the total theoretical input energy (ΔH: change in enthalpy) can be calculated as:

$$\Delta H = \Delta G + T\Delta S \tag{3.9}$$

where ΔG is the change in Gibbs free energy (the equivalent of electricity requirement) and TΔS is the thermal energy requirement.

Thus, energy efficiency is written as:

$$\eta_{\text{energy}} = \frac{\text{total useful output energy}}{\text{total input energy}} \tag{3.10}$$

and exergy efficiency is written as:

$$\eta_{\text{exergy}} = \frac{\text{total useful output exergy}}{\text{total input exergy}} \tag{3.11}$$

The efficiency of any electrochemical reactions can also be alternatively expressed in terms of current efficiency (CE). One of the major issues of the Chlor-

alkali industry is the high power consumption. Therefore, particularly current efficiency can play a major role to facilitate achieving the optimum conditions for a Chlor-alkali process. So, it is calculated as:

$$\eta_{CE} = \frac{\text{theoretical value of current}}{\text{practical value of current}} \times 100 \tag{3.12}$$

or,

$$\eta_{CE} = \frac{\text{actual deposited mass}}{\text{theoretical mass}} \times 100 \tag{3.13}$$

4. EXPERIMENTAL DESIGN AND SETUP

4.1. System Description

Figure 4.1 shows the schematic of the experimental setup. The present setup has nine main components namely a Chlor-alkali reactor, electrolyte feed containers (EFC_1 and EFC_2), electrolyte dump containers (EDC_1 and EDC_2), peristaltic pumps (P_1 and P_2), a DC power supply, and a graduated cylinder.

The concentrated aqueous solutions of sodium chloride ($NaCl$), potassium chloride (KCl), and calcium chloride ($CaCl_2$), which are separately present in EFC_2, are pumped one by one to the anode compartment of the reactor. Similarly, diluted aqueous solutions of sodium hydroxide ($NaOH$), potassium hydroxide (KOH) and calcium hydroxide ($Ca(OH)_2$), which are separately present in EFC_1, are pumped one by one to the cathode compartment of the reactor. That is, anolyte feed is saturated $NaCl$ solution while the catholyte feed is diluted $NaOH$. A similar activity is repeated for the remaining salt and base solutions. Note that, the solutions in EFC_1 and EFC_2 were heated up to operating temperature before the experiments and the electrolyte flow rates are controlled by P_1 and P_2.

The salt solution, which passes through the anode compartment of the reactor and whose concentration decreases, is collected in the EDC_2. In the case of using the appropriate type of electrode (such as a platinum metal electrode), the chlorine gas produced in the anode compartment comes to this container along with the depleted salt solution. On the other hand, the base solution concentrated in the cathode compartment is collected in the EDC_1. The hydrogen gas produced in the cathode compartment also comes to this container with the base solution. The volume of the produced hydrogen gas is measured by the volumetric displacement technique with the help of a graduated cylinder.

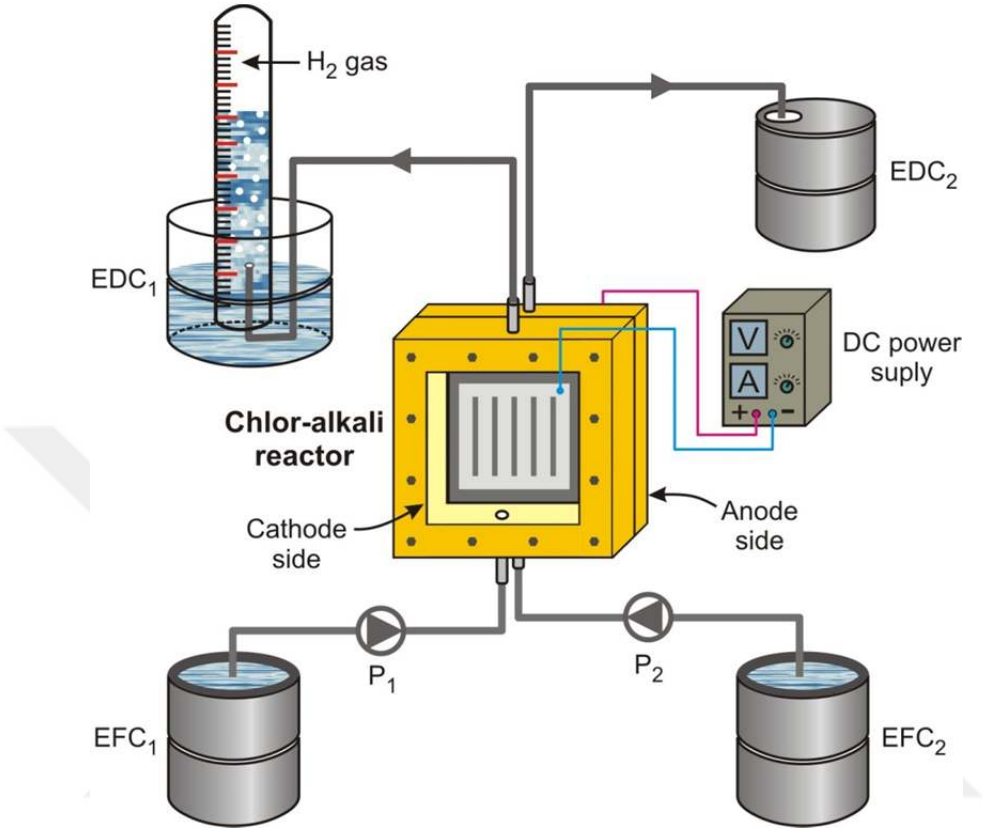

Figure 4.1. Process flow diagram of the present hydrogen production system.

Figure 4.2 shows the experimental apparatus set up in Renewable Energy Technologies Laboratory at Çukurova University. The solutions prepared with distilled water in electrolyte feeding containers and heated up to the operating temperature are pumped by the peristaltic pumps to the anode and cathode compartments of the reactor with a certain mass flow rate. Electrolytes passing through the reactor come to electrolyte dump containers through the outlet hoses. The volume of the hydrogen gas produced is measured by the volumetric displacement technique of water, by placing the outlet hose coming from the cathode compartment into a graduated cylinder. The electrical energy required for the electrolysis is also provided by a DC power supply.

Hydrogen production performance was measured by applying three different cell voltages by repeating the experiment according to three different mass flow rates for the electrolytes prepared at three different temperatures for each salt type.

In case of using suitable electrodes (such as platinum metal electrodes) in the anode compartment of the reactor, it can produce chlorine gas, which is a valuable raw material in the cleaning industry, and a base depending on the type of salt used, as well as hydrogen gas. In this experiment, 316 stainless steel electrodes with high nickel content were used instead of platinum metal electrodes due to their high cost. Chlorine, which is very active and can easily react with many metals, reacted with nickel in the structure of the electrode and formed a greenish jelly-like substance namely nickel chloride on the electrode. Consequently, serious contamination in the anode chamber and corrosion on the electrode surface was observed. Therefore, only hydrogen gas production was measured in the experiments. In addition, the energy and exergy efficiencies of the system were calculated according to the hydrogen gas production only.

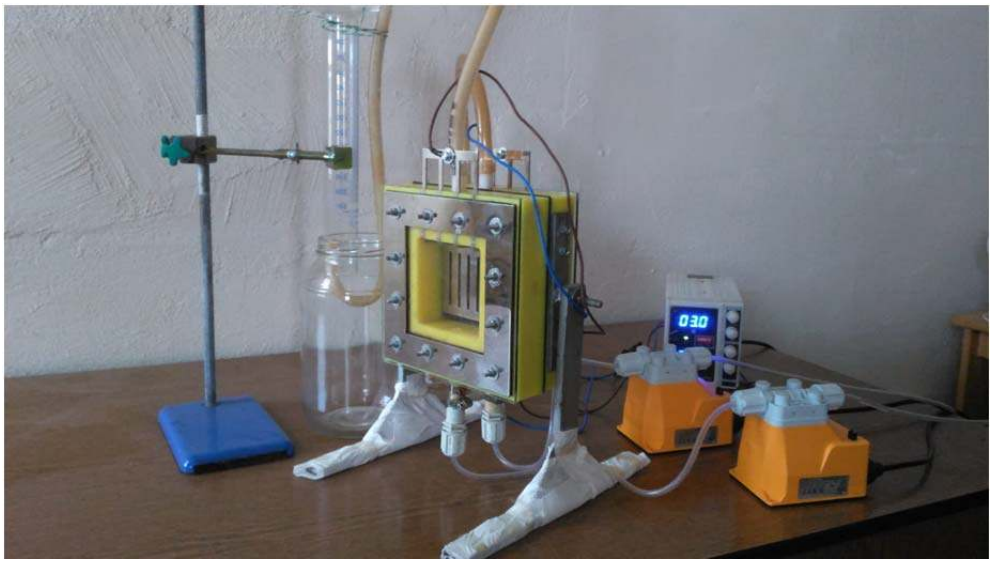

Figure 4.2. Experimental set up producing hydrogen by Chlor-alkali method.

4.2. Designing and Building the Reactor

Since the most important element of the experimental study is the reactor, computer package programs were used during the design step, then, after researching the appropriate material for the reactor production, the anode and cathode compartments were produced in CNC (computer numeric control) machine. Depending on the dimensions of the membrane used (10 cm × 10 cm), three-dimensional design drawings of the reactor were made with CorelDRAW Graphics Suite 2020, three-dimensional simulations were made with COMSOL Multiphysics 5.3 and the final step was reached for production.

Figure 4.3 shows the anode (front side) and cathode (back side) compartments of the reactor. Figure 4.3(a) shows the dimensions of the slots where the electrode is installed, the electrolyte inlet and outlet pipes, and the bolt holes. Figure 4.3(b) shows the frame dimensions of the reactor and the slot where the membrane is installed.

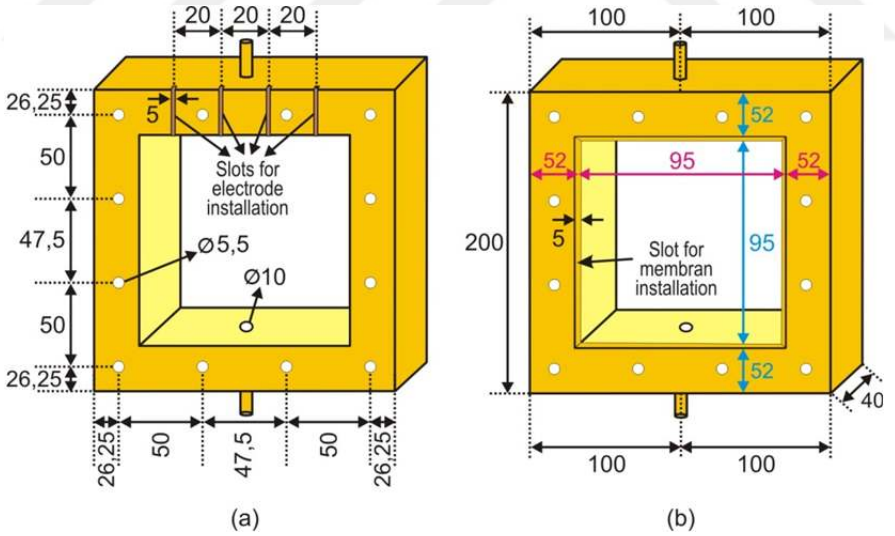

Figure 4.3 (a) Anode compartment (front side) and (b) Cathode compartment (back side) (millimeters).

Testing any designed technological system by simulating it on the computer before it is put into practice saves a significant amount of time and financial expenses. Meshing is an important step when it comes to the engineering simulation process. Meshing or mesh generation is dividing the complex geometry of a system into many suitable finite elements. In this way, computer simulation of a system can be done easily according to different operating conditions. If the mesh generation contains too many cells, it causes the computer to analyze the designed system for a very long time. On the other hand, if the mesh generation contains insufficient cells, the margin of error increases. The relationship between simulation and real application results is dependent on the mesh generation. Creating a high-quality mesh increases the simulation accuracy.

The COMSOL Multiphysics 5.3 meshing system provides the options in Table 4.1 for mesh generation. Physics-controlled mesh and finer options were used in this study.

Table 4.1. Mesh generation options of COMSOL Multiphysics 5.3.

Mesh Settings	
Sequence type:	**Element size:**
Physics-controlled mesh	Extremely fine
User-controlled mesh	Extra fine
	Finer
	Fine
	Normal
	Coarse
	Coarser
	Extra coarser
	Extremely coarser

Figure 4.4(a) shows the three-dimensional structural mesh for the designed reactor made with COMSOL Multiphysics 5.3. According to the mesh generation, the electrolyte flows in the reactor depending on the mass flow rates of 0.3 g/s, 0.5 g/s, and 0.7 g/s are shown in Figure 4.4(b, c, d), respectively.

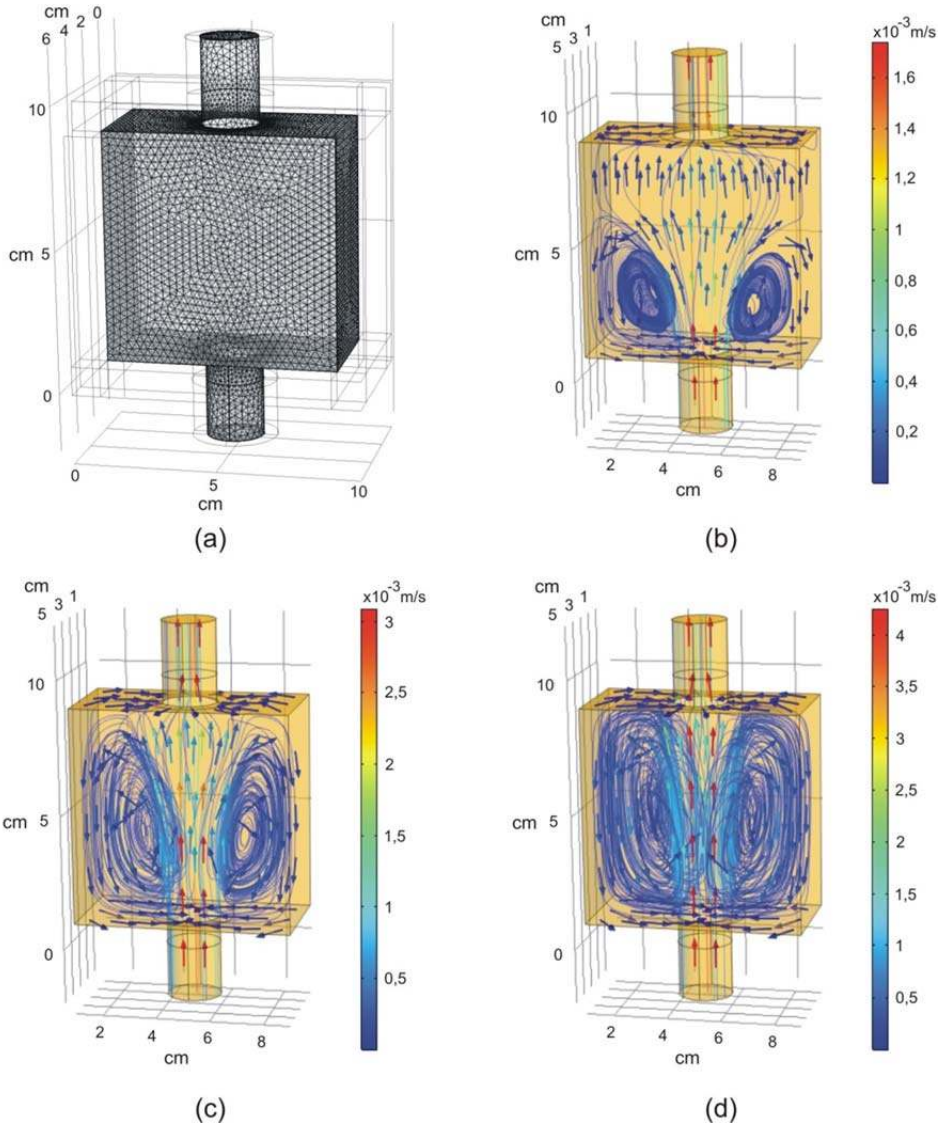

Figure 4.4. Three-dimensional mesh simulation for the reactor created with COMSOL Multiphysics 5.3.

Figure 4.5 shows the three-dimensional modeling of the anode and cathode compartments of the reactor made with SOLIDWORKS Premium 2018. This is an important step so that the reactor parts can be produced on the CNC machine.

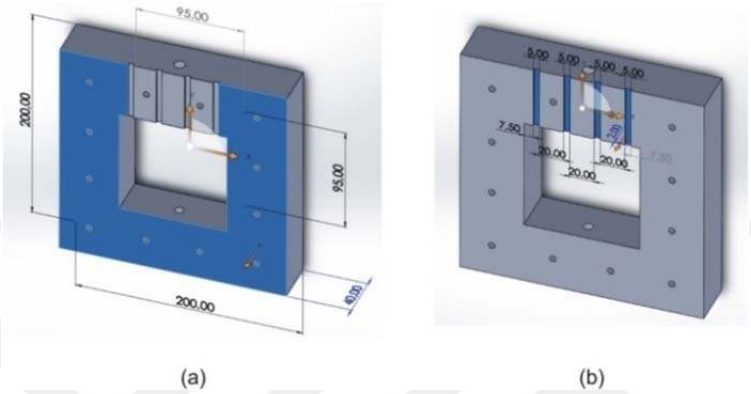

Figure 4.5 (a) Anode compartment (front side) and (b) cathode compartment (front side) modeled with SOLIDWORKS Premium 2018 (millimeters).

Figure 4.6 shows the anode and cathode compartments with inlet and outlet pipes of the reactor produced on a CNC machine from the cestamide material.

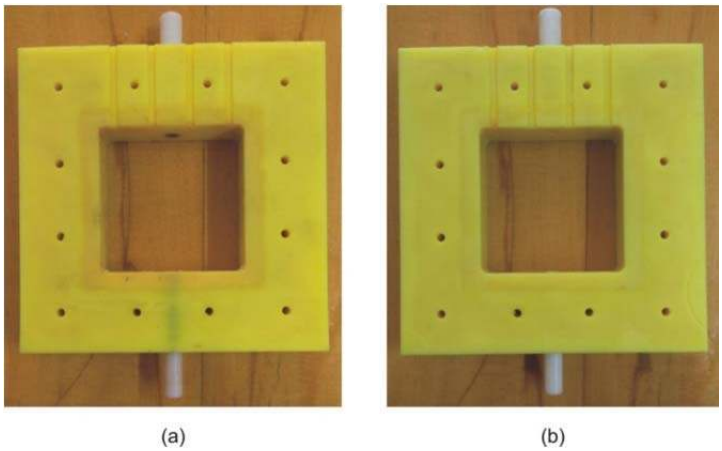

Figure 4.6 (a) Anode compartment (front side) and (b) cathode compartment (front side) made on a CNC machine from cestamide material.

Cestamide (PA6G-cast polyamide), also known as an engineering plastic, is a type of polymer with high physical and chemical properties due to its cross-linked molecular structure. Cestamide, which is in natural yellow color, can also be produced in black or other colors if desired. The operating temperature of cestamide, which melts at 220 °C, is between –30 °C and 110 °C. Although it can be easily processed in metal and woodworking machines, it has very good resistance to impact, abrasion, and bending. Cestamide, which is not affected by water and humid environments, has high resistance against acids and bases. Due to these features, system parts compatible with harsh working conditions are produced using this polymer.

Figure 4.7 shows the drawing of the designed electrode, one of the important parts of the reactor, made with CorelDRAW Graphics Suite 2020 and the three-dimensional modeling made with SOLIDWORKS Premium 2018. Oxidation and reduction reactions take place thanks to the electrodes placed symmetrically and very close to each other in the anode and cathode compartments of the reactor.

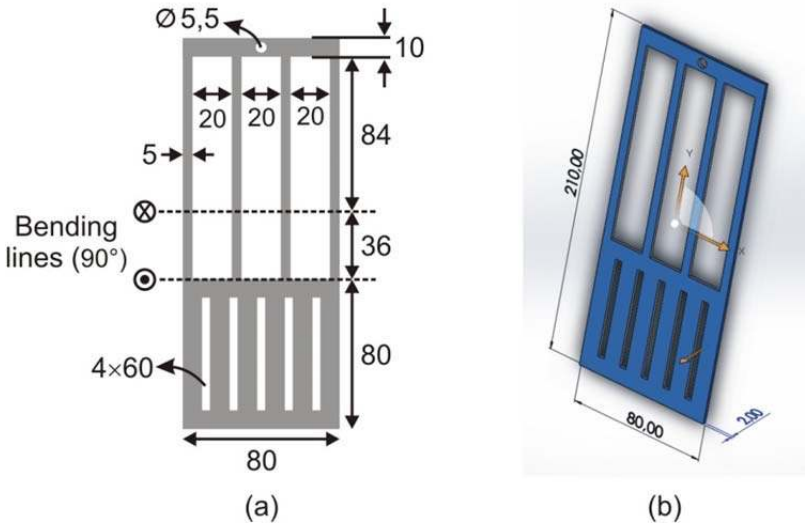

Figure 4.7. (a) Drawing of the electrode with CorelDRAW Graphics Suite 2020 and (b) three-dimensional modeling with SOLIDWORKS Premium 2018 (millimeters).

Figure 4.8 shows the electrodes made of 316 quality stainless steel sheets with a thickness of 2 mm by laser cutting. After laser cutting, 90-degree bending applications were performed at the locations shown in Figure 4.7(a). In this experiment, the electrodes were produced from 316 quality stainless steel sheet because it is low cost and resistant to corrosion from many chemicals. However, it has seen during the experiments it was not resistant to chlorine gas.

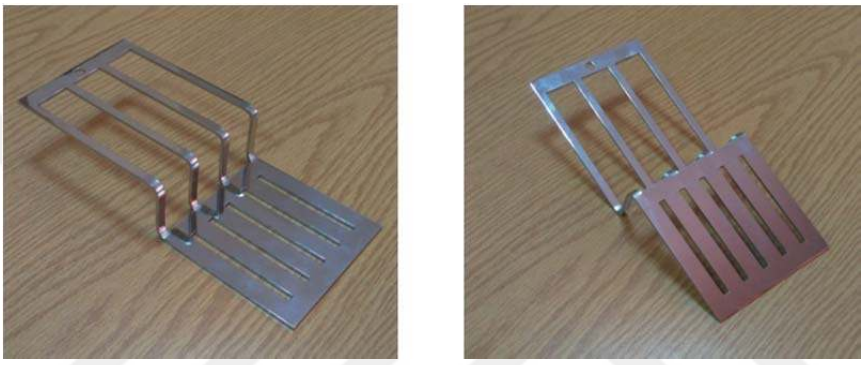

Figure 4.8. 316 quality stainless steel electrodes produced by laser cutting for anode and cathode compartments and bent 90° from the bend lines.

The most basic and most used type of stainless steel, 314 quality stainless steel, contains between 15 % and 20 % chromium and between 2 % and 10 % nickel. Furthermore, 316 quality stainless steel is obtained by adding more nickel and extra molybdenum to the 304 quality stainless steel content. Thanks to this content, the resistance of 316 quality stainless steel materials to corrosive effects such as sea water and acidic environments increases considerably. Munoz et al. (2010) studied hydrogen production by electrolysis method using stainless steel electrodes in a phosphate solution and reported that 316 quality steel electrodes in phosphate solution showed stable behavior. They also emphasized that the use of phosphate and other weak acids as catalysts could be a promising technology in the development of electrolysis units containing low-cost electrodes and building materials.

As shown in Figure 4.9, the electrodes are placed in their slots in the anode and cathode compartments. When the anode and cathode compartments of the reactor were combined and the reactor was integrated, bending was done so that the electrodes would not be far from each other. As the distance between the electrodes decreases, the voltage loss across the electrolyte decreases, so the voltage applied to the cell decreases. When the distance between the electrodes is 1.5 cm, the cell voltage is 2.83 V, and when the distance is increased to 2 cm, the cell voltage rises to 2.93 V (Domga, et al. 2017).

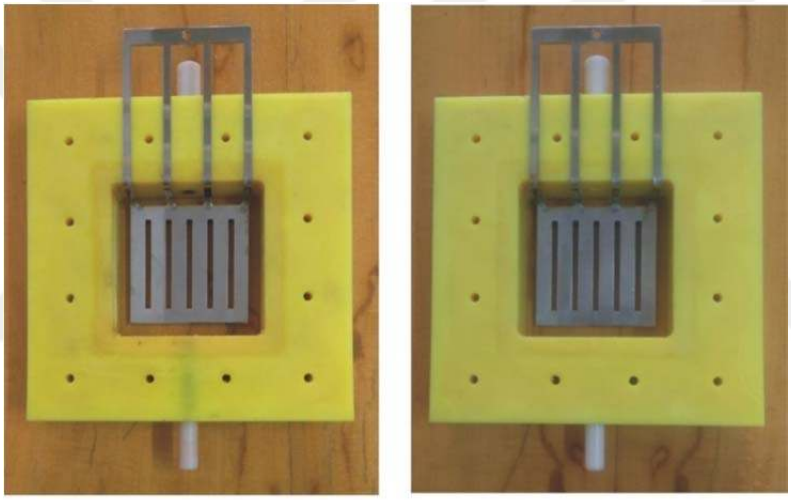

Figure 4.9. Views of the electrodes placed in the electrode slots (a) anode compartment (front side) and (b) cathode compartment (front side).

As stated in Equations (3.6) and (3.7), the voltage drop across the anolyte and catholyte is directly proportional to the distance between electrodes. To prevent this voltage loss, it is beneficial to position the electrodes as close as to each other and symmetrically. A lower gap between the electrodes ensures a significant reduction in the ohmic resistance of the cell. Consequently, higher current densities are obtained for the same cell potential.

In Figure 4.10, the cation exchange membrane (CEM) produced by Alfa Aesar, which is considered the most important part of the reactor, can be seen. The membrane is placed between the anode and cathode compartments of the reactor and acts as a barrier allowing only positive ions to pass through. In addition, the membrane prevents the electrolytes and the released gases in the anode and cathode compartments from mixing. The active surface area of the membrane is 100 cm^2 (10cm×10cm) and its thickness is about 0.3 cm. Both the anode and cathode surfaces of the membrane have a nominal Pt charge of 0.4 mg/cm^2. The content of the membrane is 50 % non-woven carbon fiber, 35 % perfluorosulfonic acid (PFSA), 5 % polytetrafluoroethylene (PTFE), 5 % carbon (black), and 5 % catalyst (finely divided Pt on C), all by weight.

Figure 4.10. Cation exchange membrane (Active area is 100 cm^2).

An ion-exchange membrane contains fixed charged ions. So, it is called a cation-exchange membrane or anion-exchange membrane according to the electrical charge type of these ions. Thanks to these fixed charged particles, the counter-ions can easily pass through the membrane. An ideal ion-exchange membrane should exclude co-ions and it should have good mechanical and chemical stability properties.

Figure 4.11 shows the order of assembly of the parts that make up the reactor. First of all, an ion exchange membrane is placed between the anode and cathode compartments to prevent the electrolytes and reaction products from mixing. A rubber gasket is placed between the anode and cathode compartments to prevent possible leakage between them. After the stainless steel electrodes (anode and cathode) are installed in their slots, the front and back sides of the reactor are covered with glass plates to observe the electrolyte flow and gas output inside. Rubber gaskets are also used to prevent leakage between the reactor frame and these plates. In order not to break the glass covers during the tightening of the bolt screws that keep the anode and the cathode compartments of the reactor together, support plates cut from steel sheets were used at the front and the back. After the reactor body was installed, the electrical and electrolyte input-output connections were made and the process was completed.

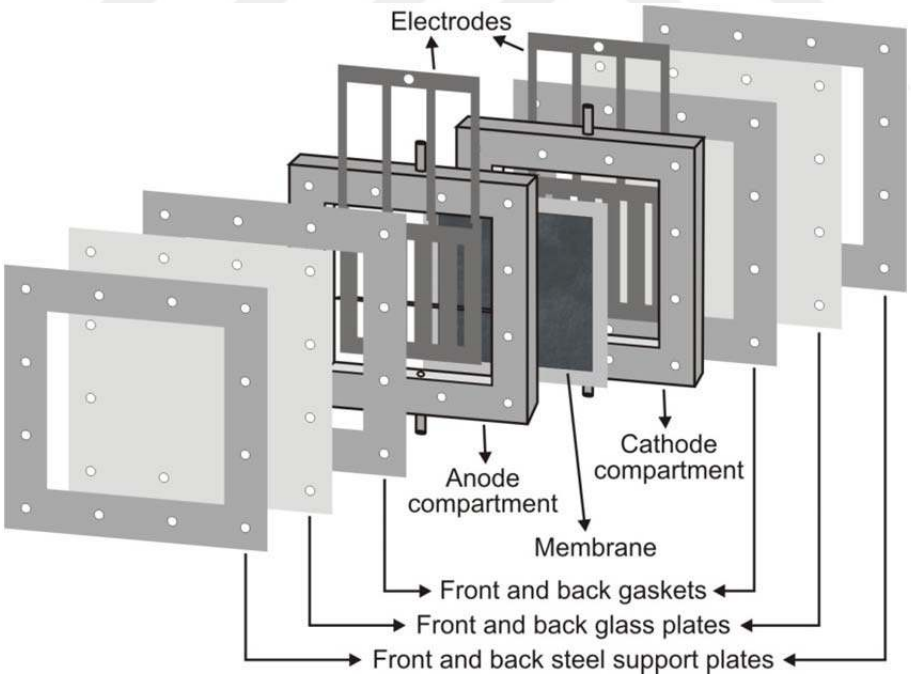

Figure 4.11. Arrangement of reactor parts in order.

Figure 4.12 shows the anode and cathode compartments of the mounted reactor. All the layers in Figure 4.11 were joined by putting rubber gaskets between them to prevent electrolyte leakage and the installation was completed. Electrolyte inlet and outlet pipes and positive and negative electrical connections are visible. It is also clearly seen how close the bent electrodes are placed to the membrane in both the cathode and anode compartments to reduce the voltage loss across the electrolytes. Electrolytes that enter separately from the inlet pipes at the bottom of the reactor to the anode and cathode compartments leave the compartments from the outlet pipes above the reactor after the Chlor-alkali processes. The anode compartment of the reactor is fed with concentrated salt solution, while the cathode compartment is fed with water. The hydrogen gas produced in the cathode compartment of the reactor comes to the graduated cylinder from the outlet pipe and its volume is measured by the volumetric displacement method of the water.

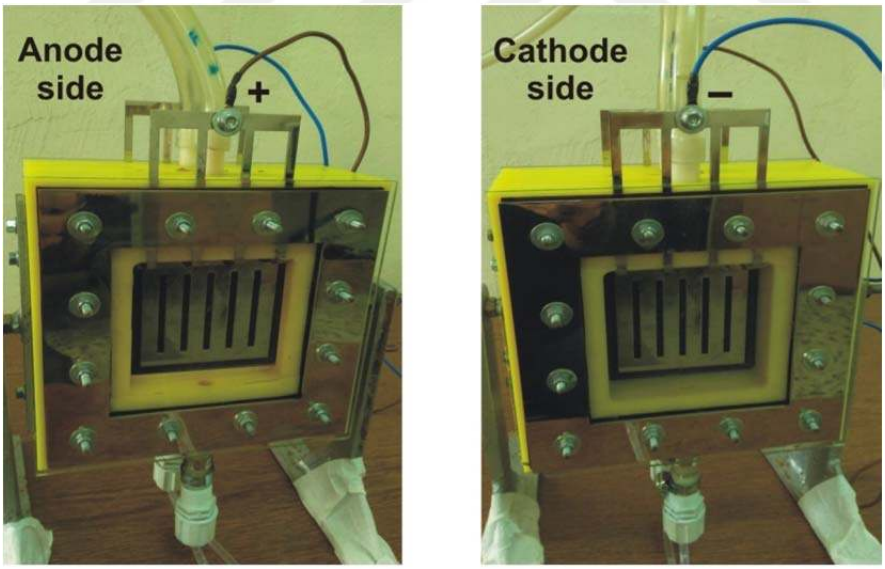

Figure 4.12. View of the (a) anode and (b) cathode sides of the completed reactor.

4.3. Instruments and Devices

In the experimental study, a DC power supply, two peristaltic pumps to provide the electrolyte flows in the cathode and anode compartments, a graduated cylinder to measure the volume of the hydrogen gas, electrolyte containers, a water heater, and a thermometer were used. To ensure that the peristaltic pumps pump electrolyte at the desired mass flow rate, first flow rate trials were carried out with the electrolyte prepared at the operating temperature for a while, then the actual experiments were carried out.

Figure 4.13(a) shows the UNI-T, UTP 3315 TFL model DC power supply used in the experiment. The maximum output voltage and the maximum output current of the power supply are 30 V and 5 A, respectively. Figure 4.13(b) shows the INJECTA, OLIMPIA model electromagnetic peristaltic pump. The pump, which has a power of 14 W, can provide a manually adjustable liquid flow rate of up to 80 mL per minute. In the experiment, two were used to provide the electrolyte flows in the cathode and anode compartments.

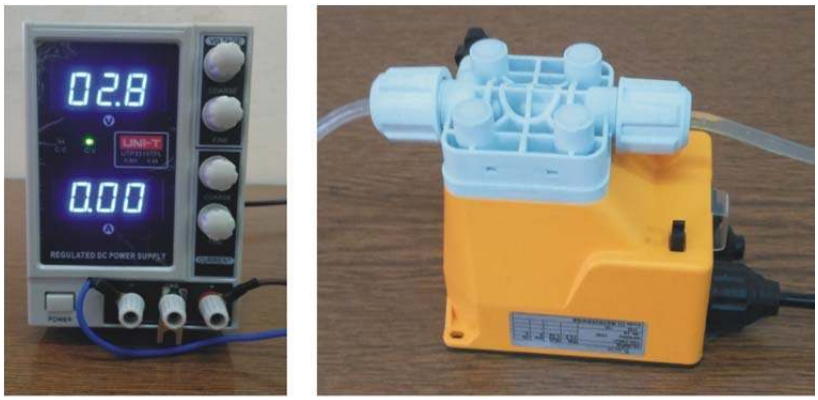

(a) (b)

Figure 4.13. (a) UNI-T, UTP 3315 TFL model DC power supply, and (b) INJECTA, OLIMPIA model electromagnetic peristaltic pump.

4.4. Physico-Chemical Properties of NaCl, KCl and $CaCl_2$

Figure 4.14 shows the extra purified NaCl, KCl, and $CaCl_2$ salts purchased from Merck for use in the experiments. For the membrane to be used for a long time without contamination, the salts used must be free from dirt and unwanted ions. Therefore, extra-purified salts were used in the experiments. In case such an experiment is carried out using sea water, a serious filtering process is required.

Figure 4.14. Extra pure NaCl, KCl, and $CaCl_2$ salts were tested in the experiments.

Some physicochemical properties of the salts used in the experiments are shown in Table 4.2.

Table 4.2. Some specifications of the salts used in the experiments.

Salts	NaCl	KCl	$CaCl_2$
Molar mass (g/mole)	58.44	74.56	147.01
Density (g/cm^3)	2.17	1.98	1.85
Solubility (g/L)	358	347	1280
Melting point (°C)	801	770	176
pH	4.5 - 7	5.5 – 8.5	4.5 – 8.5

4.5. Reactivity Series of Some Metallic Elements

Table 4.3 shows the reactivity series of some metallic elements. The reactivity of a metal depends on its atomic radius, nuclear charge, arrangement of the sublevel electrons, and shielding effect. The reactivity series of any metal is an indication of how quickly it reacts. Metals from potassium to calcium are highly reactive. Therefore they can even react with water. Metals from magnesium to lead react with acids. Metals from copper to platinum are highly unreactive. Therefore they don't react with any other substance under normal conditions. Although hydrogen is not a metal, it is included in the reactivity series for comparison.

Table 4.3. Reactivity series of some metallic elements.

Element	Symbol	Reactivity
Potassium	K	Most reactive
Sodium	Na	
Lithium	Li	
Calcium	Ca	Reactivity increases ⇧
Magnesium	Mg	
Aluminum	Al	
Zinc	Zn	
Iron	Fe	
Lead	Pb	⇩
Hydrogen	H	
Copper	Cu	
Mercury	Hg	Reactivity decreases
Silver	Ag	
Gold	Au	
Platinum	Pt	Least reactive

Table 4.4 shows how the selected elements react with water. Potassium reacts more violently and explosively with water while sodium reacts less violently with water when compared to potassium. Potassium reacts with water to form an aqueous solution of KOH with a release of H_2 gas. Sodium reacts with water to form an aqueous solution of NaOH with a release of H_2 gas. Oppose to potassium and sodium, calcium is virtually unreactive in cold water. However, calcium reacts with hot water but it is not as violent as the reaction between potassium and sodium with cold water. Consequently, increasing the temperature increases the rate of reaction of calcium with water.

Table 4.4. Comparison of reaction severity with water.

Element	Symbol	Reaction with water
Potassium	K	Violently
Sodium	Na	Very quickly
Lithium	Li	Quickly
Calcium	Ca	More slowly

Chemical equations for the reaction of K, Na, and Ca with water are written as follows:

$$K + H_2O_{(l)} \rightarrow KOH_{(aq)} + \frac{1}{2}H_{2(g)} \quad (4.1)$$

$$Na + H_2O_{(l)} \rightarrow NaOH_{(aq)} + \frac{1}{2}H_{2(g)} \quad (4.2)$$

$$Ca + H_2O_{(l)} \rightarrow Ca(OH)_{2(aq)} + \frac{1}{2}H_{2(g)} \quad (4.3)$$

The resultant solutions from these three reactions are basic because of the dissolved hydroxide.

4.6. Experimental Procedure

The experimental proceeding based on the Chlor-alkali process is illustrated in Figure 4.15. Experiments started following electrolyte preparation at operating temperature after checking the system components. When the experiments were started directly while the membrane was dry, inconsistent circuit current was observed in response to the applied voltage for several hours. To overcome this problem, it has been seen that it is beneficial to keep the membrane in the electrolyte one day beforehand. During the experimental runs, applied cell voltage and resulting current, and the hydrogen level in the graduated cylinder concerning time were monitored and registered. Each experiment was repeated to increase consistency and reliability.

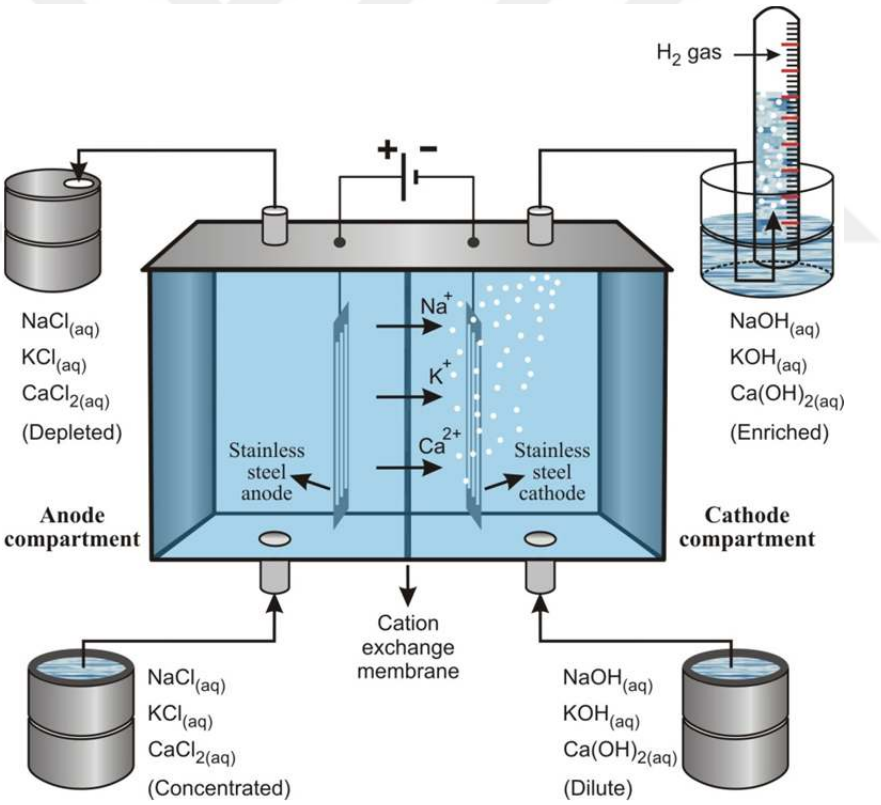

Figure 4.15. Schematic of the experimental run of Chlor-alkali process.

Experiments were continued by varying the parameters namely mass flow rate, operating temperature, and cell voltage. These experimental parameters are:

- Mass flow rate: 0.3 g/s, 0.5 g/s, 0.7 g/s.
- Operating temperature: 25 °C, 45 °C, 60 °C.
- Cell voltage: 2.5 V, 3 V, 3.5 V.

Depending on the kind of salt solution ($NaCl_{(aq)}$, $KCl_{(aq)}$ and $CaCl_{2(aq)}$) entering the anode compartment, the membrane allows positive ions only (Na^+, K^+ and Ca^{2+}) to pass from the anode compartment to the cathode compartment. Thus, hydrogen gas (H_2) is released from the cathode compartment and Sodium Hydroxide ($NaOH$), Potassium Hydroxide (KOH), and Calcium Hydroxide ($Ca(OH)_2$) solutions are formed depending on the kind of positive ion passing through the membrane in the cathode compartment simultaneously. The volume of the produced hydrogen gas is measured by the volumetric displacement technique with the help of a graduated cylinder. On the other hand, in the anode compartment, a large amount of chlorine-based chemical species such as chlorine gas, chlorate, and hypochlorous acid are available for reduction at the anode. An appropriate electrode should be used for chlorine gas discharge in the anode compartment. Although stainless steel can be used as an anode in so many chemical reactions because of its corrosion-resistant nature and good electrical conductivity, it is not stable in chlorine media. Therefore, serious contamination was observed with the formation of chlorine-based chemicals in the anode compartment instead of chlorine gas output. So, it is concluded that stainless steel cannot be used as the anode because of the unstable nature of chlorine.

5. ANALYSES

In this section, necessary basic thermodynamic concepts and equations used to evaluate the system performance thermodynamically and compare it with the experimental results, as well as the assumptions will be discussed.

5.1. Making Assumptions

Scientific studies involve making assumptions, even if we want to avoid them. Reasonable assumptions are used in scientific studies to simplify the procedure and calculations. The assumptions accepted in this study are:

- The environmental pressure (P_O) is 1 Atm.
- The environmental temperature (T_O) is 25 ºC.
- Heat losses are not considered.
- Hydrogen gas is assumed to be ideal and pure.
- Kinetic and potential energy changes are insignificant.
- Voltage losses in connecting cables are negligible.
- All processes take place in a steady state.
- All flows are laminar.
- Reactions in the control volume are assumed to be complete.

5.2. Basic Thermodynamic Concepts

To calculate the energy and exergy efficiencies of any system, mass, energy, entropy, and exergy balance equations of that system are needed. By using these balance equations, heat and work input-output, entropy production, exergy destruction rate, and energetic and exergetic activities can be evaluated.

5.2.1. Mass Balance Equation

According to the conservation of mass principle, the total mass difference entering and leaving a control volume at a certain period is equal to the change in the total mass in the control volume. This change can be in the form of an increase or decrease depending on which of the total masses entering or leaving is more than the other. Accordingly, the change in total mass for the control volume in a given period can be written as (Cengel and Boles, 2013):

$$\sum m_{in} - \sum m_{out} = \Delta m_{CV} \tag{5.1}$$

where $\sum m_{in}$ is the total mass entering the control volume, $\sum m_{out}$ is the total mass leaving the control volume, and Δm_{CV} is the change in the total mass in the control volume. Equation (5.1) can be arranged per unit time as follows:

$$\sum \dot{m}_{in} - \sum \dot{m}_{out} = \frac{dm_{CV}}{dt} \tag{5.2}$$

where $\sum \dot{m}_{in}$ is the total amount of mass entering the control volume per unit time, $\sum \dot{m}_{out}$ is the total amount of mass leaving the control volume per unit time, and $\frac{dm_{CV}}{dt}$ is the total amount of mass change per unit time in the control volume. One of the total masses entering or leaving a control volume can be more than the other or they can also be equal to each other. For incompressible fluids, since the total mass in the control volume will not change in stable systems with continuous flow, according to the principle of conservation of mass, the total fluid masses entering and leaving the control volume are equal to each other. Accordingly, Equation (5.2) can be written as:

$$\sum \dot{m}_{in} = \sum \dot{m}_{out} \tag{5.3}$$

5.2.2. Energy Balance Equation

According to the principle of conservation of energy, also known as the first law of thermodynamics, the difference between the total energies entering and leaving a control volume is equal to the change in the total energy in the control volume. This change can be in the form of an increase or a decrease depending on which of the total energies entering or leaving is greater than the other. Energy transitions in the inlet or outlet direction in the control volume can occur with heat and work transitions, and mass flow. Accordingly, the change in total energy for any control volume can be written as (Cengel and Boles, 2013):

$$E_{in} - E_{out} = \Delta E_{CV} \tag{5.4}$$

where E_{in} is the total energy entering the control volume with heat and work transitions and mass flow, E_{out} is the total energy leaving the control volume with heat and work transitions and mass flow, and ΔE_{CV} is the change in total energy in the control volume. Let's take a closer look at the factors that affect the energy transition.

- **Energy transfer with heat:** Heat input to any control volume increases the internal energy of the system as it will increase the energy of the molecules, while heat output from the control volume decreases the internal energy of the system since it means that the molecules will lose energy. For example, when a water heater is started, the temperature of the water inside it increases, while when it is stopped, the temperature of the water inside decreases over time.
- **Energy transfer with work:** If there is no temperature difference with the surroundings of any control volume, the energy transfer can only be by work transfer. This event can be in the form of the movement of a piston, rotation

of a shaft, or the presence of a current-flowing resistor in the control volume. Work done on a system increases the energy of the system, while work done by the system decreases the energy of the system. For example, motors and turbines produce work, while pumps and compressors consume work.

- **Energy transfer with mass:** When mass input is provided to any control volume, the energy of the system increases since the incoming mass will bring with it a certain energy, while when mass output is provided from the control volume, the energy of the system decreases because the outgoing mass will take with it a certain energy. If mass input and output occur simultaneously in the control volume, the energy of the system may increase or decrease depending on which one has more energy than the other.

Accordingly, Equation (5.4) can be written more precisely as:

$$Q_{in} + W_{in} + E_{mass(in)} - Q_{out} - W_{out} - E_{mass(out)} = \Delta E_{CV} \quad (5.5)$$

where Q_{in}, W_{in}, $E_{mass(in)}$ are the energies entering the control volume with heat and work transitions and mass flow, Q_{out}, W_{out}, $E_{mass(out)}$ are the energies leaving the control volume with heat and work transitions and mass flow, and ΔE_{CV} is the change in total energy in the control volume. Equations (5.4) and (5.5) can be arranged per unit time as follows:

$$\dot{E}_{in} - \dot{E}_{out} = \frac{dE_{CV}}{dt} \quad (5.6)$$

$$\dot{Q}_{in} + \dot{W}_{in} + \dot{E}_{mass(in)} - \dot{Q}_{out} - \dot{W}_{out} - \dot{E}_{mass(out)} = \frac{dE_{CV}}{dt} \quad (5.7)$$

where $\dot{E}_{in}$ is the total energy entering the control volume with heat transfer ($\dot{Q}_{in}$), work transfer ($\dot{W}_{in}$), mass flow ($\dot{E}_{mass(in)}$), and $\dot{E}_{out}$ is the total energy leaving the control volume with heat transfer ($\dot{Q}_{out}$), work transfer ($\dot{W}_{out}$), mass flow ($\dot{E}_{mass(out)}$), and $\frac{dE_{CV}}{dt}$ is the total energy change per unit time for the control volume. Since the total energy does not change in continuous flow systems, the sum of the energies entering the control volume with heat, work transitions, and mass flow and the sum of the energies leaving the control volume with heat, work transitions, and mass flow are equal to each other. Accordingly, Equation (5.6) can be written as:

$$\dot{E}_{in} = \dot{E}_{out} \tag{5.8}$$

or Equation (5.7) can be written as:

$$\dot{Q}_{in} + \dot{W}_{in} + \dot{E}_{mass(in)} = \dot{Q}_{out} + \dot{W}_{out} + \dot{E}_{mass(out)} \tag{5.9}$$

The total energy of a simple compressible mass consists of the internal energy (u) which is related to its molecular structure and molecular mobility, kinetic energy (ke) related to its motion concerning a reference point, and potential energy (pe) related to its height in the gravitational field. But if the mass is in flow, it is necessary to add the flow energy (PV) to them. Here, P and V denote the pressure and volume of the fluid portion, respectively. Accordingly, the total energy (specific energy) of the unit mass in the flow can be written as:

$$e = PV + u + ke + pe \tag{5.10}$$

where e is the specific energy. Since $PV + u$ is known as specific enthalpy and denoted as h, Equation (5.10) can be arranged as follows:

$$e = h + ke + pe = h + \frac{v^2}{2} + gz \tag{5.11}$$

where v is speed, z is the height relative to a reference point, and g is the gravitational acceleration. Thus, the total energy carried by a fluid with uniform properties with a mass flow rate ṁ can be written as:

$$\dot{E}_{mass} = \dot{m}(h + \frac{v^2}{2} + gz) \tag{5.12}$$

If the changes in kinetic and potential energies are ignored, Equation (5.12) can be written as:

$$\dot{E}_{mass} = \dot{m}h \tag{5.13}$$

Using Equation (5.13), Equation (5.9) can be arranged as follows:

$$\dot{Q}_{in} + \dot{W}_{in} + \sum \dot{m}_{in} h = \dot{Q}_{out} + \dot{W}_{out} + \sum \dot{m}_{out} h \tag{5.14}$$

5.2.3. Entropy Balance Equation

Entropy is a measure of the molecular disorder of a system. Since the molecules of a solid substance do not move relative to each other, they behave more regularly. However, since the molecules of a gaseous substance are mobile, it is difficult to define the microscopic state of the system at any given moment. Therefore, entropy also increases in the gaseous state compared to the solid state. The second law of thermodynamics states that entropy can be produced and not destroyed in a system. This is caused by irreversibilities in the system such as friction, chemical reactions, compression, and expansion. Therefore, the difference in total entropies entering and leaving any control volume will not equal the change in total entropy. Entropy production should also be added to this difference.

Entropy transitions in the inlet or outlet direction in the control volume can only occur with heat transfer and mass flow. It is also worth emphasizing that there is no entropy transfer with work. Accordingly, the change in total entropy for the control volume can be written as (Cengel and Boles, 2013):

$$S_{in} - S_{out} + S_{pro.} = \Delta S_{CV} \tag{5.15}$$

where S_{in} is the total entropy entering the control volume by heat transfer and mass flow, S_{out} is the total entropy leaving the control volume by heat transfer and mass flow, $S_{pro.}$ is the total entropy produced in the control volume due to irreversibility, and ΔS_{CV} is the change in total entropy in the control volume. Let's take a closer look at the factors that affect the entropy transition.

- **Entropy transfer with heat:** When heat transfer to a system is provided, the entropy of the system increases together with its molecular disorder, since the energy of the system increases. The entropy transfer (S_{heat}) associated with the heat transfer is defined as the ratio of the heat transferred to a control volume (Q_{CV}) to the absolute temperature (T_0) at the system boundary.

Accordingly, the entropy transition through heat transfer can be written as:

$$S_{heat} = \frac{Q_{CV}}{T_0} \tag{5.16}$$

- **Entropy transfer with mass:** If the entropy of unit mass (specific entropy) is denoted by s, the entropy transition associated with the mass flow (S_{mass}) is defined as the mass (m) entering or leaving a control volume multiplied by the specific entropy (s).

Accordingly, the entropy transition with the mass flow can be written as:

$$S_{mass} = ms \tag{5.17}$$

Thus, Equation (5.15) can be written more precisely as:

$$\sum \frac{Q_{CV}}{T_o} + \sum m_{in} s_{in} - \sum m_{out} s_{out} + S_{pro.} = \Delta S_{CV} \tag{5.18}$$

Equation (5.18) can be arranged per unit time as follows:

$$\sum \frac{\dot{Q}_{CV}}{T_o} + \sum \dot{m}_{in} s_{in} - \sum \dot{m}_{out} s_{out} + \dot{S}_{pro.} = \frac{dS_{CV}}{dt} \tag{5.19}$$

where $\sum \frac{\dot{Q}_{CV}}{T_o}$ and $\sum \dot{m}_{in} s_{in}$ are the total entropies entering the control volume per unit time through a heat transfer and mass flow, $\sum \dot{m}_{out} s_{out}$ is the total entropy leaving the control volume via mass flow per unit time, $\dot{S}_{pro.}$ is the entropy produced per unit time in the control volume, and $\frac{dS_{CV}}{dt}$ is the entropy change per unit time in the control volume. Equation (5.19) can be arranged as follows since there will be no change in entropies of continuous flow systems:

$$\sum \frac{\dot{Q}_{CV}}{T_o} + \sum \dot{m}_{in} s_{in} + \dot{S}_{pro.} = \sum \dot{m}_{out} s_{out} \tag{5.20}$$

5.2.4. Exergy Balance Equation

Exergy is defined as the maximum work that can be extracted from a system interacting with a reference counted environment (Dincer and Rosen, 2012). While mass and energy are conserved throughout the processes in a system, entropy is produced and exergy destruction occurs due to irreversibility. So, to offer more

realistic suggestions for improving the efficiency losses caused by irreversibility in industrial processes, exergy analysis should be done as well as energy analysis (BoroumandJazi et al. 2013). While the quantity of energy is important in energy analysis, the quality of energy comes to the fore in exergy analysis. Therefore, many researchers say that the thermodynamic performance of a system should be evaluated by exergy analysis, as it gives more insight into the improvement of system efficiency (Dincer and Rosen, 2005).

To find the total exergy change in a control volume, it is necessary to subtract both the total exergy leaving and the total exergy destruction from the total exergy entering. Exergy transitions in the inlet or outlet direction of a control volume can be provided by heat, work, and mass flow, as in energy. Accordingly, the change in total exergy for a control volume can be written as (Cengel and Boles, 2013):

$$\mathrm{Ex_{in}} - \mathrm{Ex_{out}} - \mathrm{Ex_d} = \Delta \mathrm{Ex_{CV}} \tag{5.21}$$

where $\mathrm{Ex_{in}}$ is the total exergy entering the control volume with heat, work, and mass flow, $\mathrm{Ex_{out}}$ is the total exergy leaving the control volume with heat, work, and mass flow, $\mathrm{Ex_d}$ is the exergy destruction in the control volume, and $\Delta \mathrm{Ex_{CV}}$ is the change in total exergy in the control volume.

- **Exergy transfer with heat:** In an environment where the reference temperature is $\mathrm{T_0}$ only a part of the energy of a heat source of temperature at T can be converted into useful work. This is also known as the Carnot efficiency $(1 - \frac{\mathrm{T_0}}{\mathrm{T}})$. Therefore, when a heat input of Q is provided to a system, exergy input is provided as much as the amount obtained by multiplying the Carnot efficiency with this heat.

Accordingly, the exergy transfer resulting from the heat transfer can be written using the Carnot efficiency as follows:

$$Ex_{heat} = \left(1 - \frac{T_0}{T}\right) Q \tag{5.22}$$

- **Exergy transfer with work:** Since exergy is a useful work potential, the work equivalent of a given energy is also an indicator of its exergy. The exergy transitions that occur in situations such as shaft work and electrical work are equal to those works themselves. However, in systems that undergo volume change, such as the piston-cylinder mechanism, the work done against the environment ($W_{env.}$) cannot be reused, so it must be removed from the moving boundary work.

Accordingly, the exergy transfer with work to a control volume can be written as:

$$Ex_{work} = W_{CV} - W_{env.} = W_{CV} - P_0 \frac{dV_{CV}}{dt} \tag{5.23}$$

where P_0 is the ambient pressure and $\frac{dV_{CV}}{dt}$ is the rate of change of the control volume. For cases where the control volume is constant, Equation (5.23) can be arranged as follows:

$$Ex_{work} = W_{CV} \tag{5.24}$$

- **Exergy transfer with mass:** Since mass includes exergy along with energy and entropy, the energy, entropy, and exergy content of a system are directly proportional to the amount of mass it has. Therefore, when a mass flow is provided in the inlet or outlet direction in a system, energy, entropy, and exergy transport takes place also along with the mass.

Accordingly, the exergy transfer that occurs with a mass flow of m to a control volume can be written as:

$$Ex_{mass} = m(ex) \tag{5.25}$$

where (ex) denotes the specific flow exergy and can be written as:

$$ex = (h - h_0) - T_0(s - s_0) + \frac{v^2}{2} + gz \tag{5.26}$$

For a fluid with negligible kinetic and potential energy, the kinetic ($\frac{v^2}{2}$) and potential energy (gz) expressions can be removed from the equation. In this case, Equation (5.26) can be arranged as:

$$ex = (h - h_0) - T_0(s - s_0) \tag{5.27}$$

Thus, Equation (5.22) can be rewritten as:

$$\sum Ex_{heat} - \sum Ex_{work} + \sum Ex_{(mass)in} - \sum Ex_{(mass)out} - Ex_d = \Delta Ex_{CV} \tag{5.28}$$

where Ex_{heat} and Ex_{work} are the exergy transitions associated with heat transfer and work transition, and Ex_{mass} is the exergy transition with the mass flow. Equation (5.28) can be arranged per unit time as follows:

$$\sum \dot{E}x_{heat} - \sum \dot{E}x_{work} + \sum \dot{E}x_{(mass)in} - \sum \dot{E}x_{(mass)out} - \dot{E}x_d = \frac{dEx_{CV}}{dt} \tag{5.29}$$

where $\sum \dot{E}x_{heat}$ ve $\sum \dot{E}x_{work}$ are the total exergy associated with heat transfer and work transition per unit time in the control volume, $\sum \dot{E}x_{(mass)in}$ is the total exergy entering the control volume through mass flow per unit time, $\sum \dot{E}x_{(mass)out}$ is the

total exergy leaving the control volume through the mass flow per unit time, $\dot{E}x_d$ is the exergy destruction per unit time in the control volume, and $\frac{dEX_{CV}}{dt}$ is the exergy change per unit time in the control volume. Since there will be no change in the exergy of a continuous flow system (steady-state and steady-flow), Equation (5.29) can be arranged as follows:

$$\sum \dot{E}x_{(heat)in} + \sum \dot{E}x_{(work)in} + \sum \dot{m}_{in} ex_{in} = \sum \dot{E}x_{(heat)out} + \sum \dot{E}x_{(work)out} + \sum \dot{m}_{out} ex_{out} + \dot{E}x_d \quad (5.30)$$

5.3. Balance Equations Adapted for a Chlor-Alkali Reactor

Balance equations are needed to evaluate thermodynamically and to make efficiency calculations for the reactor. Therefore the necessary balance equations are written according to the flow chart of the reactor in Figure 5.1.

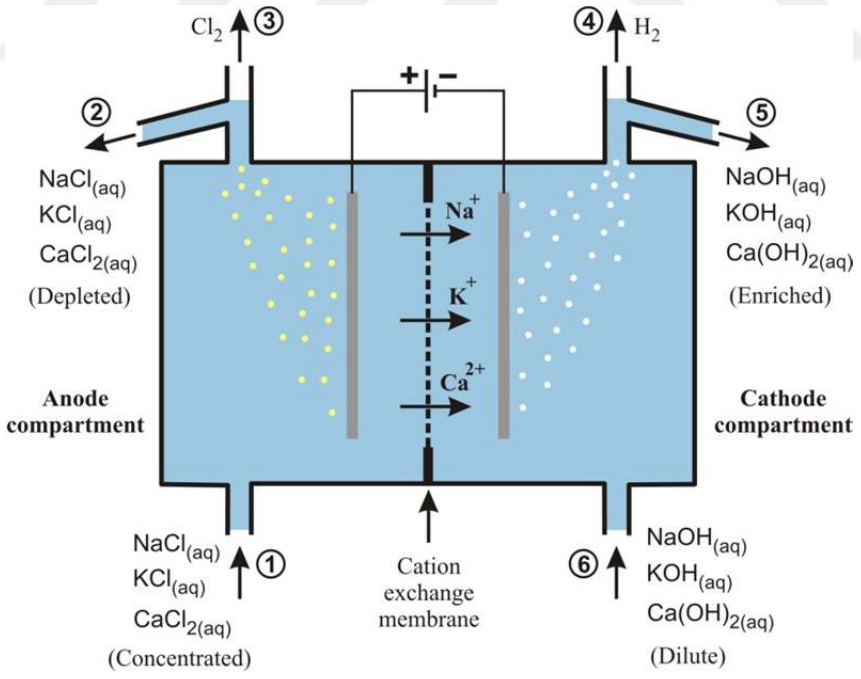

Figure5.1. Flow chart of the Chlor-alkali reactor.

5.3.1 Mass Balance Equation for the Reactor

Using Equation (5.3), the mass balance equation for the reactor per unit time can be written as:

$$\dot{m}_1 + \dot{m}_6 = \dot{m}_2 + \dot{m}_3 + \dot{m}_4 + \dot{m}_5 \tag{5.31}$$

where $\dot{m}_1$ is the mass flow rate of condensed brine entering the anode chamber of the reactor and $\dot{m}_2$ is the mass flow rate of diluted brine leaving the anode chamber. Similarly, $\dot{m}_6$ is the mass flow rate of the diluted base entering the cathode chamber of the reactor and $\dot{m}_5$ is the mass flow rate of the concentrated base leaving the cathode chamber. Mass flow rates of hydrogen and chlorine gases leaving the reactor are also shown as $\dot{m}_4$, $\dot{m}_3$, respectively.

5.3.2. Energy Balance Equation for the Reactor

Using Equation (5.14), the energy balance equation for the reactor per unit time can be written as:

$$\dot{m}_1 h_1 + \dot{m}_6 h_6 + \dot{W}_{in} + \dot{Q}_{in} = \dot{m}_2 h_2 + \dot{m}_3 h_3 + \dot{m}_4 h_4 + \dot{m}_5 h_5 \tag{5.32}$$

where h_{1-6} are the specific enthalpies entering and leaving the reactor together with the mass flow rates at the inlet and outlet points, $\dot{W}_{in}$ is the electrical power supplied to the reactor per unit time by the power source, and $\dot{Q}_{in}$ is the amount of heat required per unit time for the operating temperature above the ambient temperature. It is clear that the $\dot{Q}_{in}$ will be taken as zero for an experiment performed at ambient temperature. The electrical power applied to the reactor is calculated as:

$$\dot{W}_{in} = Vi \tag{5.33}$$

where V is the voltage applied to the reactor in volts, i is the current flowing through the reactor in amperes in response to this applied voltage.

5.3.3. Entropy Balance Equation for the Reactor

Using Equation (5.20), the entropy balance equation for the reactor per unit time can be written as:

$$\frac{\dot{Q}_{in}}{T_0} + \dot{m}_1 s_1 + \dot{m}_6 s_6 + \dot{S}_{pro.} = \dot{m}_2 s_2 + \dot{m}_3 s_3 + \dot{m}_4 s_4 + \dot{m}_5 s_5 \quad (5.34)$$

where s_{1-6} are the specific entropies entering and leaving the reactor together with the mass flow rates at the inlet and outlet points, $\frac{\dot{Q}_{in}}{T_0}$ is the rate of entropy entering the reactor through heat transfer, and $\dot{S}_{pro.}$ is the amount of entropy produced per unit of time.

5.3.4. Exergy Balance Equation for the Reactor

Using Equation (5.30), the exergy balance equation for the reactor per unit time can be written as:

$$\left(1 - \frac{T_0}{T}\right)\dot{Q}_{in} + \dot{W}_{in} + \dot{m}_1 ex_1 + \dot{m}_6 ex_6 = \dot{m}_2 ex_2 + \dot{m}_3 ex_3 + \dot{m}_4 ex_4 + \dot{m}_5 ex_5 + \dot{E}x_d \quad (5.35)$$

where ex_{1-6} are the specific exergies entering and leaving the reactor together with the mass flow rates at the inlet and outlet points, T_0 is the ambient temperature, T is the operating temperature, $\dot{Q}_{in}$ and $\dot{W}_{in}$ are the amounts of heat and work inputs per unit time, $\dot{E}x_d$ is the exergy destruction per unit time. Since exergy destruction is directly proportional to entropy generation, $\dot{E}x_d$ can be written as:

$$\dot{E}x_d = T_0 \dot{S}_{pro.} \quad (5.36)$$

5.3.5. Energy Efficiency

Systems can have more than one useful energy output. Energy efficiency calculations can be made according to a single output or include more than one output. Since this study focuses only on hydrogen production, the energy efficiency of the system will be calculated based on hydrogen production only. So, the energy efficiency equation of the present Chlor-alkali reactor according to Equation 3.10 can be written as follows:

$$\eta_{en} = \frac{\dot{m}_4 HHV_{H_2}}{\dot{W}_{in} + \dot{m}_1 h_1 + \dot{m}_6 h_6} \quad (5.37)$$

where HHV is the higher heating value of hydrogen (142 MJ/kg).

5.3.6. Exergy Efficiency

Exergy efficiency is based on the second law of thermodynamics and is important for a better understanding of system performance. That is the exergy efficiency gives an idea about the improvements that can be made by drawing attention to the losses and irreversibilities in the system. So, the exergy efficiency equation of the present Chlor-alkali reactor concerning only hydrogen production according to Equation 3.11 can be written as:

$$\eta_{ex} = \frac{\dot{m}_4 ex_4}{\dot{W}_{in} + \dot{m}_1 ex_1 + \dot{m}_6 ex_6} \quad (5.38)$$

5.3.7. Current Efficiency

Current density can be defined as the ratio of the actual mass of a substance liberated by the passage of current through an electrolyte to the theoretical mass that must be released according to Faraday's law. So, the current efficiency (CA) equation of the present Chlor-alkali reactor concerning only hydrogen production according to Equation 3.13 can be written as:

$$\eta_{CA} = \frac{m_{H_2}}{\tilde{m}_{H_2}} \times 100 \quad (5.39)$$

where m_{H_2} is the mass of produced hydrogen in the experiments and $\tilde{m}_{H_2}$ is the mass of hydrogen that should theoretically be produced.

6. RESULTS AND DISCUSSION

6.1. Hydrogen Production at a Constant Temperature of 25 °C

Figures 6.1, 6.2, and 6.3 shows the hydrogen production rate of tested salts concerning the applied voltage for the three different mass flow rate cases separately at a constant operating temperature of 25 °C.

As shown in Figure 6.1, when the cell voltage is 2.5 V, the minimum hydrogen production rate of NaCl salt is 78.48 mL/h, 79.58 mL/h, and 80.76 mL/h related to the mass flow rates of 0.3 g/s, 0.5 g/s, and 0.7 g/s, respectively. When the cell voltage is 3.5 V, the maximum hydrogen production rate of NaCl salt is 126.84 mL/h, 137.95 mL/h, and 149.16 mL/h related to the same mass flow rates, respectively.

As shown in Figure 6.2, when the cell voltage is 2.5 V, the minimum hydrogen production rate of KCl salt is 95.52 mL/h, 97.32 mL/h, and 98.76 mL/h related to the mass flow rates of 0.3 g/s, 0.5 g/s, and 0.7 g/s, respectively. When the cell voltage is 3.5 V, the maximum hydrogen production rate is 146.28 mL/h, 158.64 mL/h, and 169.8 mL/h for the same mass flow rates.

As shown in Figure 6.3, when the cell voltage is 2.5 V, the minimum hydrogen production rate of $CaCl_2$ salt is 27.36 mL/h, 27.72 mL/h, and 28.2 mL/h related with the mass flow rates of 0.3 g/s, 0.5 g/s, and 0.7 g/s, respectively. When the cell voltage is 3.5 V, the maximum hydrogen production rate is 37.14 mL/h, 37.98 mL/h, and 39.36 mL/h for the same mass flow rates.

As illustrated in Figures 6.1-6.3 hydrogen production exponentially increases since the mobility of the ions also increases with the increase in the cell voltage.

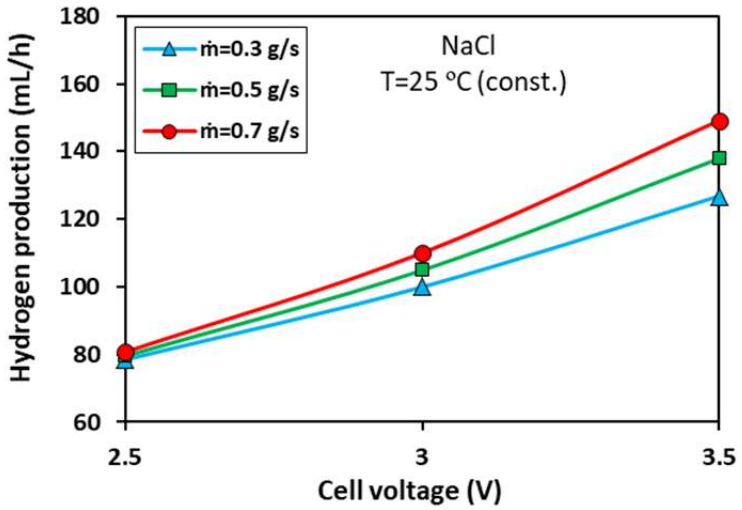

Figure 6.1. Hydrogen production of NaCl according to the applied cell voltage when the operating temperature is constant at 25 ºC.

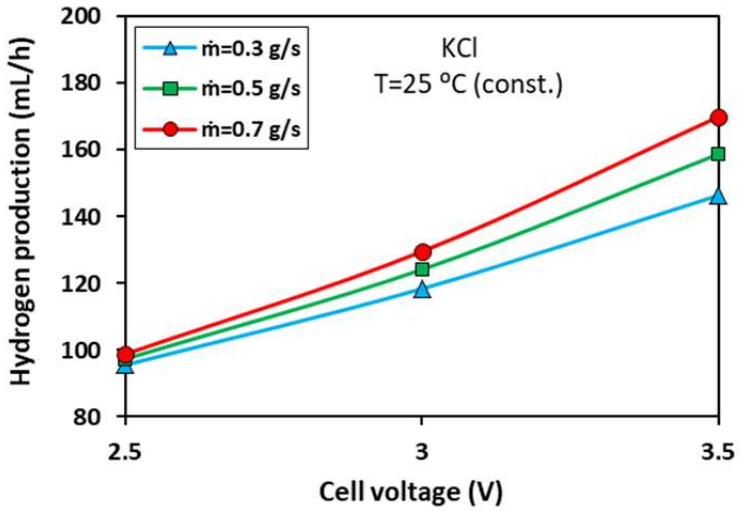

Figure 6.2. Hydrogen production of KCl according to the applied cell voltage when the operating temperature is constant at 25 ºC.

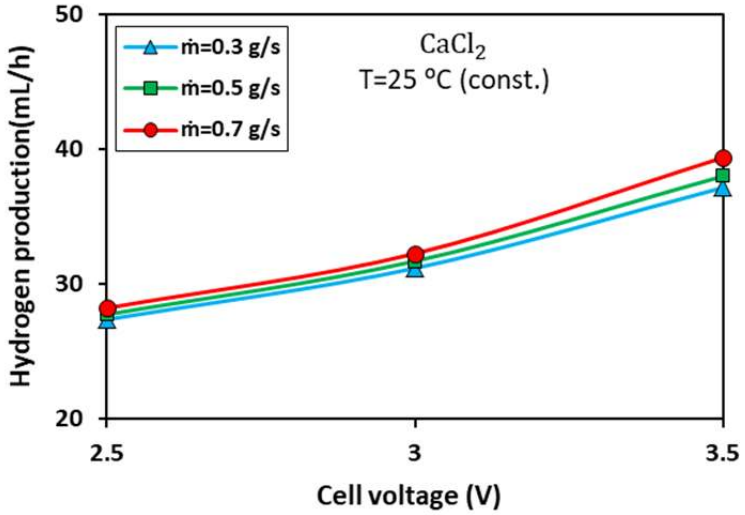

Figure 6.3. Hydrogen production of $CaCl_2$ according to the applied cell voltage when the operating temperature is constant at 25 ºC.

Figures 6.4, 6.5, and 6.6 show the hydrogen production rate of tested salts concerning the mass flow rate for the three different applied cell voltage cases separately at a constant operating temperature of 25 °C.

As shown in Figure 6.4, when the mass flow rate is 0.3 g/s, the minimum hydrogen production rate of NaCl salt is 78.48 mL/h, 99.96 mL/h, and 126.84 mL/h related to the cell voltage of 2.5 V, 3 V, and 3.5 V, respectively. When the mass flow rate is 0.7 g/s, the maximum hydrogen production rate of NaCl salt is 80.76 mL/h, 110.04 mL/h, and 149.16 mL/h related to the same cell voltages, respectively.

As shown in Figure 6.5, when the mass flow rate is 0.3 g/s, the minimum hydrogen production rate of KCl salt is 95.52 mL/h, 118.32 mL/h, and 146.28 mL/h related to the cell voltage of 2.5 V, 3 V, and 3.5 V, respectively. When the mass flow rate is 0.7 g/s, the maximum hydrogen production rate of KCl salt is 98.76 mL/h, 129.48 mL/h, and 169.8 mL/h related to the same cell voltages, respectively.

As shown in Figure 6.6, when the mass flow rate is 0.3 g/s, the minimum hydrogen production rate of $CaCl_2$ salt is 27.36 mL/h, 31.16 mL/h, and 37.14 mL/h related to the cell voltage of 2.5 V, 3 V, and 3.5 V, respectively. When the mass flow rate is 0.7 g/s, the maximum hydrogen production rate of $CaCl_2$ salt is 28.2 mL/h, 32.24 mL/h, and 39.36 mL/h related with the same cell voltages, respectively.

As illustrated in Figures 6.4-6.6 hydrogen production slightly increased since the amount of the ions in the cell also increases with the increase in the mass flow rate.

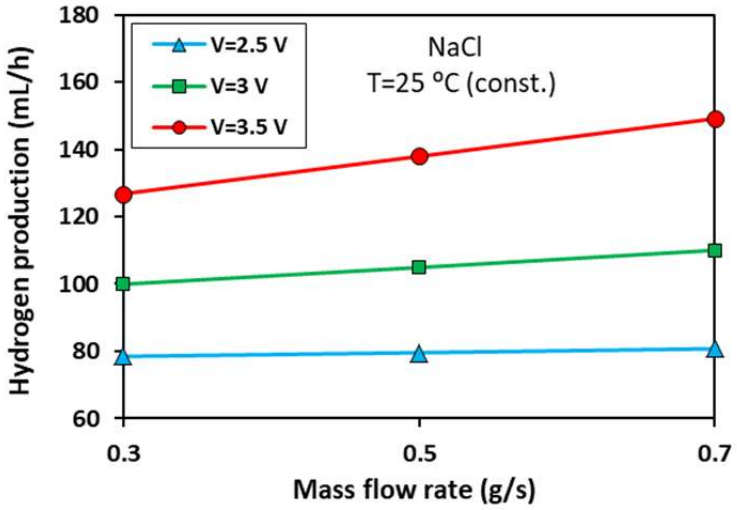

Figure 6.4. Hydrogen production of NaCl according to the mass flow rate when the operating temperature is constant at 25 ºC.

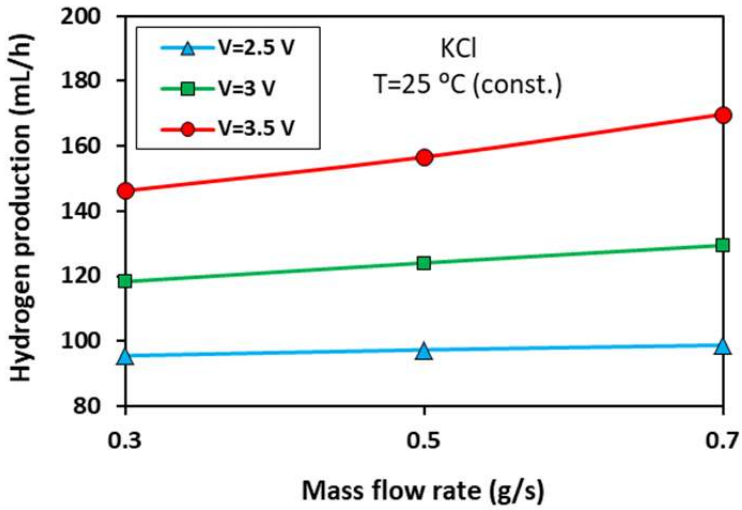

Figure 6.5. Hydrogen production of KCl according to the mass flow rate when the operating temperature is constant at 25 ºC.

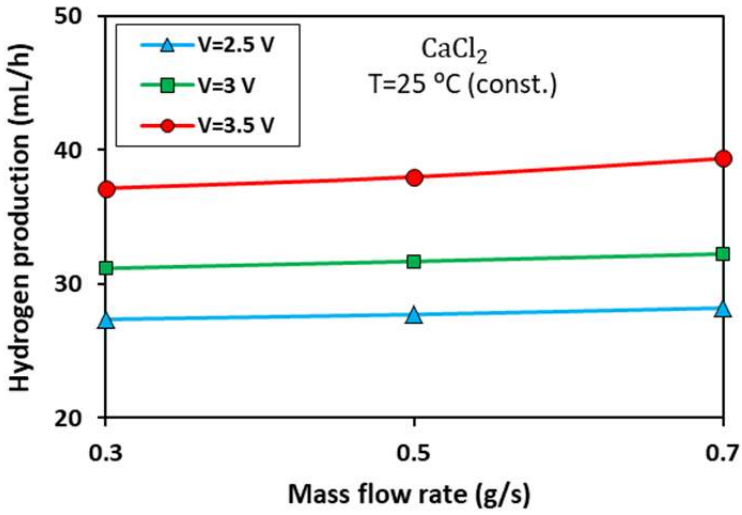

Figure 6.6. Hydrogen production of $CaCl_2$ according to the mass flow rate when the operating temperature is constant at 25 ºC.

6.2. Hydrogen Production at a Constant Temperature of 45 °C

Figures 6.7, 6.8, and 6.9 show the hydrogen production rate of tested salts concerning the applied voltage for the three different mass flow rate cases separately at a constant operating temperature of 45 °C.

As shown in Figure 6.7, when the cell voltage is 2.5 V, the minimum hydrogen production rate of NaCl salt is 95.27 mL/h, 98.38 mL/h, and 101.56 mL/h related to the mass flow rates of 0.3 g/s, 0.5 g/s, and 0.7 g/s, respectively. When the cell voltage is 3.5 V, the maximum hydrogen production rate of NaCl salt is 156.16 mL/h, 173.56 mL/h, and 195.05 mL/h related to the same mass flow rates, respectively.

As shown in Figure 6.8, when the cell voltage is 2.5 V, the minimum hydrogen production rate of KCl salt is 115.32 mL/h, 119.28 mL/h, and 123.36 mL/h related to the mass flow rates of 0.3 g/s, 0.5 g/s, and 0.7 g/s, respectively. When the cell voltage is 3.5 V, the maximum hydrogen production rate is 190.56 mL/h, 204.36 mL/h, and 221.16 mL/h for the same mass flow rates.

As shown in Figure 6.9, when the cell voltage is 2.5 V, the minimum hydrogen production rate of $CaCl_2$ salt is 48.12 mL/h, 48.6 mL/h, and 49.08 mL/h related with the mass flow rates of 0.3 g/s, 0.5 g/s, and 0.7 g/s, respectively. When the cell voltage is 3.5 V, the maximum hydrogen production rate is 85.56 mL/h, 96.68 mL/h, and 108.72 mL/h for the same mass flow rates.

As illustrated in Figures 6.7-6.9 hydrogen production exponentially increases since the mobility of the ions also increases with the increase in the cell voltage.

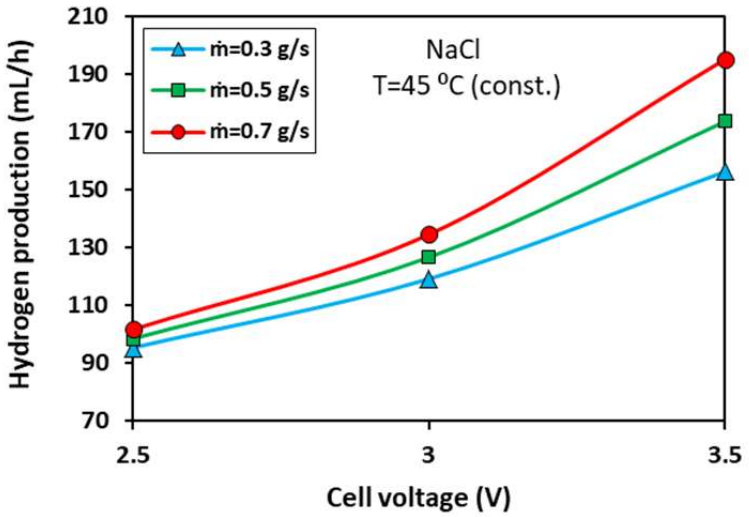

Figure 6.7. Hydrogen production of NaCl according to the applied cell voltage when the operating temperature is constant at 45 ºC.

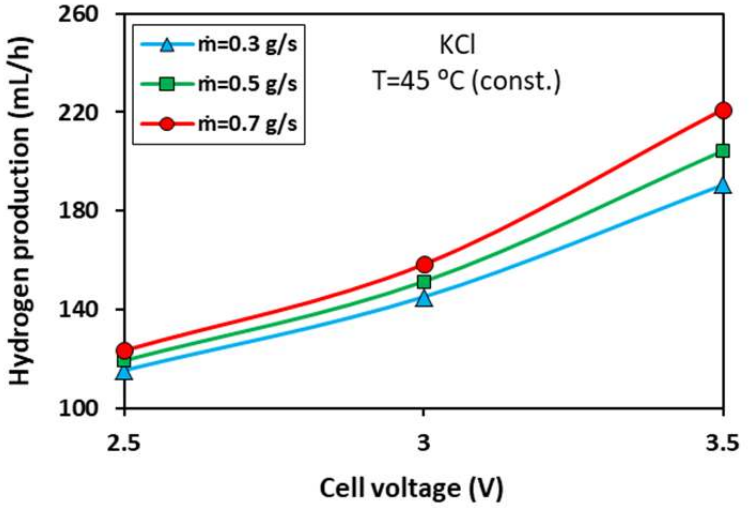

Figure 6.8. Hydrogen production of KCl according to the applied cell voltage when the operating temperature is constant at 45 ºC.

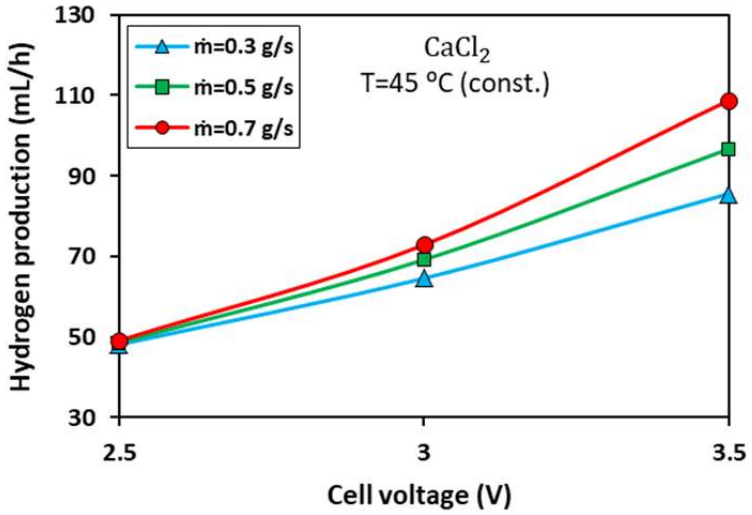

Figure 6.9. Hydrogen production of $CaCl_2$ according to the applied cell voltage when the operating temperature is constant at 45 ºC.

Figures 6.10, 6.11, and 6.12 show the hydrogen production rate of tested salts concerning the mass flow rate for the three different applied cell voltage cases separately at a constant operating temperature of 45 °C.

As shown in Figure 6.10, when the mass flow rate is 0.3 g/s, the minimum hydrogen production rate of NaCl salt is 95.27 mL/h, 119.07 mL/h, and 156.16 mL/h related to the cell voltage of 2.5 V, 3 V, and 3.5 V, respectively. When the mass flow rate is 0.7 g/s, the maximum hydrogen production rate of NaCl salt is 101.56 mL/h, 134.46 mL/h, and 195.05 mL/h related to the same cell voltages, respectively.

As shown in Figure 6.11, when the mass flow rate is 0.3 g/s, the minimum hydrogen production rate of KCl salt is 115.32 mL/h, 145.08 mL/h, and 190.56 mL/h related to the cell voltage of 2.5 V, 3 V, and 3.5 V, respectively. When the mass flow rate is 0.7 g/s, the maximum hydrogen production rate of KCl salt is 123.36 mL/h, 158.28 mL/h, and 221.16 mL/h related to the same cell voltages, respectively.

As shown in Figure 6.12, when the mass flow rate is 0.3 g/s, the minimum hydrogen production rate of $CaCl_2$ salt is 48.12 mL/h, 64.56 mL/h, and 85.56 mL/h related to the cell voltage of 2.5 V, 3 V, and 3.5 V, respectively. When the mass flow rate is 0.7 g/s, the maximum hydrogen production rate of $CaCl_2$ salt is 49.08 mL/h, 72.84 mL/h, and 108.72 mL/h related with the same cell voltages, respectively.

As illustrated in Figures 6.10-6.12 hydrogen production slightly increased since the amount of the ions in the cell also increases with the increase in the mass flow rate.

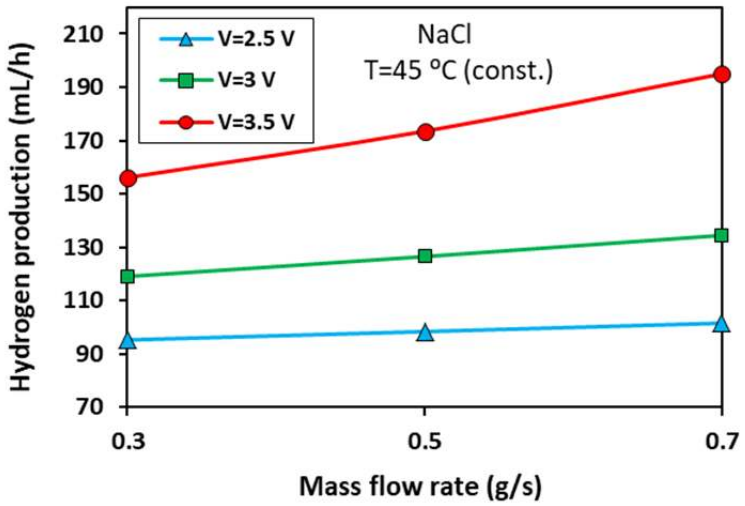

Figure 6.10 Hydrogen production of NaCl according to the mass flow rate when the operating temperature is constant at 45 ºC.

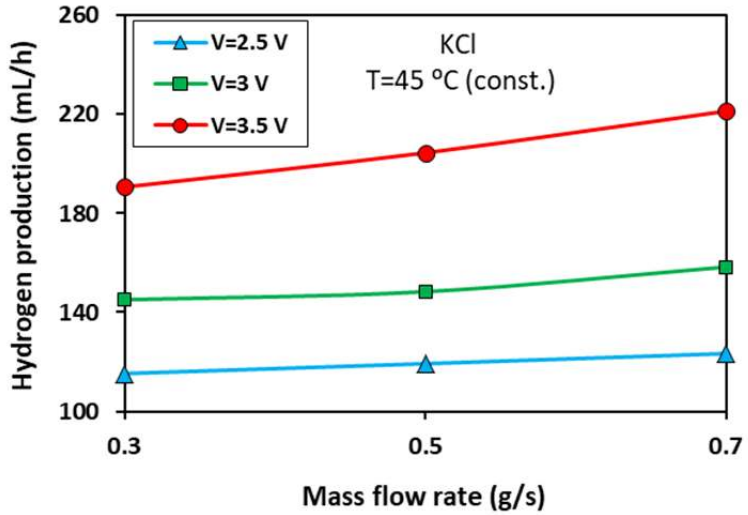

Figure 6.11. Hydrogen production of KCl according to the mass flow rate when the operating temperature is constant at 45 ºC.

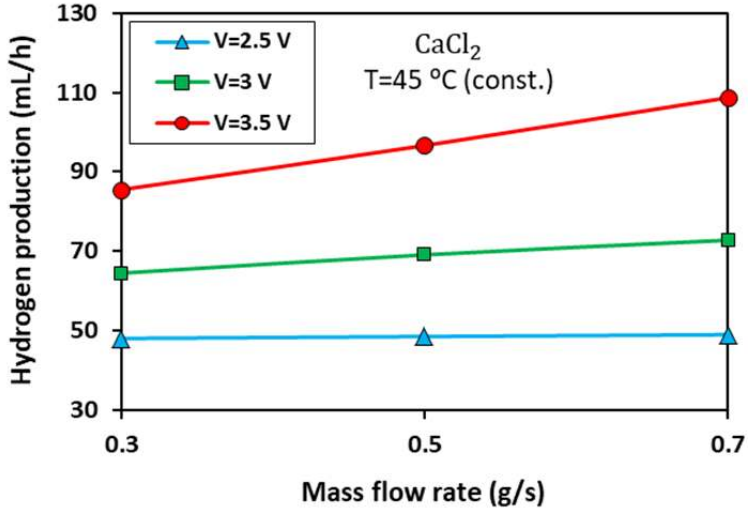

Figure 6.12. Hydrogen production of $CaCl_2$ according to the mass flow rate when the operating temperature is constant at 45 ºC.

6.3. Hydrogen Production at a Constant Temperature of 60 °C

Figures 6.13, 6.14, and 6.15 show the hydrogen production rate of tested salts concerning the applied voltage for the three different mass flow rate cases separately at a constant operating temperature of 60 °C.

As shown in Figure 6.13, when the cell voltage is 2.5 V, the minimum hydrogen production rate of NaCl salt is 111.43 mL/h, 115.48 mL/h, and 119.64 mL/h related to the mass flow rates of 0.3 g/s, 0.5 g/s, and 0.7 g/s, respectively. When the cell voltage is 3.5 V, the maximum hydrogen production rate of NaCl salt is 201.56 mL/h, 225.84 mL/h, and 254.36 mL/h related to the same mass flow rates, respectively.

As shown in Figure 6.14, when the cell voltage is 2.5 V, the minimum hydrogen production rate of KCl salt is 133.8 mL/h, 143.88 mL/h, and 153.36 mL/h related to the mass flow rates of 0.3 g/s, 0.5 g/s, and 0.7 g/s, respectively. When the cell voltage is 3.5 V, the maximum hydrogen production rate is 238.92 mL/h, 260.64 mL/h, and 295.68 mL/h for the same mass flow rates.

As shown in Figure 6.15, when the cell voltage is 2.5 V, the minimum hydrogen production rate of $CaCl_2$ salt is 83.64 mL/h, 87.12 mL/h, and 94.08 mL/h related with the mass flow rates of 0.3 g/s, 0.5 g/s, and 0.7 g/s, respectively. When the cell voltage is 3.5 V, the maximum hydrogen production rate is 179.16 mL/h, 202.08 mL/h, and 225.48 mL/h for the same mass flow rates.

As illustrated in Figures 6.13-6.15 hydrogen production exponentially increases since the mobility of the ions also increases with the increase in the cell voltage.

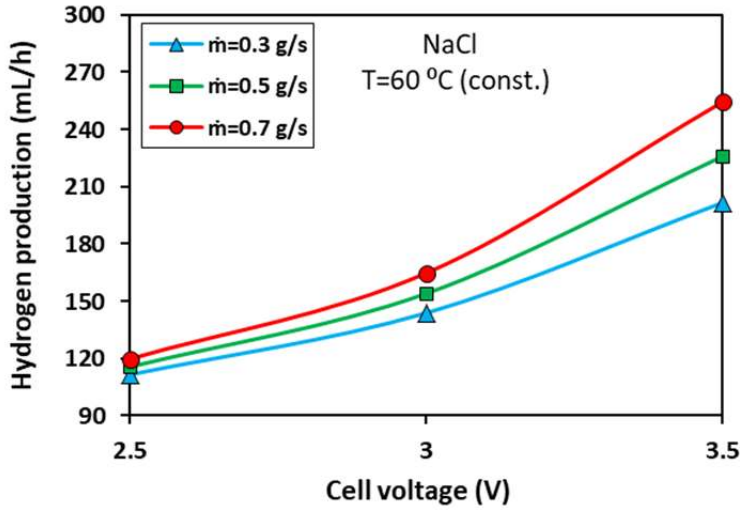

Figure 6.13. Hydrogen production of NaCl according to the cell voltage when the operating temperature is constant at 60 ºC.

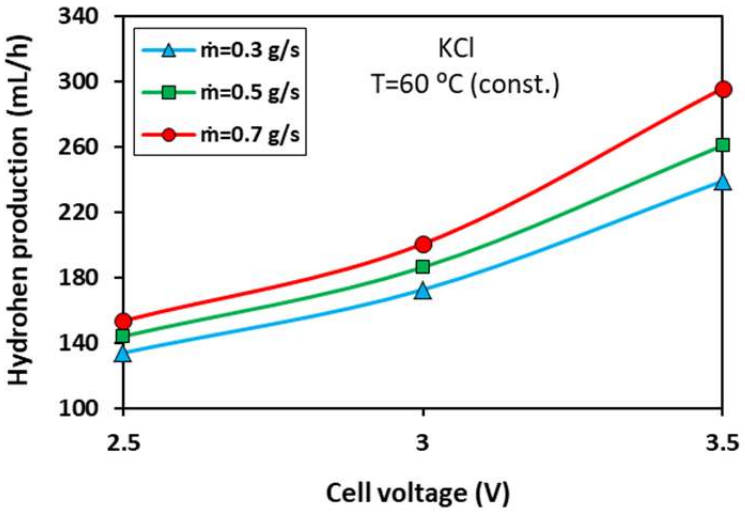

Figure 6.14. Hydrogen production of KCl according to the cell voltage when the operating temperature is constant at 60 ºC.

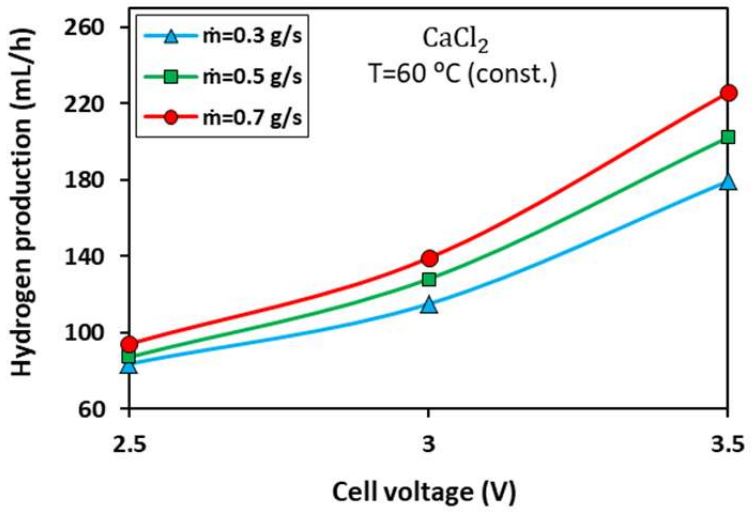

Figure 6.15. Hydrogen production of $CaCl_2$ according to the cell voltage when the operating temperature is constant at 60 ºC.

Figures 6.16, 6.17, and 6.18 show the hydrogen production rate of tested salts concerning the mass flow rate for the three different applied cell voltage cases separately at a constant operating temperature of 60 °C.

As shown in Figure 6.16, when the mass flow rate is 0.3 g/s, the minimum hydrogen production rate of NaCl salt is 95.27 mL/h, 119.07 mL/h, and 156.16 mL/h related to the cell voltage of 2.5 V, 3 V, and 3.5 V, respectively. When the mass flow rate is 0.7 g/s, the maximum hydrogen production rate of NaCl salt is 101.56 mL/h, 134.46 mL/h, and 195.05 mL/h related to the same cell voltages, respectively.

As shown in Figure 6.17, when the mass flow rate is 0.3 g/s, the minimum hydrogen production rate of KCl salt is 115.32 mL/h, 145.08 mL/h, and 190.56 mL/h related to the cell voltage of 2.5 V, 3 V, and 3.5 V, respectively. When the mass flow rate is 0.7 g/s, the maximum hydrogen production rate of KCl salt is 123.36 mL/h, 158.28 mL/h, and 221.16 mL/h related to the same cell voltages, respectively.

As shown in Figure 6.18, when the mass flow rate is 0.3 g/s, the minimum hydrogen production rate of $CaCl_2$ salt is 48.12 mL/h, 64.56 mL/h, and 85.56 mL/h related to the cell voltage of 2.5 V, 3 V, and 3.5 V, respectively. When the mass flow rate is 0.7 g/s, the maximum hydrogen production rate of $CaCl_2$ salt is 49.08 mL/h, 72.84 mL/h, and 108.72 mL/h related with the same cell voltages, respectively.

As illustrated in Figures 6.16-6.18 hydrogen production slightly increased since the amount of the ions in the cell also increases with the increase in the mass flow rate.

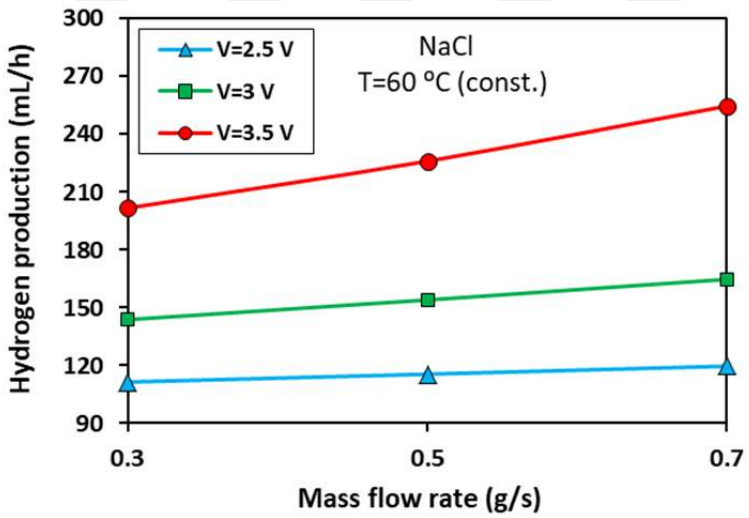

Figure 6.16. Hydrogen production of NaCl according to the mass flow rate when the operating temperature is constant at 60 ºC.

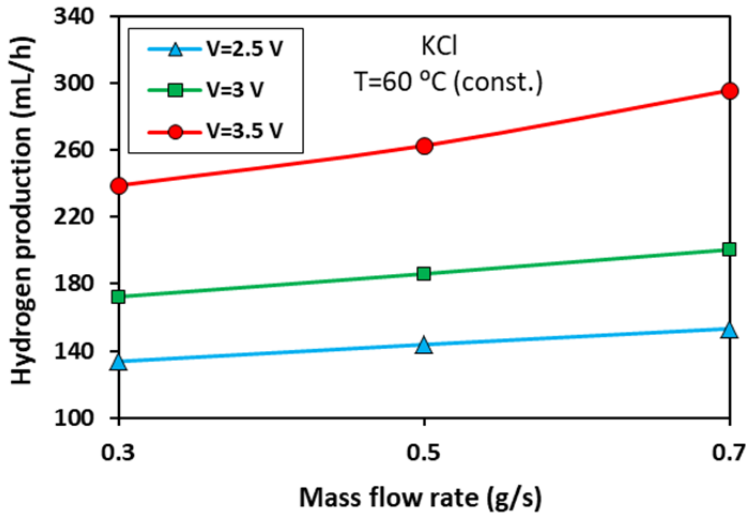

Figure 6.17. Hydrogen production of KCl according to the mass flow rate when the operating temperature is constant at 60 ºC.

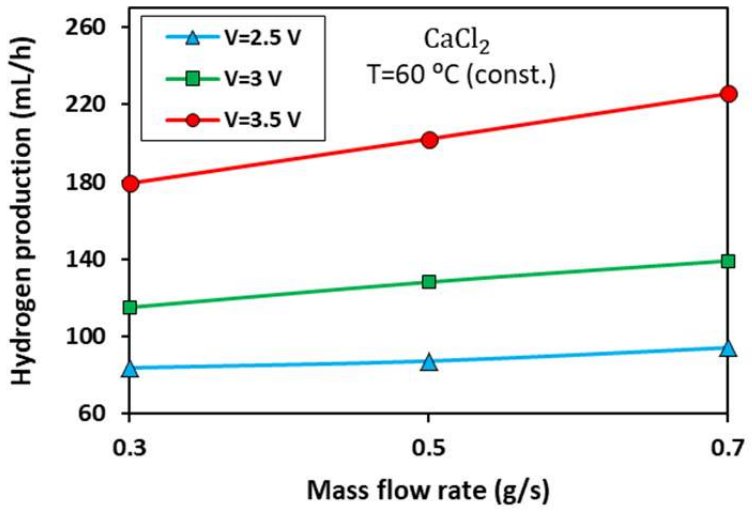

Figure 6.18 Hydrogen production of $CaCl_2$ according to the mass flow rate when the operating temperature is constant at 60 ºC.

6.4. Hydrogen Production at a Constant Mass Flow Rate of 0.3 g/s

Figures 6.19, 6.20, and 6.21 show the hydrogen production rate of tested salts concerning the operating temperature for the three different cell voltage cases separately at a constant mass flow rate of 0.3 g/s.

As shown in Figure 6.19, when the operating temperature is 25 °C, the minimum hydrogen production rate of NaCl salt is 78.48 mL/h, 99.96 mL/h, and 126.84 mL/h related with the cell voltage of 2.5 V, 3 V, and 3.5 V, respectively. When the operating temperature is 60 °C, the maximum hydrogen production rate of NaCl salt is 111.43 mL/h, 143.76 mL/h, and 201.56 mL/h related to the same cell voltages, respectively.

As shown in Figure 6.20, when the operating temperature is 25 °C, the minimum hydrogen production rate of KCl salt is 95.92 mL/h, 118.32 mL/h, and 146.28 mL/h related to the cell voltage of 2.5 V, 3 V, and 3.5 V, respectively. When the operating temperature is 60 °C, the maximum hydrogen production rate is 133.8 mL/h, 172.44 mL/h, and 238.92 mL/h for the same cell voltages.

As shown in Figure 6.21, when the operating temperature is 25 °C, the minimum hydrogen production rate of $CaCl_2$ salt is 27.36 mL/h, 31.16 mL/h, and 37.14 mL/h related to the cell voltage of 2.5 V, 3 V, and 3.5 V, respectively. When the operating temperature is 60 °C, the maximum hydrogen production rate is 83.64 mL/h, 114.96 mL/h, and 179.16 mL/h for the same cell voltages.

As illustrated in Figures 6.19-6.21 hydrogen production exponentially increases since the mobility of the ions also increases with the increase in the operating temperature.

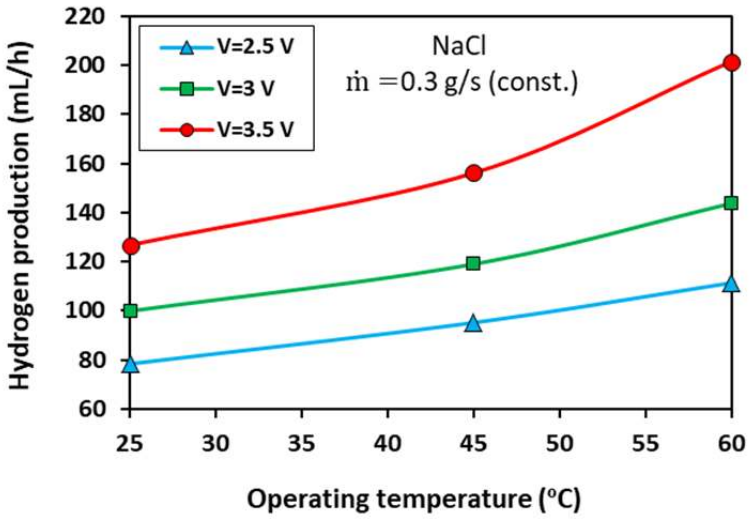

Figure 6.19. Hydrogen production of NaCl according to the operating temperature when the mass flow rate is constant at 0.3 g/s.

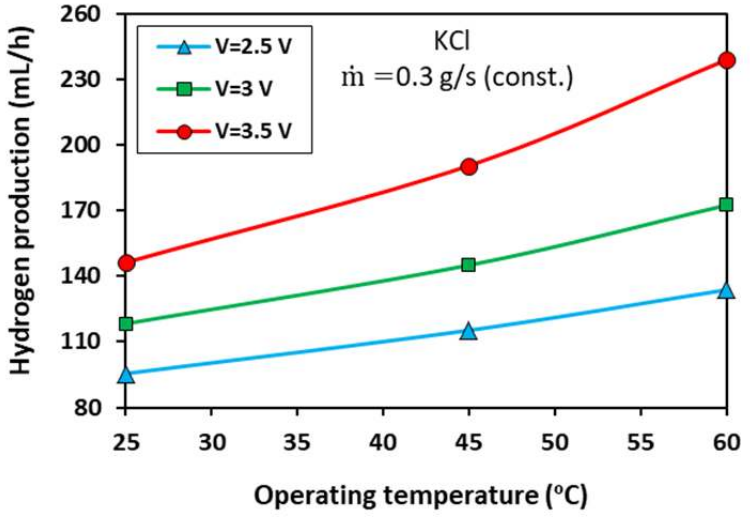

Figure 6.20. Hydrogen production of KCl according to the operating temperature when the mass flow rate is constant at 0.3 g/s.

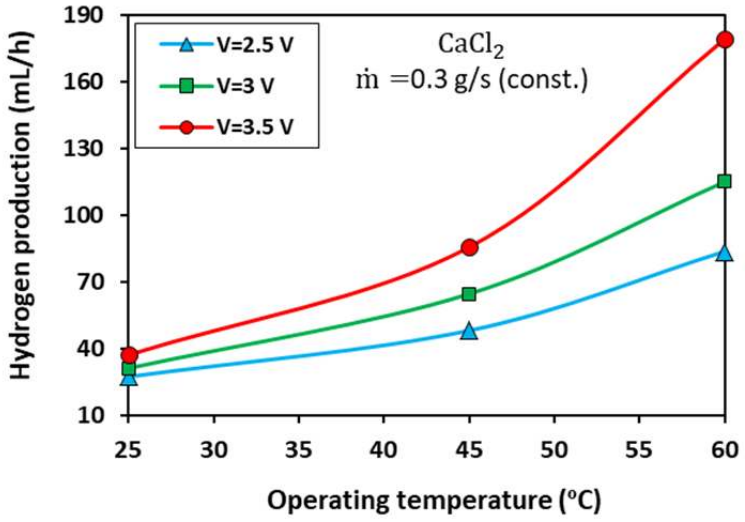

Figure 6.21. Hydrogen production of $CaCl_2$ according to the operating temperature when the mass flow rate is constant at 0.3 g/s.

Figures 6.22, 6.23, and 6.24 show the hydrogen production rate of tested salts concerning the cell voltage for the three different operating temperature cases separately at a constant mass flow rate of 0.3 g/s.

As shown in Figure 6.22, when the cell voltage is 2.5 V, the minimum hydrogen production rate of NaCl salt is 78.46 mL/h, 95.27 mL/h, and 111.43 mL/h related to the operating temperatures of 25 °C, 45 °C, and 60 °C, respectively. When the cell voltage is 3.5 V, the maximum hydrogen production rate of NaCl salt is 126.84 mL/h, 156.16 mL/h, and 201.56 mL/h related to the same operating temperatures, respectively.

As shown in Figure 6.23, when the cell voltage is 2.5 V, the minimum hydrogen production rate of KCl salt is 95.52 mL/h, 115.32 mL/h, and 133.8 mL/h related to the operating temperatures of 25 °C, 45 °C, and 60 °C, respectively. When the cell voltage is 3.5 V, the maximum hydrogen production rate of KCl salt is 146.28 mL/h, 190.56 mL/h, and 238.92 mL/h related to the same operating temperatures, respectively.

As shown in Figure 6.24, when the cell voltage is 2.5 V, the minimum hydrogen production rate of $CaCl_2$ salt is 27.36 mL/h, 48.12 mL/h, and 83.64 mL/h related to the operating temperatures of 25 °C, 45 °C, and 60 °C, respectively. When the cell voltage is 3.5 V, the maximum hydrogen production rate of $CaCl_2$ salt is 37.14 mL/h, 85.56 mL/h, and 179.16 mL/h related to the same operating temperatures, respectively.

As illustrated in Figures 6.22-6.24 hydrogen production exponentially increases since the mobility of the ions also increases with the increase in the operating temperature.

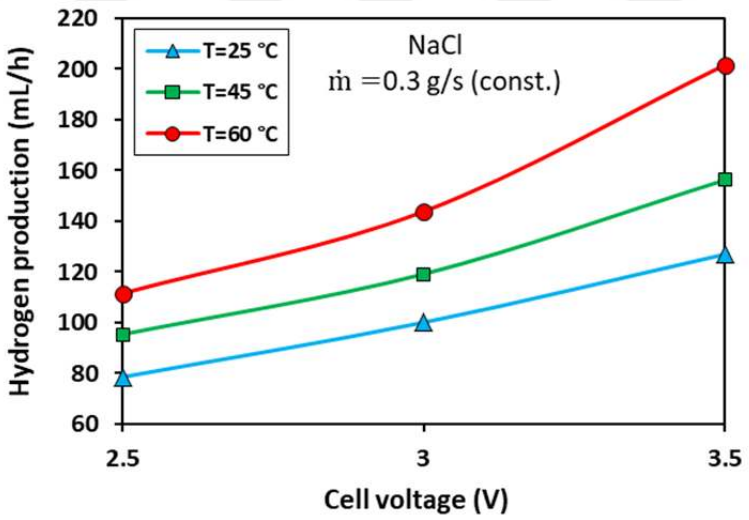

Figure 6.22 Hydrogen production of NaCl according to the cell voltage when the mass flow rate is constant at 0.3 g/s.

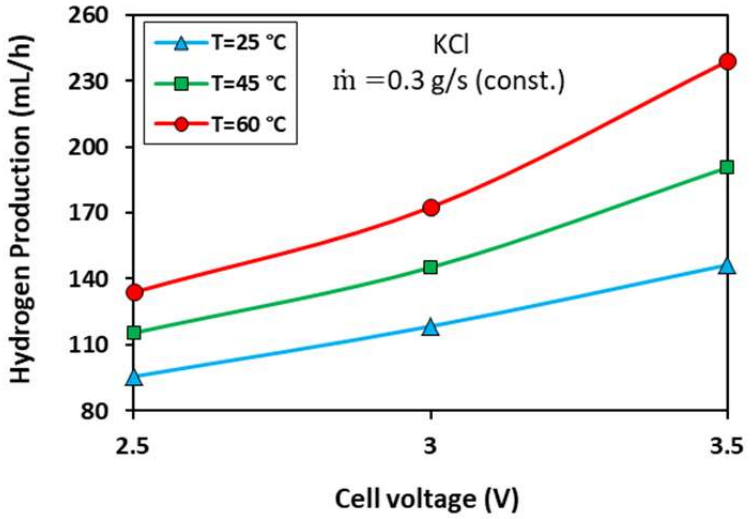

Figure 6.23. Hydrogen production of KCl according to the cell voltage when the mass flow rate is constant at 0.3 g/s.

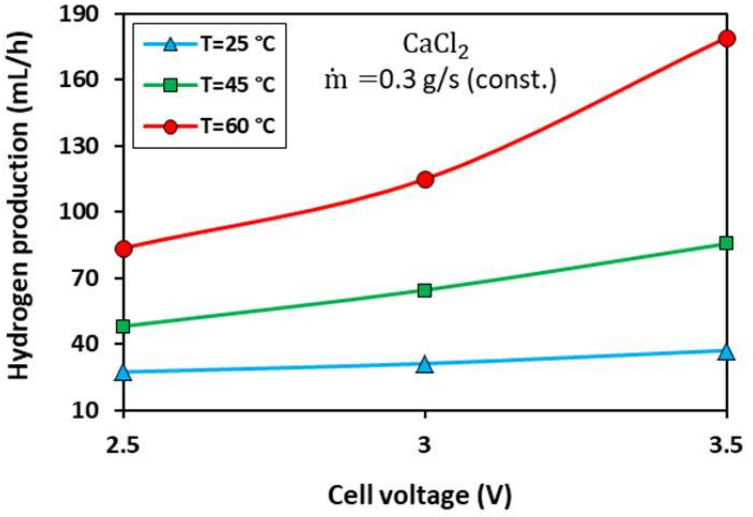

Figure 6.24 Hydrogen production of $CaCl_2$ according to the cell voltage when the mass flow rate is constant at 0.3 g/s.

6.5. Hydrogen Production at a Constant Mass Flow Rate of 0.5 g/s

Figures 6.25, 6.26, and 6.27 show the hydrogen production rate of tested salts concerning the operating temperature for the three different cell voltage cases separately at a constant mass flow rate of 0.5 g/s.

As shown in Figure 6.25, when the operating temperature is 25 °C, the minimum hydrogen production rate of NaCl salt is 79.58 mL/h, 104.92 mL/h, and 137.95 mL/h related to the cell voltage of 2.5 V, 3 V, and 3.5 V, respectively. When the operating temperature is 60 °C, the maximum hydrogen production rate of NaCl salt is 115.48 mL/h, 153.96 mL/h, and 225.84 mL/h related to the same cell voltages, respectively.

As shown in Figure 6.26, when the operating temperature is 25 °C, the minimum hydrogen production rate of KCl salt is 97.32 mL/h, 124.08 mL/h, and 156.64 mL/h related to the cell voltage of 2.5 V, 3 V, and 3.5 V, respectively. When the operating temperature is 60 °C, the maximum hydrogen production rate is 143.88 mL/h, 186.12 mL/h, and 260.64 mL/h for the same cell voltages.

As shown in Figure 6.27, when the operating temperature is 25 °C, the minimum hydrogen production rate of $CaCl_2$ salt is 27.72 mL/h, 31.68 mL/h, and 37.98 mL/h related to the cell voltage of 2.5 V, 3 V, and 3.5 V, respectively. When the operating temperature is 60 °C, the maximum hydrogen production rate is 87.12 mL/h, 128.04 mL/h, and 202.08 mL/h for the same cell voltages.

As illustrated in Figures 6.25-6.27 hydrogen production exponentially increases since the mobility of the ions also increases with the increase in the operating temperature.

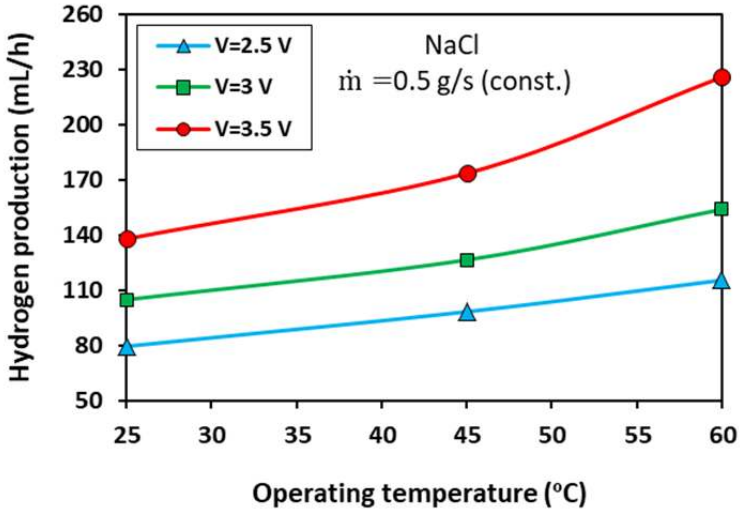

Figure 6.25. Hydrogen production of NaCl according to the operating temperature when the mass flow rate is constant at 0.5 g/s.

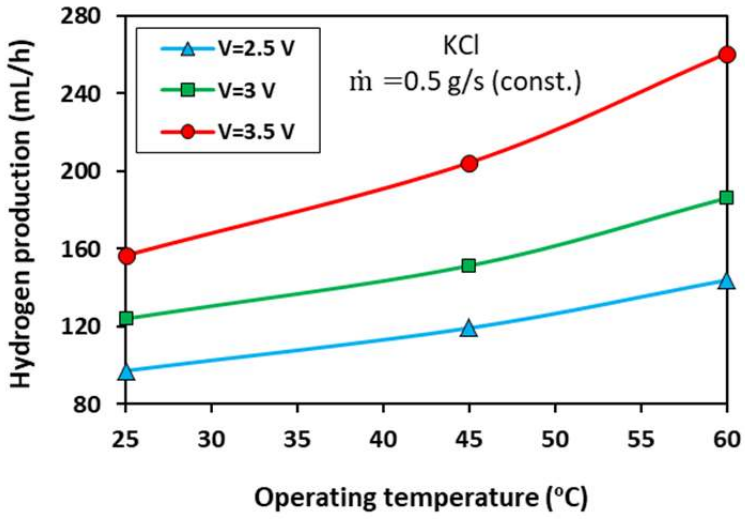

Figure 6 26. Hydrogen production of KCl according to the operating temperature when the mass flow rate is constant at 0.5 g/s.

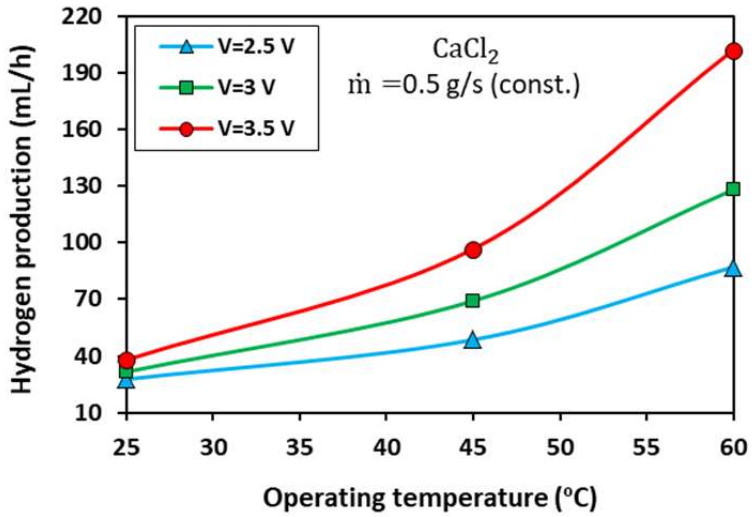

Figure 6.27 Hydrogen production of $CaCl_2$ according to the operating temperature when the mass flow rate is constant at 0.5 g/s.

Figures 6.28, 6.29, and 6.30 show the hydrogen production rate of tested salts concerning the cell voltage for the three different operating temperature cases separately at a constant mass flow rate of 0.5 g/s.

As shown in Figure 6.28, when the cell voltage is 2.5 V, the minimum hydrogen production rate of NaCl salt is 79.58 mL/h, 98.38 mL/h, and 115.48 mL/h related to the operating temperatures of 25 °C, 45 °C, and 60 °C, respectively. When the cell voltage is 3.5 V, the maximum hydrogen production rate of NaCl salt is 137.95 mL/h, 173.51 mL/h, and 225.84 mL/h related to the same operating temperatures, respectively.

As shown in Figure 6.29, when the cell voltage is 2.5 V, the minimum hydrogen production rate of KCl salt is 97.32 mL/h, 119.28 mL/h, and 143.88 mL/h related to the operating temperatures of 25 °C, 45 °C, and 60 °C, respectively. When the cell voltage is 3.5 V, the maximum hydrogen production rate of KCl salt is 158.64 mL/h, 204.36 mL/h, and 262.64 mL/h related to the same operating temperatures, respectively.

As shown in Figure 6.30, when the cell voltage is 2.5 V, the minimum hydrogen production rate of $CaCl_2$ salt is 27.72 mL/h, 48.6 mL/h, and 87.12 mL/h related to the operating temperatures of 25 °C, 45 °C, and 60 °C, respectively. When the cell voltage is 3.5 V, the maximum hydrogen production rate of $CaCl_2$ salt is 37.98 mL/h, 96.68 mL/h, and 202.08 mL/h related with the same operating temperatures, respectively.

As illustrated in Figures 6.28-6.30 hydrogen production exponentially increases since the mobility of the ions also increases with the increase in the cell voltage.

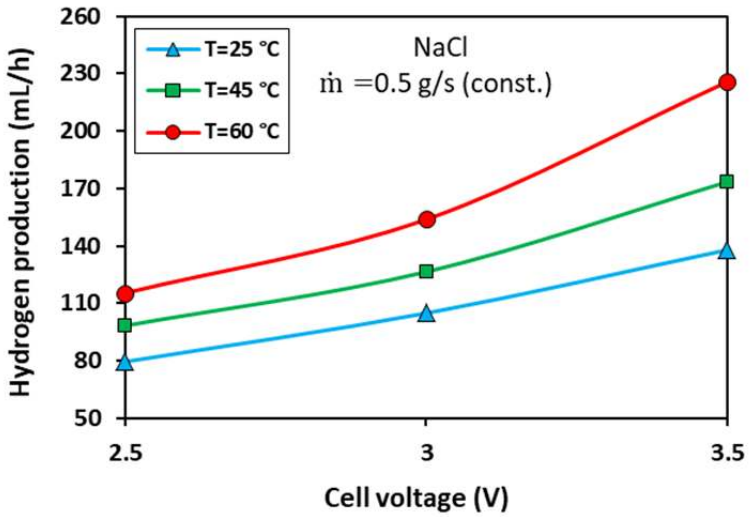

Figure 6.28. Hydrogen production of NaCl according to the cell voltage when the mass flow rate is constant at 0.5 g/s.

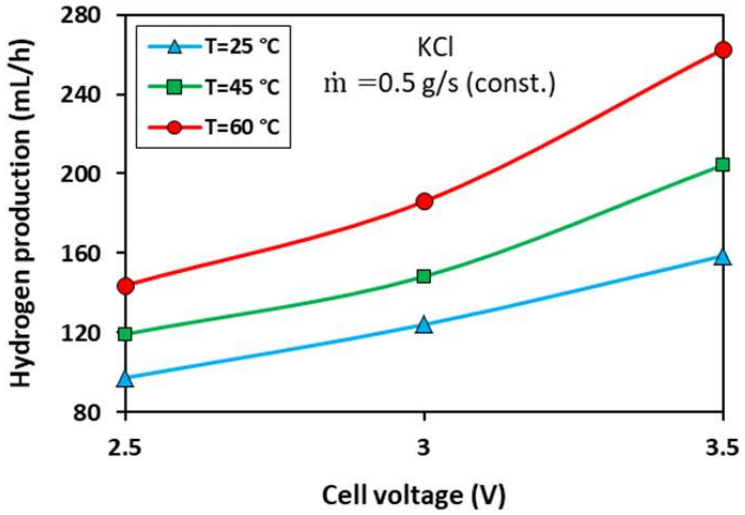

Figure 6.29. Hydrogen production of KCl according to the cell voltage when the mass flow rate is constant at 0.5 g/s.

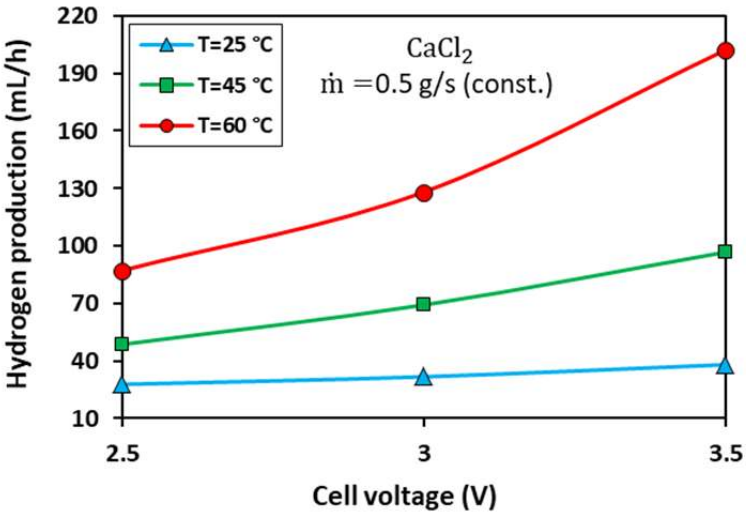

Figure 6.30. Hydrogen production of $CaCl_2$ according to the cell voltage when the mass flow rate is constant at 0.5 g/s.

6.6. Hydrogen Production at a Constant Mass Flow Rate of 0.7 g/s

Figures 6.31, 6.32, and 6.33 show the hydrogen production rate of tested salts concerning the operating temperature for the three different cell voltage cases separately at a constant mass flow rate of 0.7 g/s.

As shown in Figure 6.31, when the operating temperature is 25 °C, the minimum hydrogen production rate of NaCl salt is 80.76 mL/h, 110.04 mL/h, and 149.16 mL/h related to the cell voltage of 2.5 V, 3 V, and 3.5 V, respectively. When the operating temperature is 60 °C, the maximum hydrogen production rate of NaCl salt is 119.64 mL/h, 164.65 mL/h, and 254.36 mL/h related to the same cell voltages, respectively.

As shown in Figure 6.32, when the operating temperature is 25 °C, the minimum hydrogen production rate of KCl salt is 98.76 mL/h, 129.48 mL/h, and 169.8 mL/h related with the cell voltage of 2.5 V, 3 V, and 3.5 V, respectively. When the operating temperature is 60 °C, the maximum hydrogen production rate is 153.36 mL/h, 200.52 mL/h, and 295.68 mL/h for the same cell voltages.

As shown in Figure 6.33, when the operating temperature is 25 °C, the minimum hydrogen production rate of $CaCl_2$ salt is 28.2 mL/h, 32.24 mL/h, and 39.36 mL/h related to the cell voltage of 2.5 V, 3 V, and 3.5 V, respectively. When the operating temperature is 60 °C, the maximum hydrogen production rate is 94.08 mL/h, 138.96 mL/h, and 225.48 mL/h for the same cell voltages.

As illustrated in Figures 6.31-6.33 hydrogen production exponentially increases since the mobility of the ions also increases with the increase in the operating temperature.

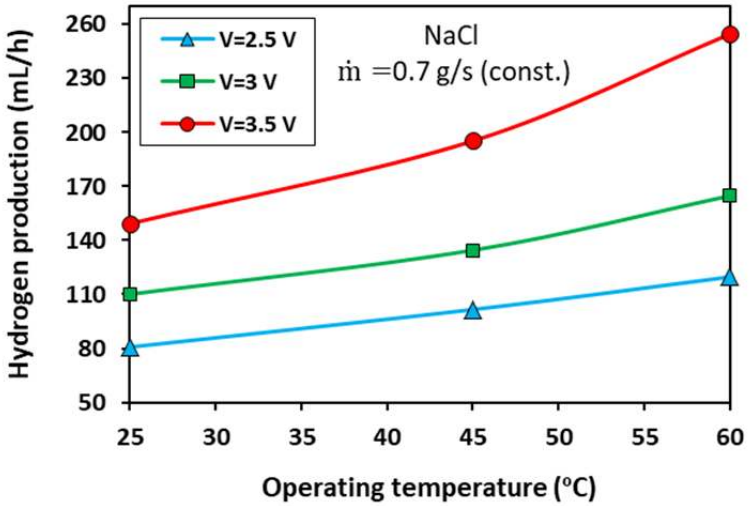

Figure 6.31. Hydrogen production of NaCl according to the operating temperature when the mass flow rate is constant at 0.7 g/s.

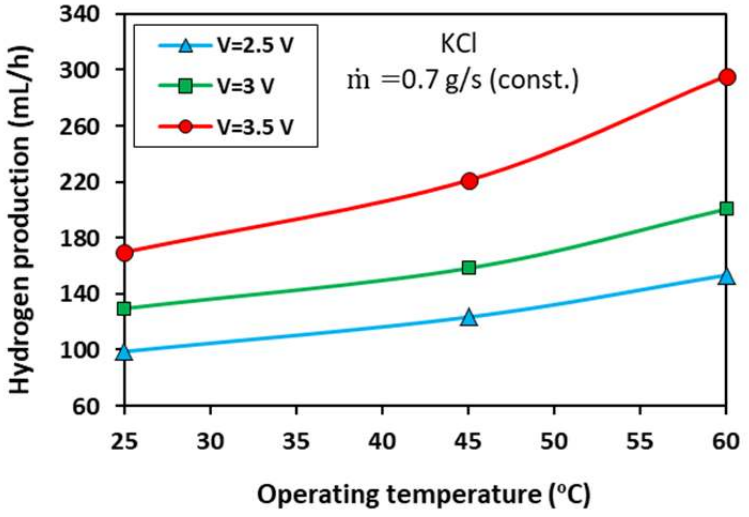

Figure 6.32. Hydrogen production of KCl according to the operating temperature when the mass flow rate is constant at 0.7 g/s.

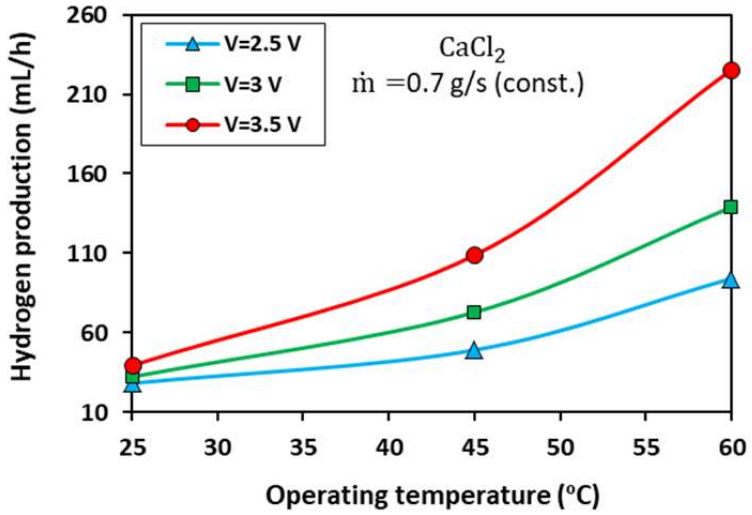

Figure 6.33. Hydrogen production of $CaCl_2$ according to the operating temperature when the mass flow rate is constant at 0.7 g/s.

Figures 6.34, 6.35, and 6.36 show the hydrogen production rate of tested salts concerning the cell voltage for the three different operating temperature cases separately at a constant mass flow rate of 0.7 g/s.

As shown in Figure 6.34, when the cell voltage is 2.5 V, the minimum hydrogen production rate of NaCl salt is 80.76 mL/h, 101.56 mL/h, and 119.64 mL/h related to the operating temperatures of 25 °C, 45 °C, and 60 °C, respectively. When the cell voltage is 3.5 V, the maximum hydrogen production rate of NaCl salt is 149.16 mL/h, 195.05 mL/h, and 254.36 mL/h related to the same operating temperatures, respectively.

As shown in Figure 6.35, when the cell voltage is 2.5 V, the minimum hydrogen production rate of KCl salt is 98.76 mL/h, 123.36 mL/h, and 153.36 mL/h related to the operating temperatures of 25 °C, 45 °C, and 60 °C, respectively. When the cell voltage is 3.5 V, the maximum hydrogen production rate of KCl salt is 169.8 mL/h, 221.16 mL/h, and 295.68 mL/h related to the same operating temperatures, respectively.

As shown in Figure 6.36, when the cell voltage is 2.5 V, the minimum hydrogen production rate of $CaCl_2$ salt is 28.2 mL/h, 49.08 mL/h, and 94.08 mL/h related to the operating temperatures of 25 °C, 45 °C, and 60 °C, respectively. When the cell voltage is 3.5 V, the maximum hydrogen production rate of $CaCl_2$ salt is 39.36 mL/h, 108.72 mL/h, and 225.48 mL/h related with the same operating temperatures, respectively.

As illustrated in Figures 6.34-6.36 hydrogen production exponentially increases since the mobility of the ions also increases with the increase in the cell voltage.

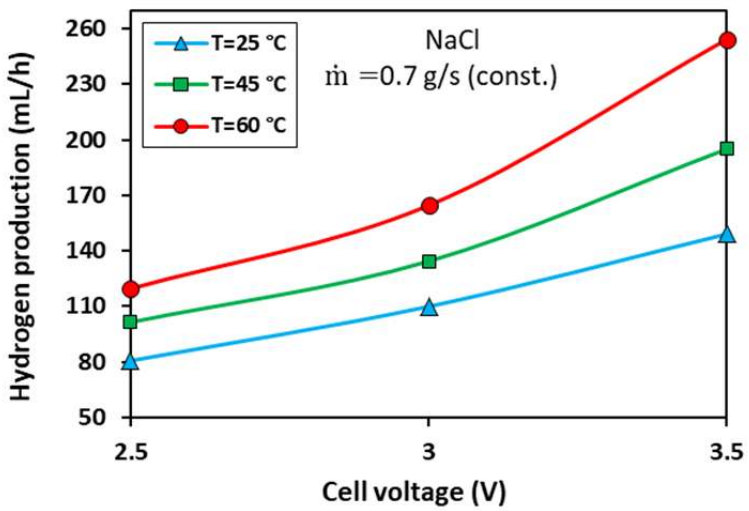

Figure 6.34 Hydrogen production of NaCl according to the cell voltage when the mass flow rate is constant at 0.7 g/s.

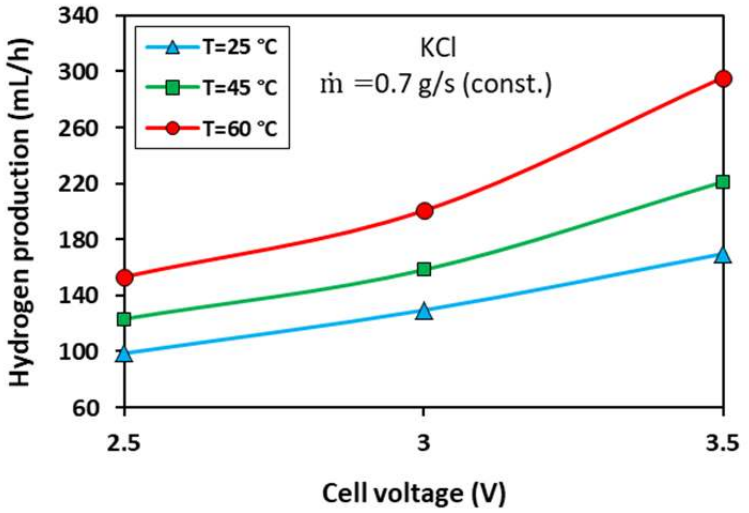

Figure 6.35. Hydrogen production of KCl according to the cell voltage when the mass flow rate is constant at 0.7 g/s.

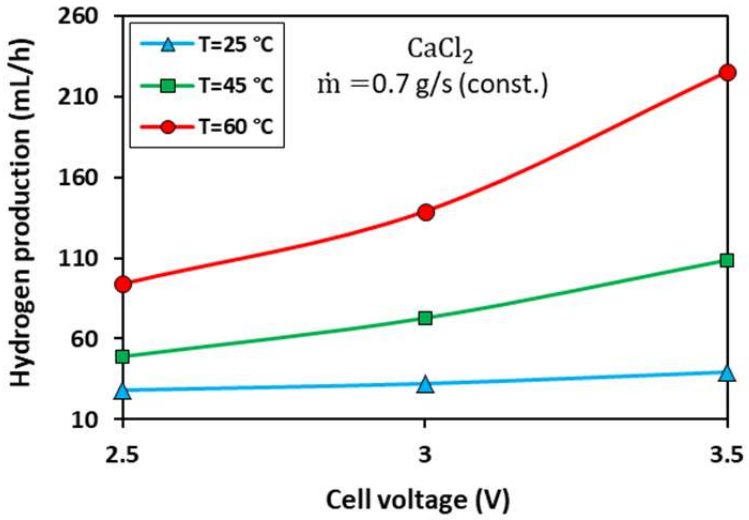

Figure 6.36. Hydrogen production of $CaCl_2$ according to the cell voltage when the mass flow rate is constant at 0.7 g/s.

6.7. Hydrogen Production at a Constant Cell Voltage of 2.5 V

Figures 6.37, 6.38, and 6.39 show the hydrogen production rate of tested salts concerning the operating temperature for the three different mass flow rate cases separately at a constant cell voltage of 2.5 V.

As shown in Figure 6.37, when the operating temperature is 25 °C, the minimum hydrogen production rate of NaCl salt is 78.48 mL/h, 79.58 mL/h, and 80.76 mL/h related to the mass flow rate of 0.3 g/s, 0.5 g/s, and 0.7 g/s, respectively. When the operating temperature is 60 °C, the maximum hydrogen production rate of NaCl salt is 111.43 mL/h, 111.48 mL/h, and 119.64 mL/h related to the same mass flow rates, respectively.

As shown in Figure 6.38, when the operating temperature is 25 °C, the minimum hydrogen production rate of KCl salt is 95.52 mL/h, 97.32 mL/h, and 98.76 mL/h related to the mass flow rate of 0.3 g/s, 0.5 g/s, and 0.7 g/s, respectively. When the operating temperature is 60 °C, the maximum hydrogen production rate of KCl salt is 133.8 mL/h, 143.88 mL/h, and 153.36 mL/h related to the same mass flow rates, respectively.

As shown in Figure 6.39, when the operating temperature is 25 °C, the minimum hydrogen production rate of $CaCl_2$ salt is 27.36 mL/h, 27.72 mL/h, and 28.2 mL/h related with the mass flow rate of 0.3 g/s, 0.5 g/s, and 0.7 g/s, respectively. When the operating temperature is 60 °C, the maximum hydrogen production rate of $CaCl_2$ salt is 83.64 mL/h, 87.12 mL/h, and 94.08 mL/h related with the same mass flow rates, respectively.

As illustrated in Figures 6.37-6.39 hydrogen production exponentially increases since the mobility of the ions also increases with the increase in the operating temperature.

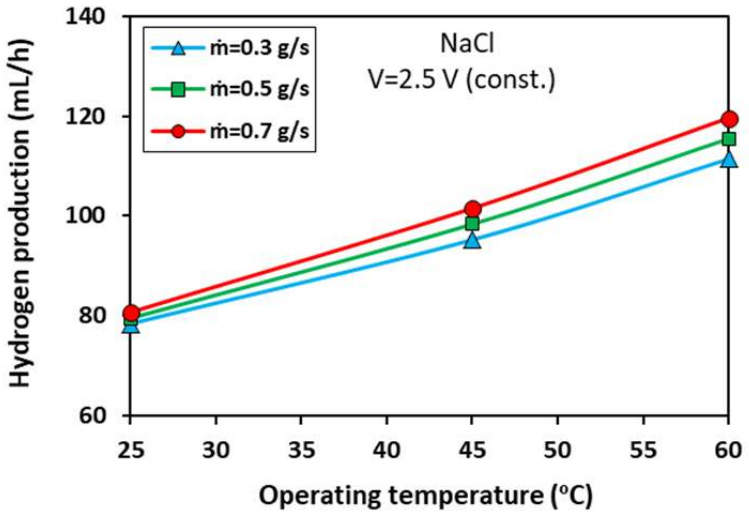

Figure 6.37. Hydrogen production of NaCl according to the operating temperature when the cell voltage is constant at 2.5 V.

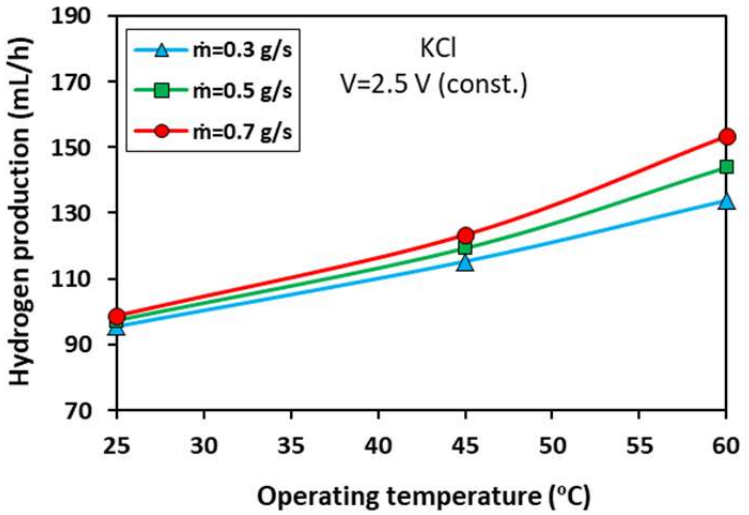

Figure 6.38. Hydrogen production of KCl according to the operating temperature when the cell voltage is constant at 2.5 V.

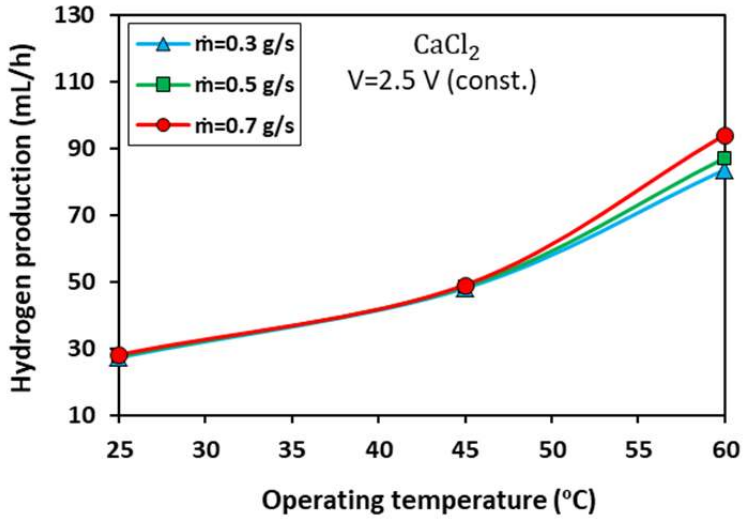

Figure 6.39. Hydrogen production of $CaCl_2$ according to the operating temperature when the cell voltage is constant at 2.5 V.

Figures 6.40, 6.41, and 6.42 show the hydrogen production rate of tested salts concerning the mass flow rate for the three different operating temperature cases separately at a constant cell voltage of 2.5 V.

As shown in Figure 6.40, when the mass flow rate is 0.3 g/s, the minimum hydrogen production rate of NaCl salt is 78.48 mL/h, 95.27 mL/h, and 111.46 mL/h related to the operating temperature of 25 °C, 45 °C, and 60 °C, respectively. When the mass flow rate is 0.7 g/s, the maximum hydrogen production rate of NaCl salt is 80.76 mL/h, 101.56 mL/h, and 119.64 mL/h related to the same operating temperatures, respectively.

As shown in Figure 6.41, when the mass flow rate is 0.3 g/s, the minimum hydrogen production rate of KCl salt is 95.52 mL/h, 115.32 mL/h, and 133.8 mL/h related to the operating temperature of 25 °C, 45 °C, and 60 °C, respectively. When the mass flow rate is 0.7 g/s, the maximum hydrogen production rate of KCl salt is 98.76 mL/h, 123.36 mL/h, and 153.36 mL/h related to the same operating temperatures, respectively.

As shown in Figure 6.42, when the mass flow rate is 0.3 g/s, the minimum hydrogen production rate of $CaCl_2$ salt is 27.36 mL/h, 48.12 mL/h, and 83.64 mL/h related to the operating temperature of 25 °C, 45 °C, and 60 °C, respectively. When the mass flow rate is 0.7 g/s, the maximum hydrogen production rate of $CaCl_2$ salt is 28.2 mL/h, 49.08 mL/h, and 94.08 mL/h related to the same operating temperatures, respectively.

As illustrated in Figures 6.40-6.42 hydrogen production slightly increases since the number of ions also increases with the increase in the mass flow rate.

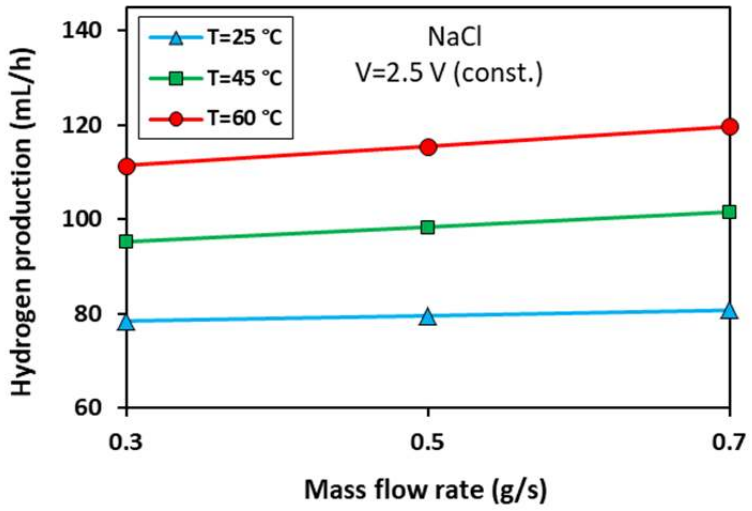

Figure 6.40 Hydrogen production of NaCl according to the mass flow rate when the cell voltage is constant at 2.5 V.

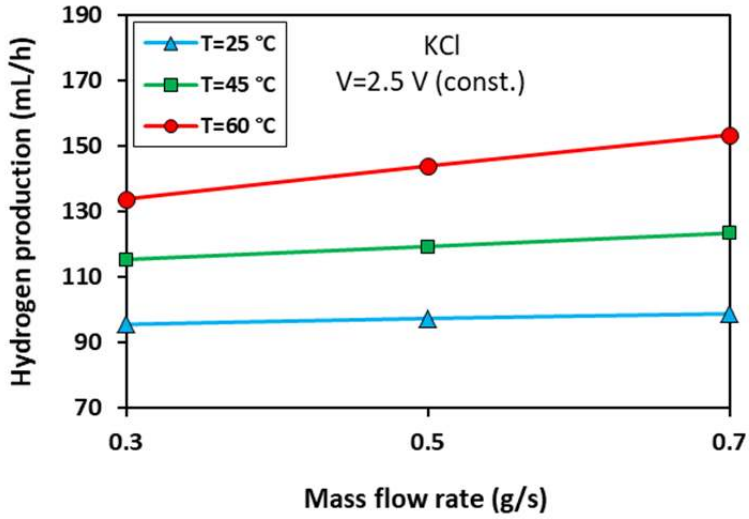

Figure 6.41 Hydrogen production of KCl according to the mass flow rate when the cell voltage is constant at 2.5 V.

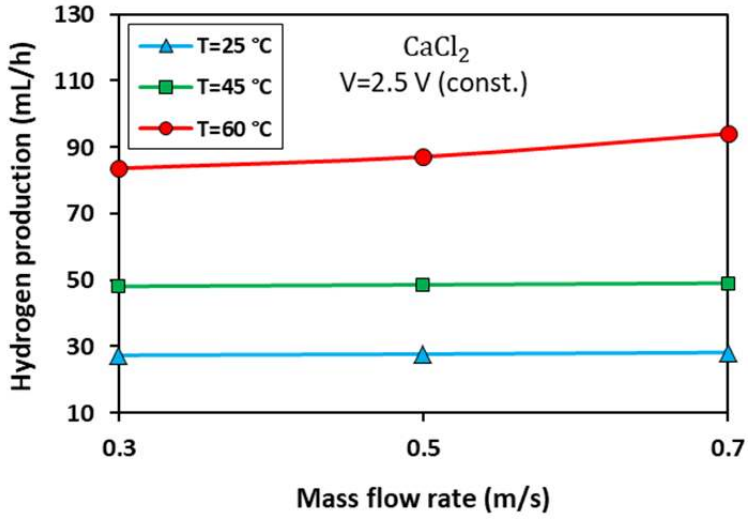

Figure 6.42. Hydrogen production of $CaCl_2$ according to the mass flow rate when the cell voltage is constant at 2.5 V.

6.8. Hydrogen Production at a Constant Cell Voltage of 3 V

Figures 6.43, 6.44, and 6.45 show the hydrogen production rate of tested salts concerning the operating temperature for the three different mass flow rate cases separately at a constant cell voltage of 3 V.

As shown in Figure 6.43, when the operating temperature is 25 °C, the minimum hydrogen production rate of NaCl salt is 99.96 mL/h, 104.92 mL/h, and 110.04 mL/h related to the mass flow rate of 0.3 g/s, 0.5 g/s, and 0.7 g/s, respectively. When the operating temperature is 60 °C, the maximum hydrogen production rate of NaCl salt is 143.76 mL/h, 153.96 mL/h, and 164.65 mL/h related to the same mass flow rates, respectively.

As shown in Figure 6.44, when the operating temperature is 25 °C, the minimum hydrogen production rate of KCl salt is 118.32 mL/h, 124.08 mL/h, and 129.48 mL/h related to the mass flow rate of 0.3 g/s, 0.5 g/s, and 0.7 g/s, respectively. When the operating temperature is 60 °C, the maximum hydrogen production rate of KCl salt is 172.44 mL/h, 186.12 mL/h, and 200.52 mL/h related to the same mass flow rates, respectively.

As shown in Figure 6.45, when the operating temperature is 25 °C, the minimum hydrogen production rate of $CaCl_2$ salt is 31.16 mL/h, 31.68 mL/h, and 32.24 mL/h related with the mass flow rate of 0.3 g/s, 0.5 g/s, and 0.7 g/s, respectively. When the operating temperature is 60 °C, the maximum hydrogen production rate of $CaCl_2$ salt is 114.96 mL/h, 128.04 mL/h, and 138.96 mL/h related with the same mass flow rates, respectively.

As illustrated in Figures 6.43-6.45 hydrogen production exponentially increases since the mobility of the ions also increases with the increase in the operating temperature.

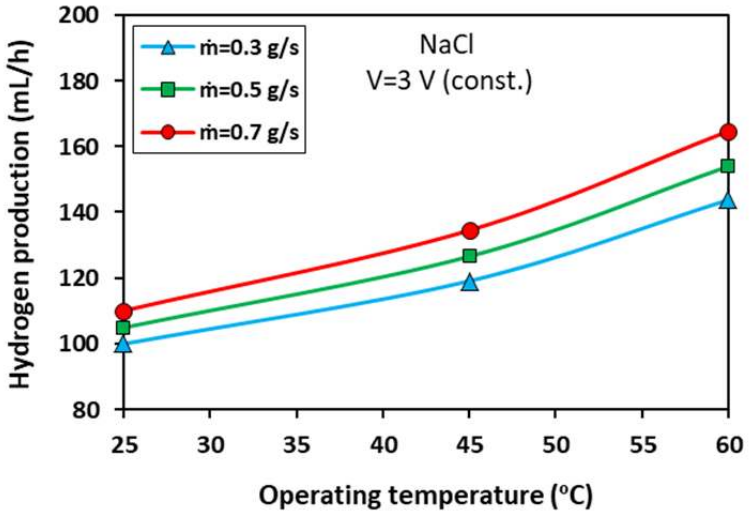

Figure 6.43. Hydrogen production of NaCl according to the operating temperature when the cell voltage is constant at 3 V.

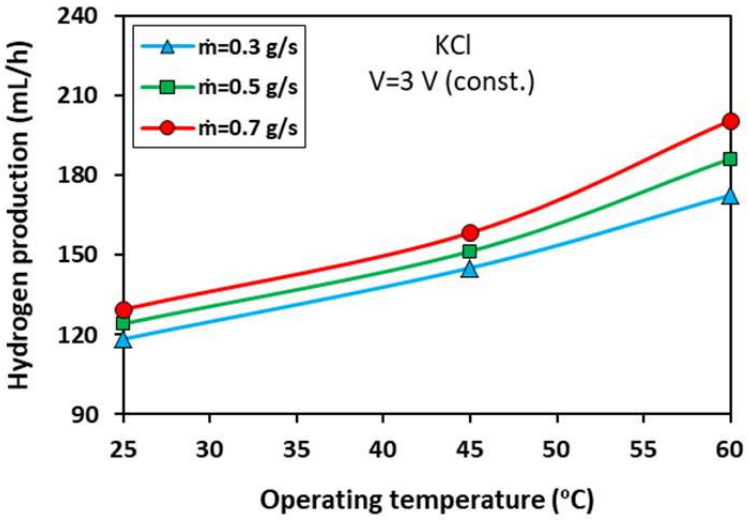

Figure 6.44. Hydrogen production of KCl according to the operating temperature when the cell voltage is constant at 3 V.

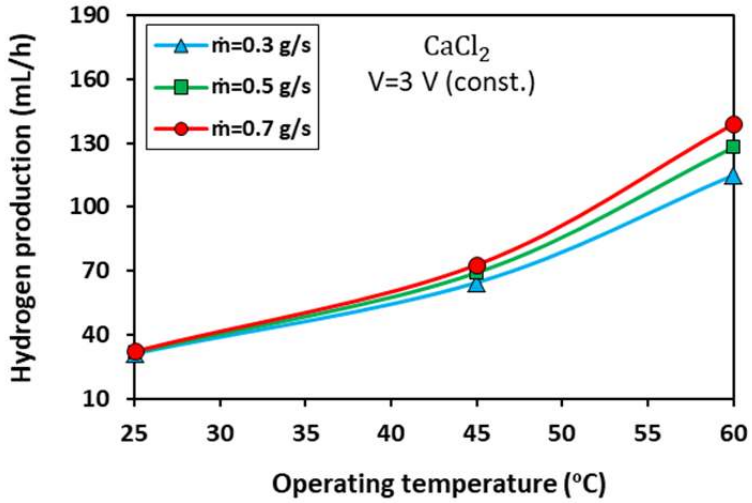

Figure 6.45. Hydrogen production of $CaCl_2$ according to the operating temperature when the cell voltage is constant at 3 V.

Figures 6.46, 6.47, and 6.48 show the hydrogen production rate of tested salts concerning the mass flow rate for the three different operating temperature cases separately at a constant cell voltage of 3 V.

As shown in Figure 6.46, when the mass flow rate is 0.3 g/s, the minimum hydrogen production rate of NaCl salt is 99.96 mL/h, 119.07 mL/h, and 143.76 mL/h related to the operating temperature of 25 °C, 45 °C, and 60 °C, respectively. When the mass flow rate is 0.7 g/s, the maximum hydrogen production rate of NaCl salt is 110.04 mL/h, 134.46 mL/h, and 164.65 mL/h related to the same operating temperatures, respectively.

As shown in Figure 6.47, when the mass flow rate is 0.3 g/s, the minimum hydrogen production rate of KCl salt is 118.32 mL/h, 145.08 mL/h, and 172.44 mL/h related to the operating temperature of 25 °C, 45 °C, and 60 °C, respectively. When the mass flow rate is 0.7 g/s, the maximum hydrogen production rate of KCl salt is 129.48 mL/h, 158.28 mL/h, and 200.52 mL/h related to the same operating temperatures, respectively.

As shown in Figure 6.48, when the mass flow rate is 0.3 g/s, the minimum hydrogen production rate of $CaCl_2$ salt is 31.16 mL/h, 64.56 mL/h, and 114.96 mL/h related to the operating temperature of 25 °C, 45 °C, and 60 °C, respectively. When the mass flow rate is 0.7 g/s, the maximum hydrogen production rate of $CaCl_2$ salt is 32.24 mL/h, 72.84 mL/h, and 138.96 mL/h related with the same operating temperatures, respectively.

As illustrated in Figures 6.46-6.48 hydrogen production slightly increases since the number of ions also increases with the increase in the mass flow rate.

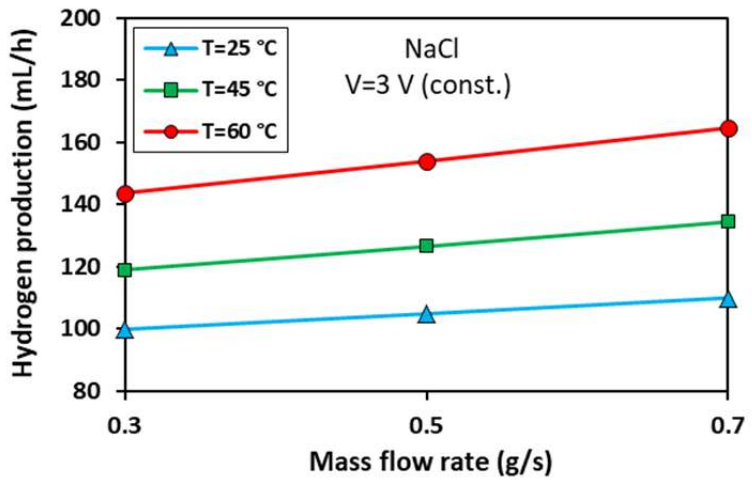

Figure 6.46 Hydrogen production of NaCl according to the mass flow rate when the cell voltage is constant at 3 V.

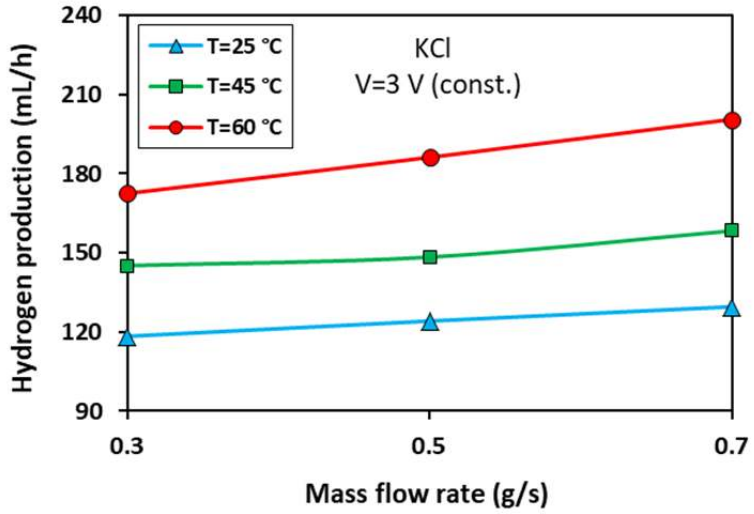

Figure 6.47. Hydrogen production of KCl according to the mass flow rate when the cell voltage is constant at 3 V.

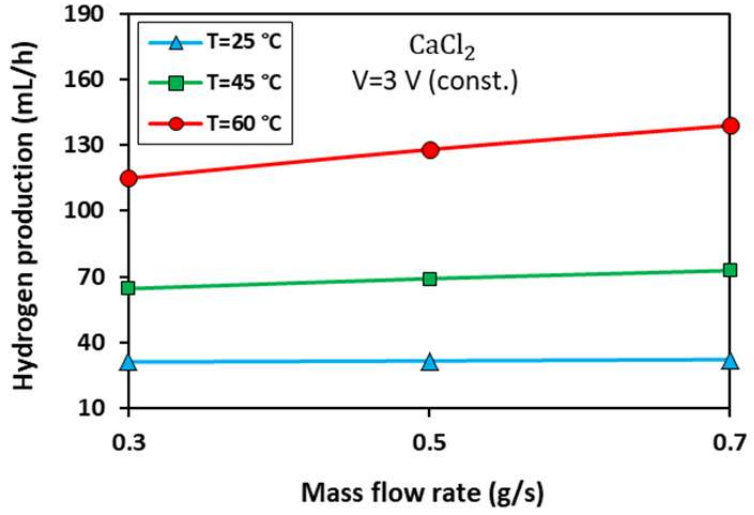

Figure 6.48. Hydrogen production of $CaCl_2$ according to the mass flow rate when the cell voltage is constant at 3 V.

6.9. Hydrogen Production at a Constant Cell Voltage of 3.5 V

Figures 6.49, 6.50, and 6.51 show the hydrogen production rate of tested salts concerning the operating temperature for the three different mass flow rate cases separately at a constant cell voltage of 3.5 V.

As shown in Figure 6.49, when the operating temperature is 25 °C, the minimum hydrogen production rate of NaCl salt is 126.84 mL/h, 137.95 mL/h, and 149.16 mL/h related to the mass flow rate of 0.3 g/s, 0.5 g/s, and 0.7 g/s, respectively. When the operating temperature is 60 °C, the maximum hydrogen production rate of NaCl salt is 201.56 mL/h, 222.84 mL/h, and 254.36 mL/h related to the same mass flow rates, respectively.

As shown in Figure 6.50, when the operating temperature is 25 °C, the minimum hydrogen production rate of KCl salt is 146.28 mL/h, 156.64 mL/h, and 169.8 mL/h related to the mass flow rate of 0.3 g/s, 0.5 g/s, and 0.7 g/s, respectively. When the operating temperature is 60 °C, the maximum hydrogen production rate of KCl salt is 238.92 mL/h, 260.64 mL/h, and 295.68 mL/h related to the same mass flow rates, respectively.

As shown in Figure 6.51, when the operating temperature is 25 °C, the minimum hydrogen production rate of $CaCl_2$ salt is 37.14 mL/h, 37.98 mL/h, and 39.36 mL/h related with the mass flow rate of 0.3 g/s, 0.5 g/s, and 0.7 g/s, respectively. When the operating temperature is 60 °C, the maximum hydrogen production rate of $CaCl_2$ salt is 179.16 mL/h, 202.08 mL/h, and 225.48 mL/h related with the same mass flow rates, respectively.

As illustrated in Figures 6.49-6.51 hydrogen production exponentially increases since the mobility of the ions also increases with the increase in the operating temperature.

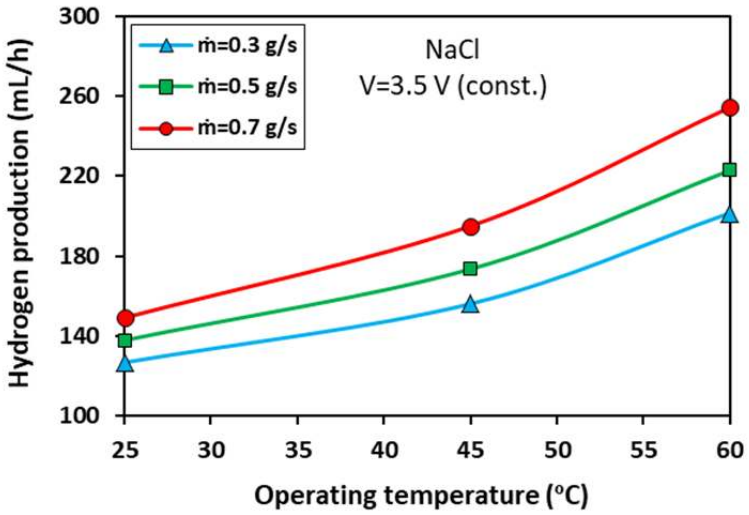

Figure 6.49. Hydrogen production of NaCl according to the operating temperature when the cell voltage is constant at 3.5 V.

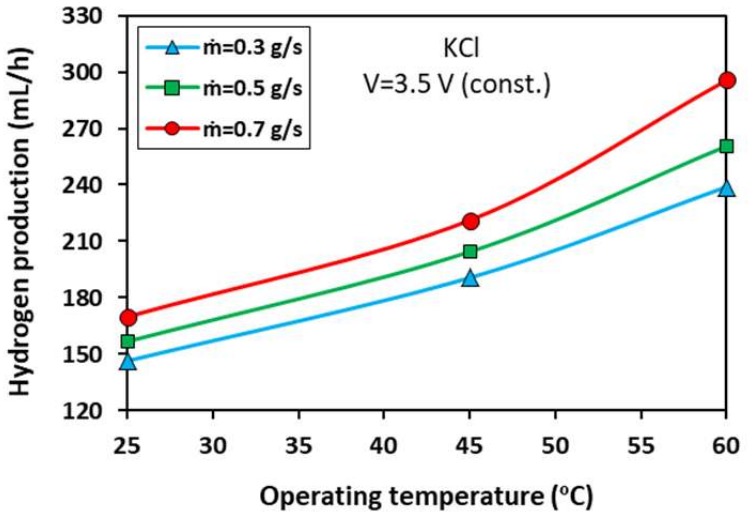

Figure 6.50. Hydrogen production of KCl according to the operating temperature when the cell voltage is constant at 3.5 V.

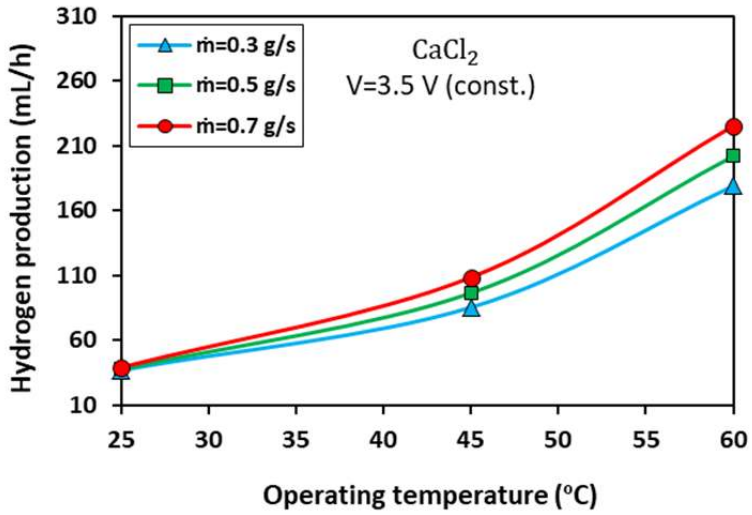

Figure 6.51. Hydrogen production of $CaCl_2$ according to the operating temperature when the cell voltage is constant at 3.5 V.

Figures 6.52, 6.53, and 6.54 show the hydrogen production rate of tested salts concerning the mass flow rate for the three different operating temperature cases separately at a constant cell voltage of 3.5 V.

As shown in Figure 6.52, when the mass flow rate is 0.3 g/s, the minimum hydrogen production rate of NaCl salt is 126.84 mL/h, 156.16 mL/h, and 201.56 mL/h related to the operating temperature of 25 °C, 45 °C, and 60 °C, respectively. When the mass flow rate is 0.7 g/s, the maximum hydrogen production rate of NaCl salt is 149.16 mL/h, 195.05 mL/h, and 254.36 mL/h related to the same operating temperatures, respectively.

As shown in Figure 6.53, when the mass flow rate is 0.3 g/s, the minimum hydrogen production rate of KCl salt is 146.28 mL/h, 190.56 mL/h, and 238.92 mL/h related to the operating temperature of 25 °C, 45 °C, and 60 °C, respectively. When the mass flow rate is 0.7 g/s, the maximum hydrogen production rate of KCl salt is 169.8 mL/h, 221.16 mL/h, and 295.68 mL/h related to the same operating temperatures, respectively.

As shown in Figure 6.54, when the mass flow rate is 0.3 g/s, the minimum hydrogen production rate of $CaCl_2$ salt is 37.14 mL/h, 85.56 mL/h, and 179.16 mL/h related to the operating temperature of 25 °C, 45 °C, and 60 °C, respectively. When the mass flow rate is 0.7 g/s, the maximum hydrogen production rate of $CaCl_2$ salt is 39.36 mL/h, 108.72 mL/h, and 225.48 mL/h related with the same operating temperatures, respectively.

As illustrated in Figures 6.52-6.54 hydrogen production slightly increases since the number of ions also increases with the increase in the mass flow rate.

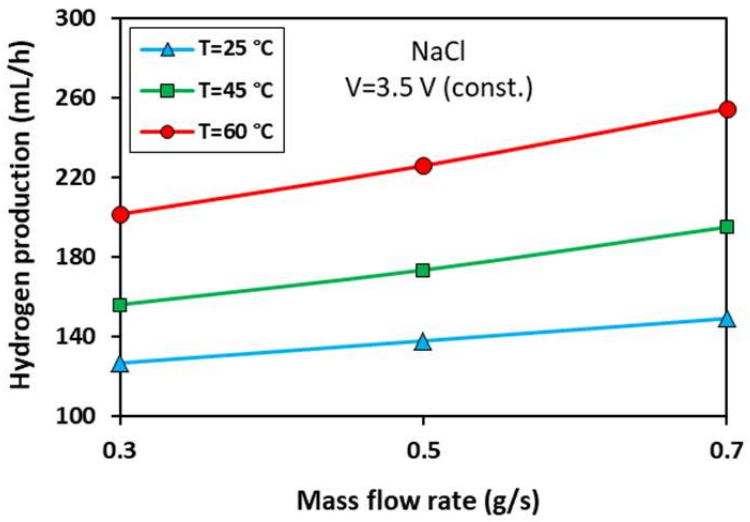

Figure 6.52 Hydrogen production of NaCl according to the mass flow rate when the cell voltage is constant at 3.5 V.

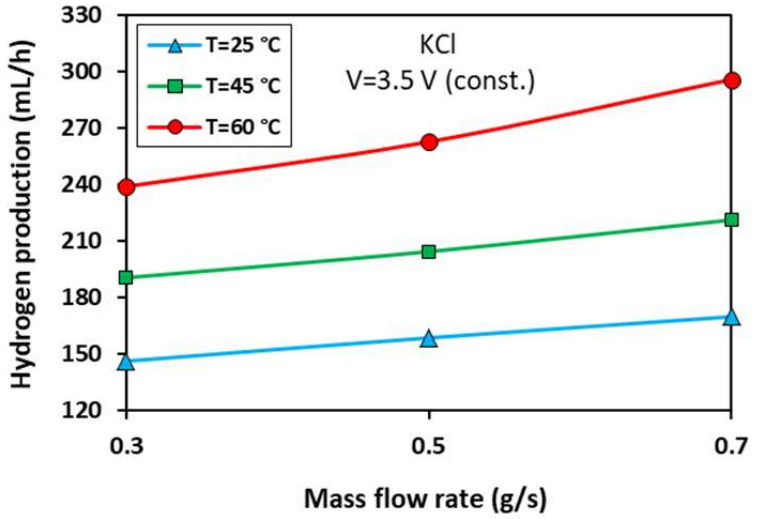

Figure 6.53 Hydrogen production of KCl according to the mass flow rate when the cell voltage is constant at 3.5 V.

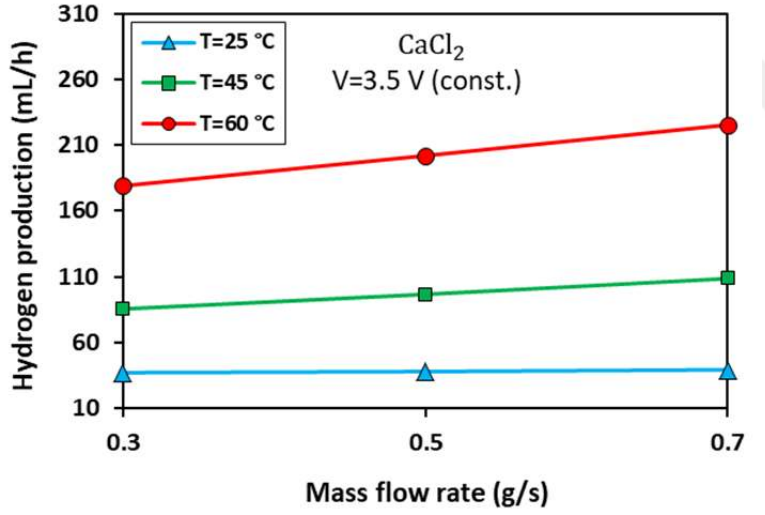

Figure 6.54. Hydrogen production of $CaCl_2$ according to the mass flow rate when the cell voltage is constant at 3.5 V.

6.10. Comparison of Hydrogen Production of Tested Salts

Figure 6.55 shows the measured cell current for each tested salt concerning the operating temperature when the cell voltage and the mass flow rate are kept constant at 3 V and 0.5 g/s, respectively. As the electrical conductivity of the electrolytes increased with the operating temperature, the cell current also increased. This means that voltage losses throughout the reactor are decreasing while measured cell current increases at high temperatures. While the $CaCl_2$ salt remains very passive at low temperatures, its activity increases considerably at high temperatures. Table 4.3 shows the cell currents depending on KCl, NaCl, and $CaCl_2$ salts. The minimum measured cell currents for KCl, NaCl, and $CaCl_2$ are 0.34 A, 0.29 A, and 0.09 A at 25 °C, respectively. The maximum measured cell currents for KCl, NaCl, and $CaCl_2$ are 0.51 A, 0.42 A, and 0.35 A at 60 °C, respectively.

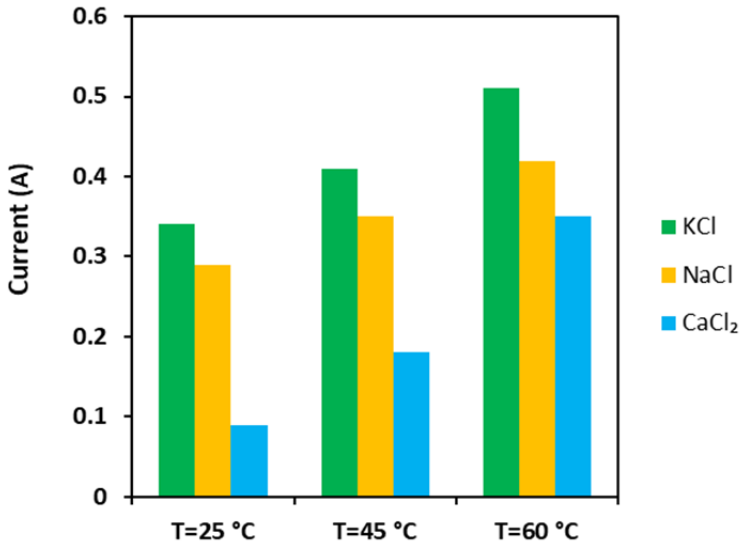

Figure 6.55. Comparing cell currents for tested salts concerning the operating temperature.

Figure 6.56 shows the hydrogen production rate of tested salts concerning the operating temperature (25 °C, 45 °C, and 60 °C) when the cell voltage and the mass flow rate are kept constant at 3 V and 0.5 g/s, respectively. As seen in Figure 6.56, hydrogen production increased with the increase in temperature for all three salt types since the electric charge movement increased with the temperature. In all three operating temperature conditions, calcium produced the least hydrogen, while potassium produced the most hydrogen. In addition, the hydrogen production of potassium and sodium salts increases relatively smoothly with the increase in temperature. However, while the hydrogen production of calcium salt at low temperatures remains low, it is observed that this product grows and increases with increasing temperature. The minimum hydrogen production rate for KCl, NaCl, and $CaCl_2$ are 124.08 mL/h, 104.92 mL/h, and 31.68 mL/h at the operating temperature of 25 °C, respectively. The maximum hydrogen production rate for KCl, NaCl, and $CaCl_2$ are 186.12 mL/h, 153.96 mL/h, and 128.04 mL/h at the operating temperature of 60 °C, respectively.

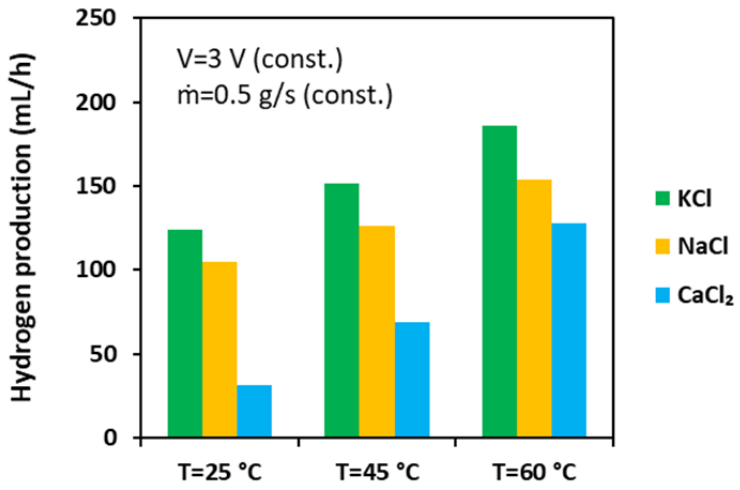

Figure 6.56. Comparing hydrogen production of tested salts concerning the operating temperature.

Figure 6.57 shows the hydrogen production rate of tested salts concerning the cell voltage (2.5 V, 3 V, and 3.5 V) when the operating temperature and the mass flow rate are kept constant at 45 °C and 0.5 g/s, respectively. As seen in Figure 6.57, hydrogen production increased with the increase in cell voltage for all three salt types since the electric charge movement increased with the voltage. In all three voltage conditions, calcium produced the least hydrogen, while potassium produced the most hydrogen. In all three voltage conditions, calcium produced the least hydrogen depending on its place in the activity series while potassium produced the most hydrogen. Hydrogen production increased uniformly with increasing cell voltage for all three salt types. The minimum hydrogen production rate for KCl, NaCl, and $CaCl_2$ are 119.28 mL/h, 98.38 mL/h, and 48.6 mL/h at the cell voltage of 2.5 V, respectively. The maximum hydrogen production rate for KCl, NaCl, and $CaCl_2$ are 204.36 mL/h, 173.51 mL/h, and 96.68 mL/h at the cell voltage of 3.5 V, respectively.

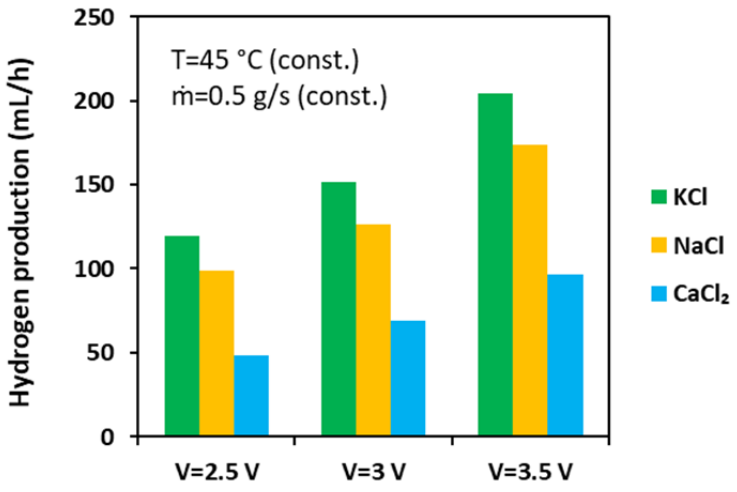

Figure 6.57. Comparing hydrogen production of tested salts concerning the cell voltage.

Figure 6.58 shows the hydrogen production rate of tested salts concerning the mass flow rate (0.3 g/s, 0.5 g/s, and 0.7 g/s) when the cell voltage and the operating temperature are kept constant at 3 V and 45 °C, respectively. As seen in Figure 6.58, hydrogen production increased with the increase in mass flow rate for all three salt types since the amount of the ions in the cell also increases with the increase in the mass flow rate. In all three voltage conditions, calcium produced the least hydrogen, while potassium produced the most hydrogen. In all three mass flow conditions, calcium produced the least hydrogen depending on its place in the activity series while potassium produced the most hydrogen. Hydrogen production increased uniformly with increasing mass flow rate for all three salt types. The minimum hydrogen production rate for KCl, NaCl, and $CaCl_2$ are 145.08 mL/h, 119.07 mL/h and 64.56 mL/h at the mass flow rate of 0.3 g/s, respectively. The maximum hydrogen production rate for KCl, NaCl, and $CaCl_2$ are 158.28 mL/h, 134.46 mL/h and 72.84 mL/h the mass flow rate of 0.5 g/s, respectively.

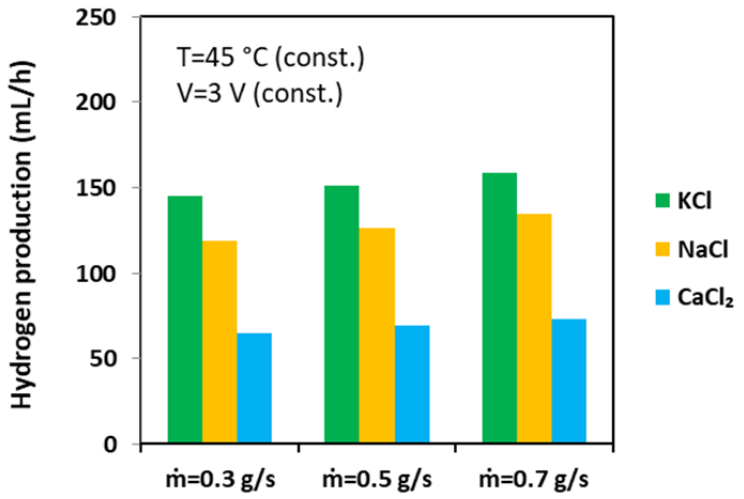

Figure 6.58. Comparing hydrogen production of tested salts concerning the mass flow rate.

Figure 6.59 shows the energy efficiencies of the tested salts concerning the operating temperature of 25 °C, 45 °C, and 60 °C. The energy efficiencies of hydrogen production of KCl, NaCl, and $CaCl_2$ at 25 °C are 28.42 %, 24.28 % and 11.25 %, respectively. The efficiency values of KCl and NaCl decreased to 26.03 % and 21.12 % at 60 °C. The efficiency decrease for KCl and NaCl with increasing temperature results due to the additional heat input even though hydrogen production increases. Conversely, the efficiency of $CaCl_2$ increased to 17.89 % at 60 °C since it reacts violently with water at high temperatures.

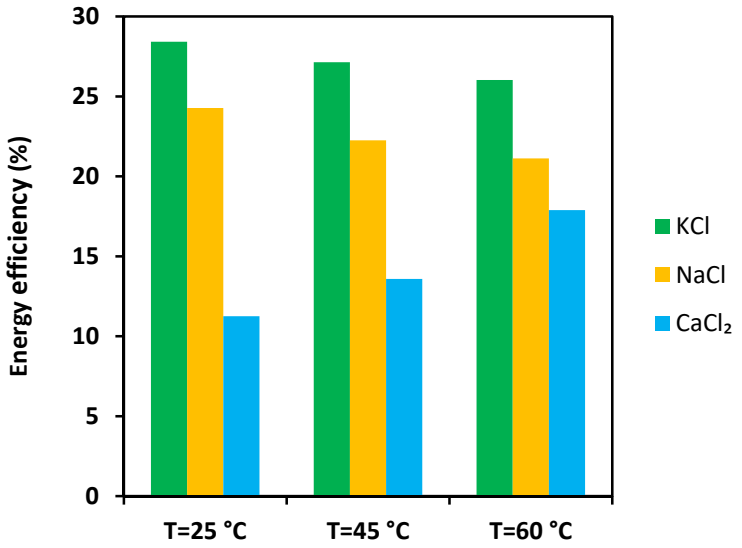

Figure 6.59. Energy efficiencies of the tested salts concerning the operating temperatures.

Figure 6.60 shows the exergy efficiencies of the tested salts concerning the operating temperature of 25 °C, 45 °C, and 60 °C. The exergy efficiencies of hydrogen production of KCl, NaCl, and $CaCl_2$ at 25 °C are 23.62 %, 19.81 % and 10.92 %, respectively. The exergy efficiency values of KCl and NaCl decreased to 22.74 % and 18.89 % at 60 °C due to additional heat input. As in the energy efficiency, the exergy efficiency of $CaCl_2$ increased to 16.14 % at 60 °C.

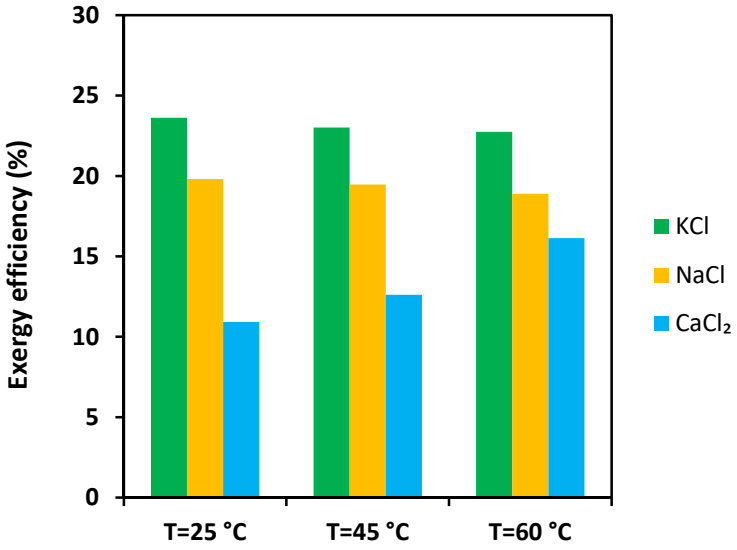

Figure 6.60. Exergy efficiencies of the tested salts concerning the operating temperatures.

The yield values calculated for the NaCl salt were found to be close to the yield values found in Acar and Dincer 2017a.

7. CONCLUSIONS AND RECOMMENDATIONS

7.1 Conclusions

The need for new and clean energy sources has become very important today. So humanity needs a sustainable system to replace fossil fuels and their harmful effects in the long run. Hydrogen is considered a key element to replacing fossil fuels in the long term since it can be a major contributor to a fully decarbonised energy system. Produced with renewable electricity by electrolysis, green hydrogen is a carbon-free raw material for many applications. Whether as a raw material for industry (production of green chemicals such as ammonia and methanol), as a fuel for fuel cells, or as a synthetic energy carrier, hydrogen is becoming more and more important.

Three important products, namely chlorine gas, caustic soda, and hydrogen gas, are obtained with the Chlor-alkali method. Therefore, a Chlor-alkali process powered by electricity generated from renewable sources is an important industrial application as it produces three important products without emitting carbon.

Depending on the activity series of K, Na, and Ca metals, KCl salt produced the most hydrogen, while $CaCl_2$ salt produced the least hydrogen in a certain time interval. Increasing the operating temperature, cell voltage, or mass flow rate increased the hydrogen production rate for all three salt types. However, the least effective of these three parameters is the mass flow rate. As the cell voltage and operating temperature increased, more hydrogen was produced as a result of increasing the mobility of the ions. For the rate of hydrogen production, the voltage increase was more effective than the increase in the operating temperature.

The hydrogen production rate of tested salts concerning the operating temperature (25 °C, 45 °C, and 60 °C) when the cell voltage and the mass flow rate are kept constant at 3 V and 0.5 g/s as followings: The minimum hydrogen production rate for KCl, NaCl and $CaCl_2$ are 124.08 mL/h, 104.92 mL/h and 31.68

mL/h at the operating temperature of 25 °C, respectively. The maximum hydrogen production rate for KCl, NaCl, and $CaCl_2$ are 186.12 mL/h, 153.96 mL/h, and 128.04 mL/h at the operating temperature of 60 °C, respectively.

The hydrogen production rate of tested salts concerning the cell voltage (2.5 V, 3 V, and 3.5 V) when the operating temperature and the mass flow rate are kept constant at 45 °C and 0.5 g/s as followings: The minimum hydrogen production rate for KCl, NaCl and $CaCl_2$ are 119.28 mL/h, 98.38 mL/h, and 48.6 mL/h at the cell voltage of 2.5 V, respectively. The maximum hydrogen production rate for KCl, NaCl, and $CaCl_2$ are 204.36 mL/h, 173.51 mL/h, and 96.68 mL/h at the cell voltage of 3.5 V, respectively.

The hydrogen production rate of tested salts concerning the mass flow rate (0.3 g/s, 0.5 g/s, and 0.7 g/s) when the cell voltage and the operating temperature are kept constant at 3 V and 45 °C as followings: The minimum hydrogen production rate for KCl, NaCl and $CaCl_2$ are 145.08 mL/h, 119.07 mL/h and 64.56 mL/h at the mass flow rate of 0.3 g/s, respectively. The maximum hydrogen production rate for KCl, NaCl, and $CaCl_2$ are 158.28 mL/h, 134.46 mL/h and 72.84 mL/h the mass flow rate of 0.5 g/s, respectively.

The energy efficiencies of hydrogen production of KCl, NaCl, and $CaCl_2$ at 25 °C are 28.42 %, 24.28 % and 11.25 %, respectively. The exergy efficiencies of hydrogen production of KCl, NaCl, and $CaCl_2$ at 25 °C are 23.62 %, 19.81 % and 10.92 %, respectively.

Since an electrode resistant to the activity of chlorine gas, such as platinum metal, was not used in the anode compartment, no chlorine gas releasing was observed, instead, chlorate-based contaminations and also serious erosions were observed on the electrode. Due to this contamination, the reactor had to be cleaned frequently during the experiments.

7.2 Recommendations

- Different reactor designs can be tried.
- Different types of electrodes can be tried.
- Different types of salts can be tried.
- Studies can be carried out to extend membrane life and improve ion transfer.
- Since the increase in operating temperature increases the hydrogen production rate, studies can be conducted on the integration of Chlor-alkali systems into a heat sources such as solar collector systems and geothermal sources.

REFERENCES

Acar, C., Dincer, I., 2017a. Experimental investigation and analysis of a hybrid photoelectrochemical hydrogen production system. International Journal of Hydrogen Energy, 42:2504-2511.

Acar, C., Dincer, I., 2017b. Testing and performance evaluation of a hybrid photoelectrochemical hydrogen production system. International Journal of Hydrogen Energy, 42:3605-3613.

Acar, C., Dincer, I., 2017c. Energy and exergy analyses of a novel photoelectrochemical hydrogen production system. International Journal of Hydrogen Energy, 42:30550-30558.

Acar, C., Dincer, I., 2019b. Review and evaluation of hydrogen production options for better environment. Journal of Cleaner Production, 218:835-849.

Acar, C., Beskese, A., Temur, G.T., 2018. Sustainability analysis of different hydrogen production options using hesitant fuzzy AHP. International Journal of Hydrogen Energy, 43:18059-18076.

Ahmad, H., Kamarudin, S.K., Minggu, L.J., Kassim, M., 2015. Hydrogen from photo-catalytic water splitting process: A review. Renewable and Sustainable Energy Reviews, 43:599-610.

Bhattacharyya, R., Misra, A., Sandeep, K.C., 2017. Photovoltaic solar energy conversion for hydrogen production by alkaline water electrolysis: Conceptual design and analysis. Energy Conversion and Management, 133:1-13.

Bicer, Y., Dincer, I., 2018. Performance evaluation of a photoelectrochemical hydrogen production reactor under concentrated and non-concentrated sunlight conditions. International Journal of Hydrogen Energy, 43:10258-10267.

BoroumandJazi, G., Rismanchi, B., Saidur, R., 2013. A review on exergy analysis of industrial sector. Renewable and Sustainable Energy Reviews, 27: 198-203.

Budiarto, T., Esche, E., Repke, J. U., Leksono, E., 2017. Dynamic model of chloralkali membrane process. Procedia Engineering, 170:473-481.

Cengel, Y.A., Boles M.A., 2013. Termodinamik. Yedinci baskı. Palme yayıncılık, Ankara.

Chehade, D., Demir, M.E., Dincer, I., Yuzer, B., Selcuk, H., 2018. Experimental investigation and analysis of a new photoelectrochemical reactor for hydrogen production. International Journal of Hydrogen Energy, 43:12049-12058.

Dincer, I., Rosen, M.A., 2005. Thermodynamic aspects of renewables and sustainable development. Renewable and Sustainable Energy Reviews, 9:169-189.

Dincer, I., Rosen, M.A., 2012. Energy, Environment, and Sustainable Development. Elsevier: Oxford.

Domga, R.D., Noumi, G.B., Tchatchueng, J.B., 2017. Study of Some Electrolysis Parameters for Chlorine and Hydrogen Production Using a New Membrane Electrolyzer. International Journal of Chemical Engineering and Analytical Science, 2(1):1-8.

El-Shafie, M., Kambara, S., Hayakawa, Y., 2019. Hydrogen production technologies overview. Journal of Power and Energy Engineering, 7:107-154.

Eurochlor (17.) Chlor-Alkali Industry Review 2019-2020.

Foorginezhad, S., Dargah, M. M., Falahati, Z., Abbassi, R., Razmjou, A., Asadnia, M., 2021. Sensing advancement towards safety assessment of hydrogen fuel cell vehicles. Journal of Power Sources, Vol:489, 229450.

Franco, F., Prior, J., Velizarov, S., Mendes, A., 2019. A systematic performance history analysis of a chlor-alkali membrane electrolyser under Industrial operating conditions. Applies Sciences, 9:284.

Fujishima, A., Honda, K., 1972. Electrochemical photolysis of water at a semiconductor electrode. Nature 238:37-38.

Greenbaum, E., Lee, J. W., 1997. Photosynthetic hydrogen and oxygen production by green algae. Proceedings of the International Conference on Biological Hydrogen Production BioHydrogen '97, June 23-26 1997, Waikoloa, HE.

Hofmann, M., Muller, R., Christidis, A., Fischer, P., Klaucke, F., Vomberg, S., Tsatsaronis, G., 2022. Flexible and economical operation of chlor-alkali process with subsequent polyvinyl chloride production, AIChE J. 2022;68(1):e17480.

Jalali, A.A., Mohammadi, F., Ashrafizadeh, S.N., 2009. Effects of process conditions on cell voltage, current efficiency and voltage balance of a chlor-alkali membrane cell. Desalination 237:126-139.

Karakilcik, H., Karakilcik, M., 2020. Underground Large-Scale Hydrogen Storage. In: Uyar, T. (eds) Accelerating the Transition to a 100% Renewable Energy Era. Lecture Notes in Energy, vol 74. Springer.

Karakilcik, M., Erden, M., Cilogullari, M., Dincer, I., 2018. Investigation of hydrogen production performance of a reactor assisted by a solar pond via photoelectrochemical process. International Journal of Hydrogen Energy, 43:10549-10554.

Karapekmez, A., Dincer, I., 2020. Thermodynamic analysis of a novel solar and geothermal based combined energy system for hydrogen production. International Journal of Hydrogen Energy, 45:5608-5628.

Khasawneh, H., Saidan, M. N., Al-Addous, M., 2019. Utilization of hydrogen as clean energy resource in chlor-alkali process. Energy Exploration & Exploitation, 37(3):1053-1072.

Li, K., Fan, Q., Chuai, H., Liu, H., Zhang, S., Ma, X., 2021. Revisiting chlor-alkali electrolyzers: from materials to devices. Transactions of Tianjin University, 27:202-216.

Longden, T., Beck, F. J., Jotzo, F., Andrews, R., Prasad, M., 2022. 'Clean' hydrogen? – Comparing the emissions and costs of fossil fuel versus renewable electricity based hydrogen. Applied Energy, Volume 306, Part B, 118145.

Luo, Y., Wang, Q., Li, J., Xu, F., Sun, L., Zou, Y., Chu, H., Li, B., Zhang, K., 2020. Enhanced hydrogen storage/sensing of metal hydrides by nanomodification. Materials Today Nano, Vol:9.

Madaeni, S. S., Kazemi, V., 2008. Treatment of saturated brine in chlor-alkali process using membranes. Separation and Purification Technology, 61:68-74.

Mijim, J. K., Pluvinage, G., Capelle, J., Azari, Z., Benamara, M., 2020. Probabilistic design factors for pipes used for hydrogen transport. International Journal of Hydrogen Energy, 58:33860-33870.

Munoz, L.D.S., Bergel, A., Feron, D., Basseguy, R., 2010. Hydrogen production by electrolysis of a phosphate solution on a stainless steel cathode. International Journal of Hydrogen Energy, 35:8561-8568.

Noor, M. M., Wandel, A. P., Yusaf, T., 2013. The development of mild combustion open burner experimental setup. International Conference on Mechanical Engineering Research (ICMER2013), 1-3 July, Paper ID: P341.

Qureshy, A.M.M.I., Ahmed, M., Dincer, I., 2019. Performance assessment study of photo-electrochemical water-splitting reactor designs for hydrogen production. International Journal of Hydrogen Energy, 44:9237-9247.

Rabbani, M., Dincer, I., Naterer, G.F., 2014(a). Experimental investigation of processing parameters and effects on chloralkali products in an electrolysis based chloralkali reactor. Chemical Engineering and Processing, 82:9-18.

Rabbani, M., Dincer, I., Naterer, G.F., 2014(b). Electrochemical analysis of a photoelectrochemical chloralkali reactor. Chemical Engineering and Processing, 82:42-53.

Rosales-Huamani, J.A., Medina-Collana, J.T., Diaz-Cordova, Z.M., Montano-Pisfil, J.A., 2021. Factors influencing the formation of sodium hydroxide by an ion exchange membrane cell. Batteries, 7, 34.

Safari, F., Dincer, I., 2019. Development and analysis of a novel biomass-based integrated system for multigeneration with hydrogen production. International Journal of Hydrogen Energy, 44:3511-3526.

Safari, F., Dincer, I., 2020. A review and comparative evaluation of thermochemical water splitting cycles for hydrogen production. Energy Conversion and Management, Volume 205, 11218.

Safizadeh, F., Ghali, E., Houlachi, G., 2015. Electrocatalysis developments for hydrogen evolution reaction in alkaline solutions-A Review. International Journal of Hydrogen Energy, 40:256-274.

Singla, S., Shetti, N. P., Basu, S., Mondal, K., Aminabhavi, T. M., 2022. Hydrogen production technologies - Membrane based separation, storage and challenges. Journal of Environmental Management, Volume 302, Part A, 113963.

Song, H., Luo, S., Huang, H., Deng, B., Ye, J., 2022. Solar-Driven Hydrogen Production: Recent Advances, Challenges, and Future Perspectives. ACS Energy Lett. 7:1043-1065.

Thummar, K., Abang, R., Menzel, K., de Groot, M.T., 2022. Coupling a chlor-alkali membrane electrolyzer cell to a wind energy source: Dynamic Modeling and Simulations. Energies, 15, 606.

Torzillo, G., Scoma, A., Faraloni, C., Giannelli, L., 2015. Advances in the biotechnology of hydrogen production with the microalga Chlamydomonas reinhardtii, Critical Reviews in Biotechnology, 35:4, 485-496.

Xing, Z., Zong, X., Pan, J., Wang, L. 2013. On the engineering part of solar hydrogen production from water splitting: Photo reactor design. Chemical Engineering Science, 104:125-146.

Yilmaz, F., Balta, M.T., Selbas, R., 2016. A review of solar based hydrogen production methods. Renewable and Sustainable Energy Reviews, 56:171-178.

Zafar, S., Dincer, I., 2014. Thermodynamic analysis of a combined PVT-fuel-cell system for power, heat, fresh water and hydrogen production. International Journal of Hydrogen Energy, 39:9962-9972.

ÖZGEÇMİŞ

Mustafa ERDEN, Orta Doğu Teknik Üniversitesi Eğitim Fakültesi Fizik Öğretmenliği Bölümünden mezun oldu. Çukurova Üniversitesi Sosyal Bilimler Enstitüsü İlköğretim Bölümünde ve Fen Bilimleri Enstitüsü Fizik Bölümünde yüksek lisans yaptı. Halen Fizik Bölümünde doktora çalışmasına devam etmektedir.